Investigations with High Spectral Resolution Data from AIRS

Lectures in Krakow
May 2006

Paul Menzel
NOAA/NESDIS/ORA

Investigations with High Spectral Resolution Data from AIRS

Paul Menzel
NOAA/NESDIS
in collaboration with
Tim Schmit, Jun Li, Youri Plokhenko, Dave Tobin, Hank Revercomb and colleagues at CIMSS

Earth emitted spectra overlaid on Planck function envelopes

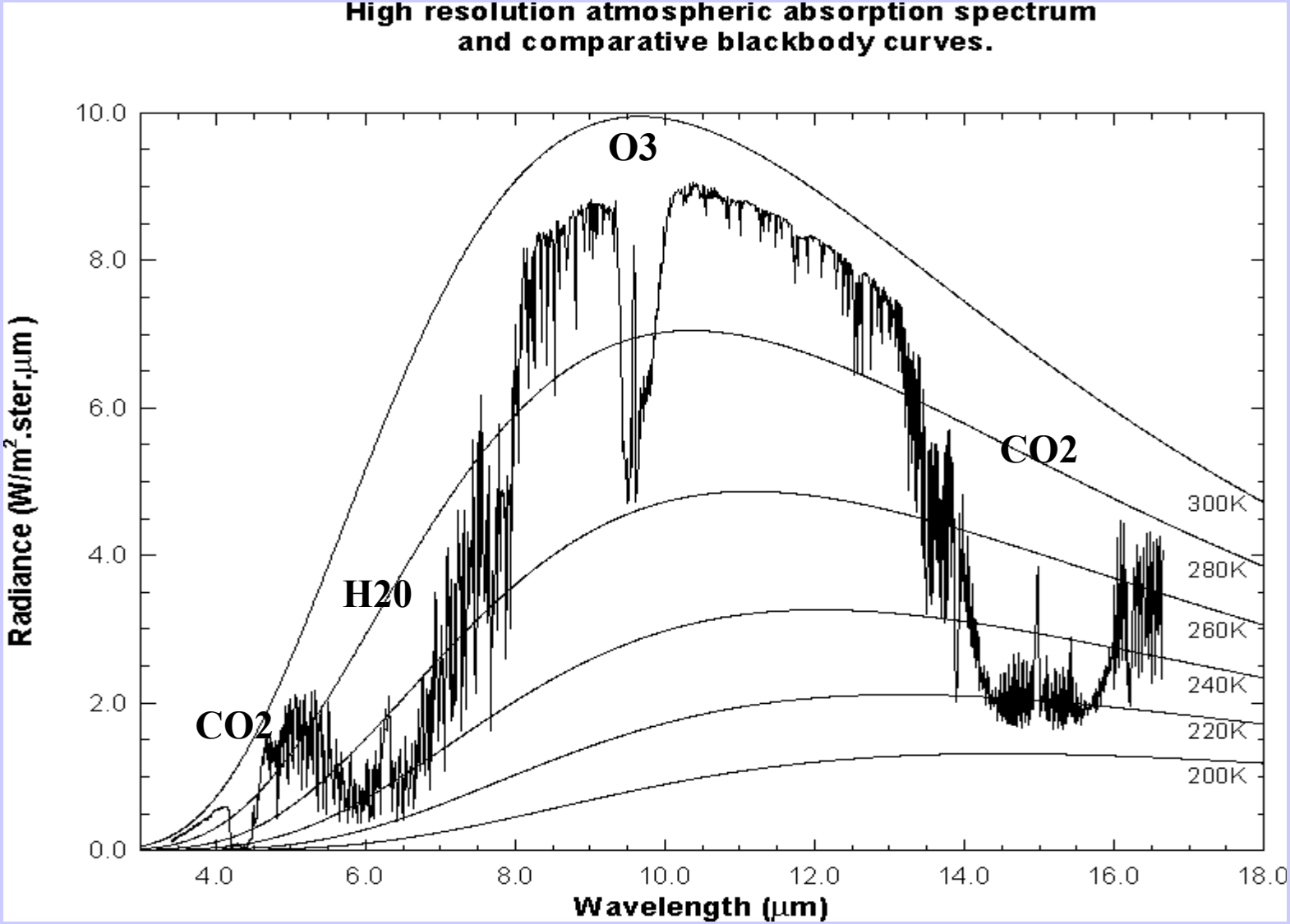

line broadening with pressure helps to explain weighting functions

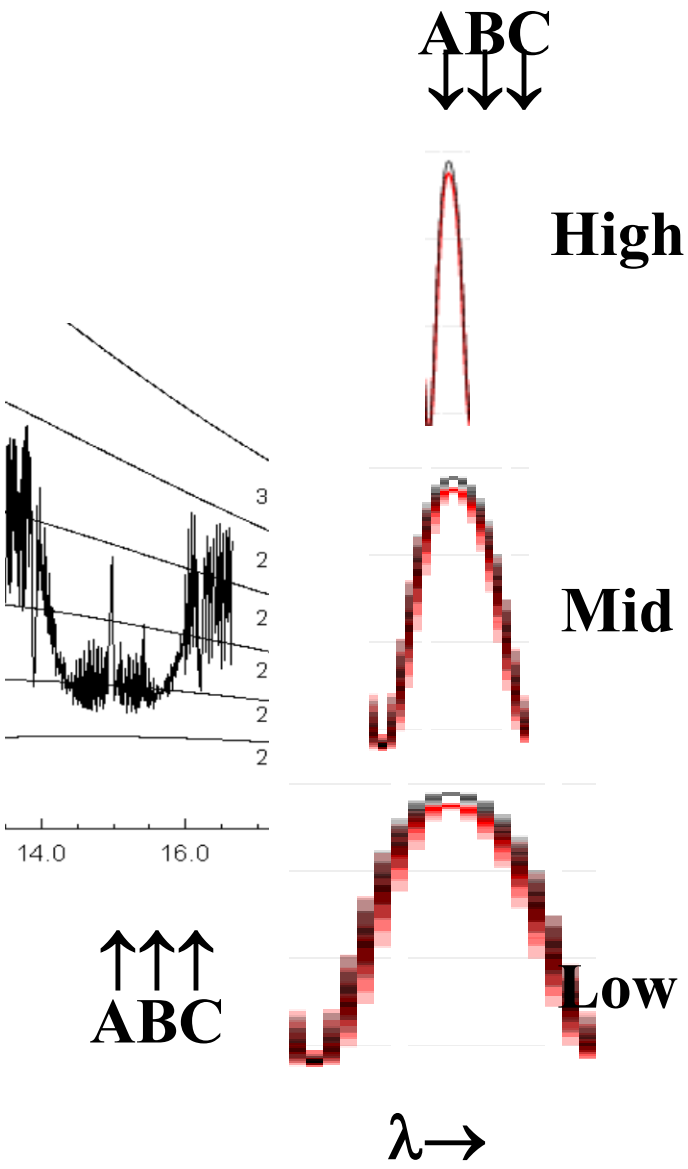

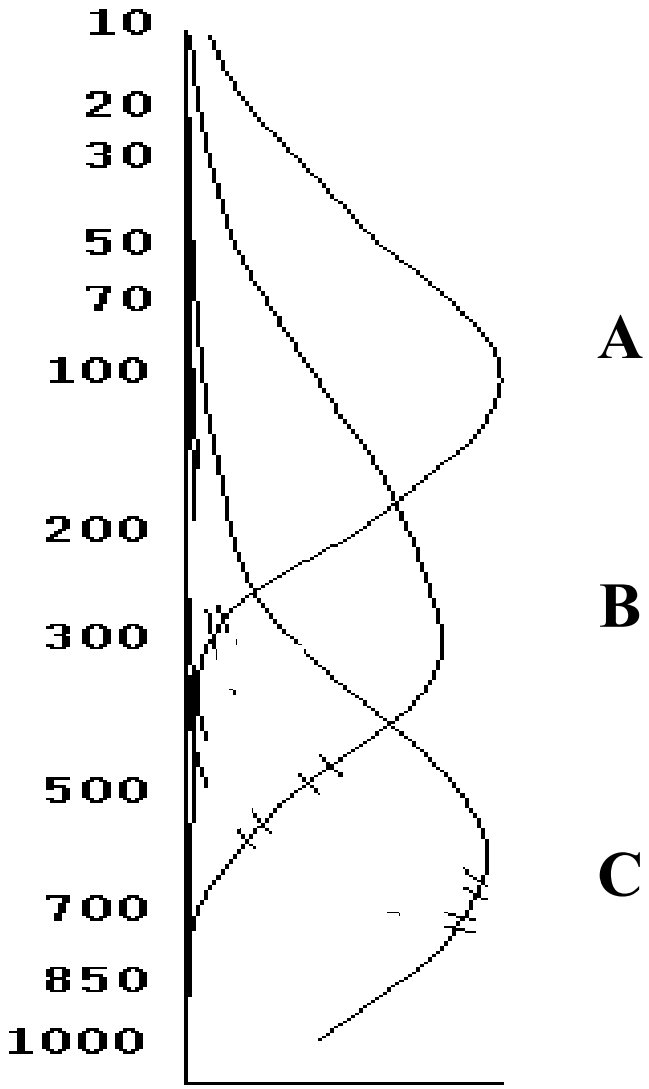

Fourier Transform Spectroscopy
Infrared Atmospheric Sounding

For a given water vapor spectral channel

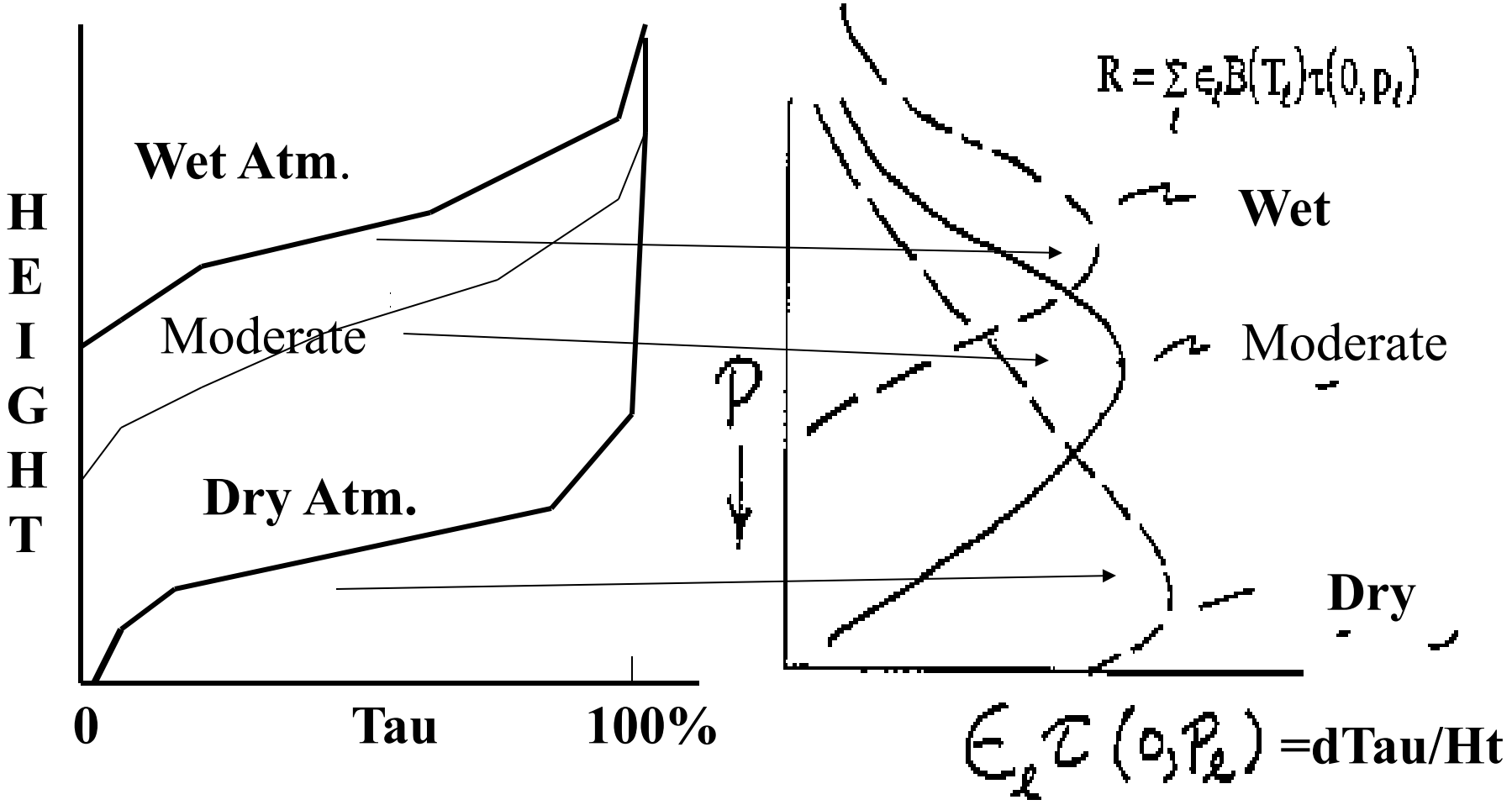

Fourier Transform Spectroscopy
Infrared Atmospheric Sounding

Wavelength Converts to Altitude

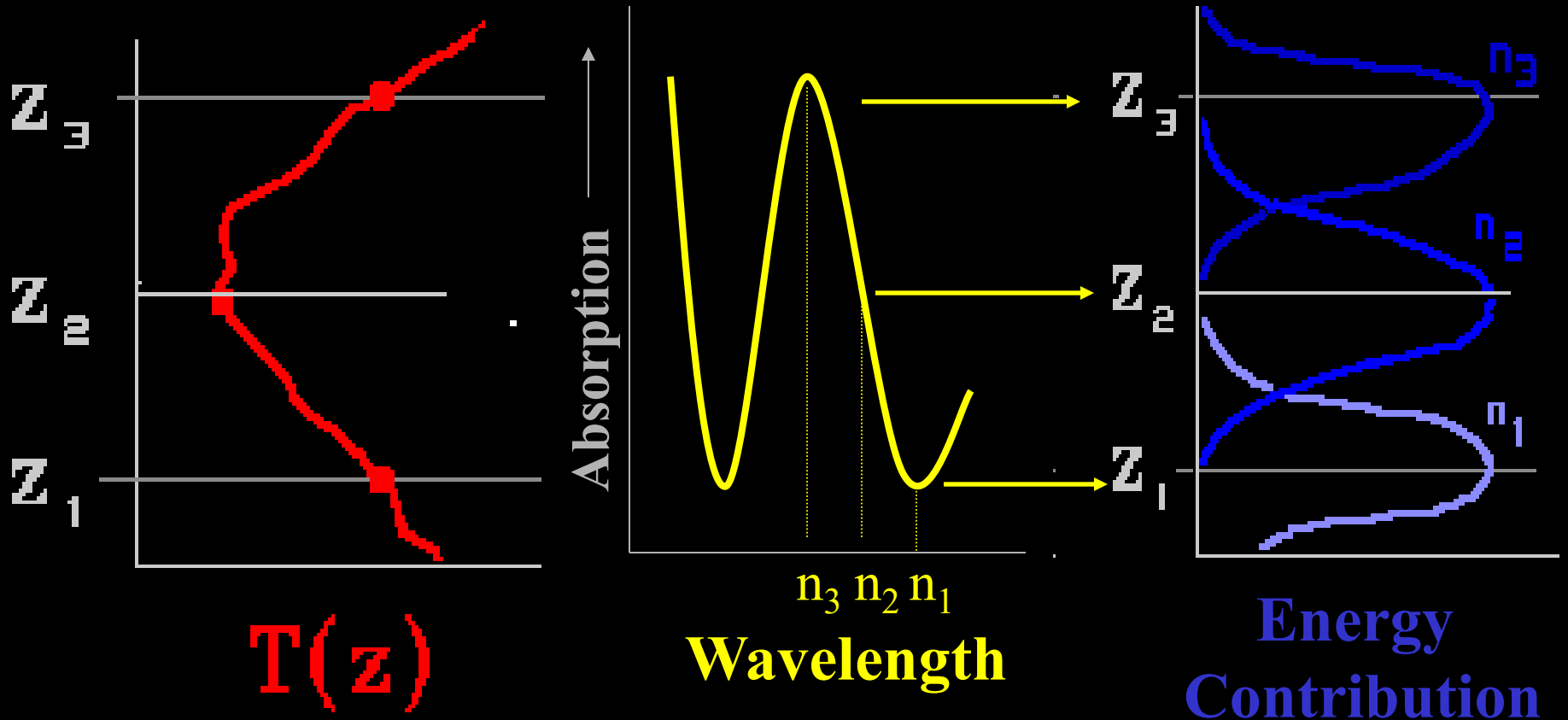

Earth emitted spectrum in CO2 sensitive 705 to 760 cm-1

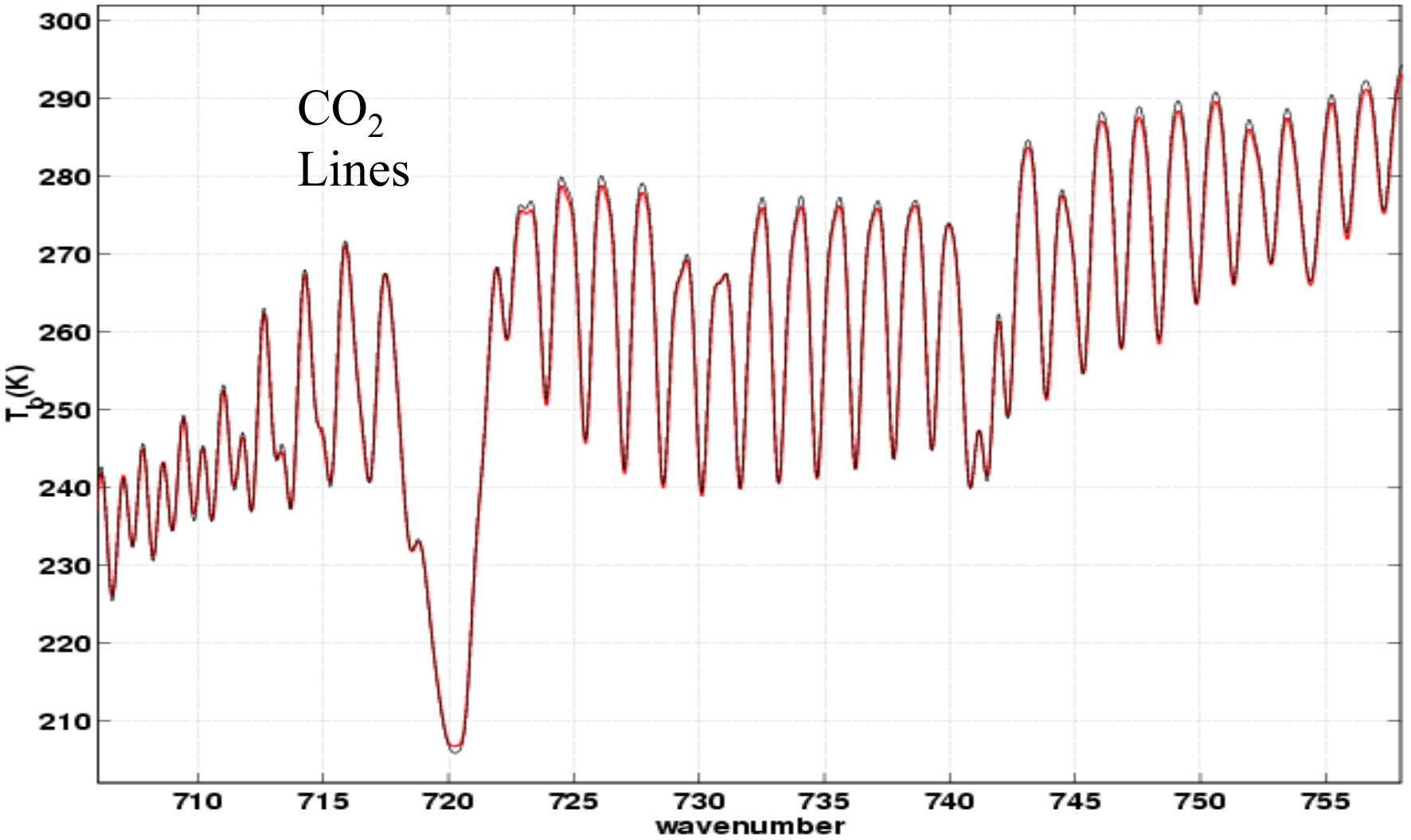

Associating relative weighting functions with the CO2 rotational bands

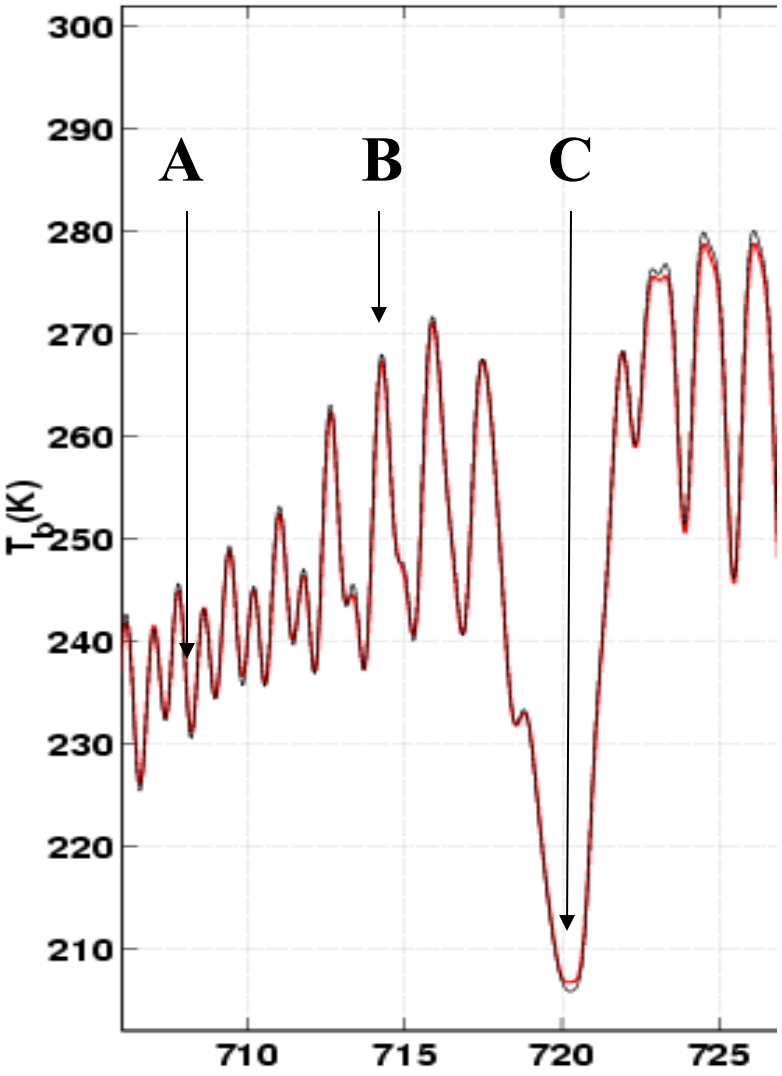

Wavenumber

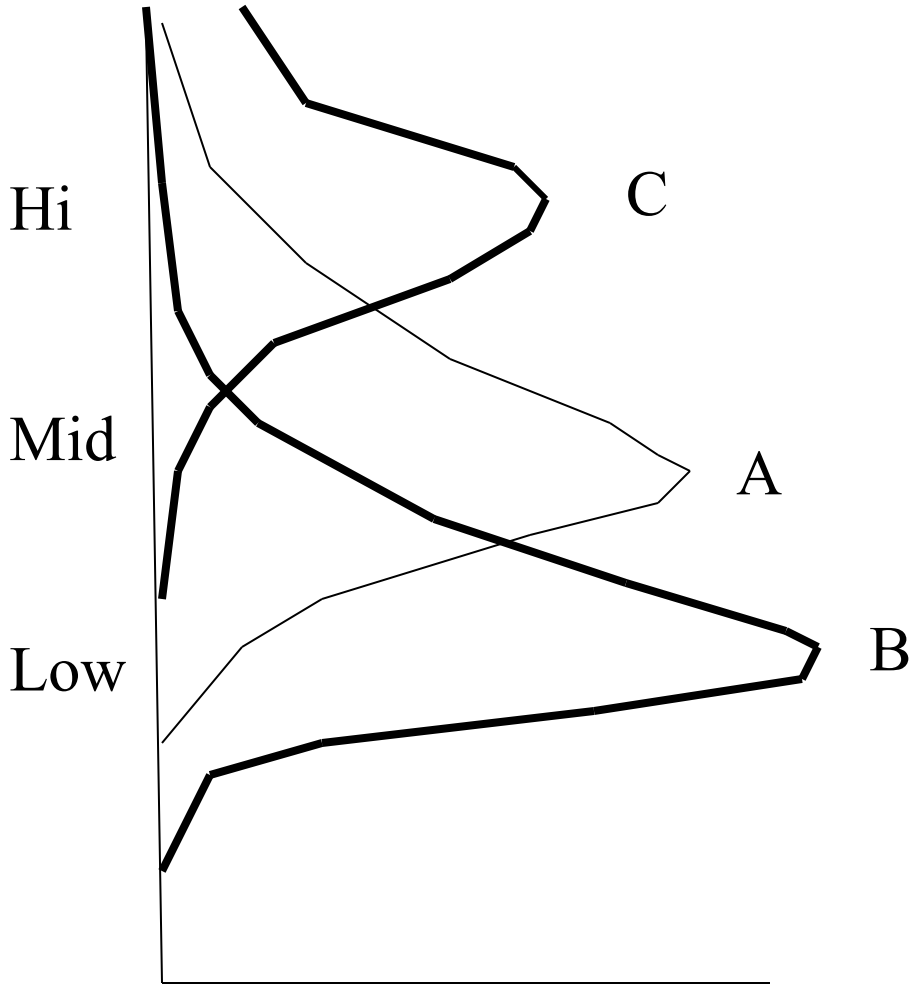

Weighting Function

Associating relative weighting functions with the CO2 rotational bands

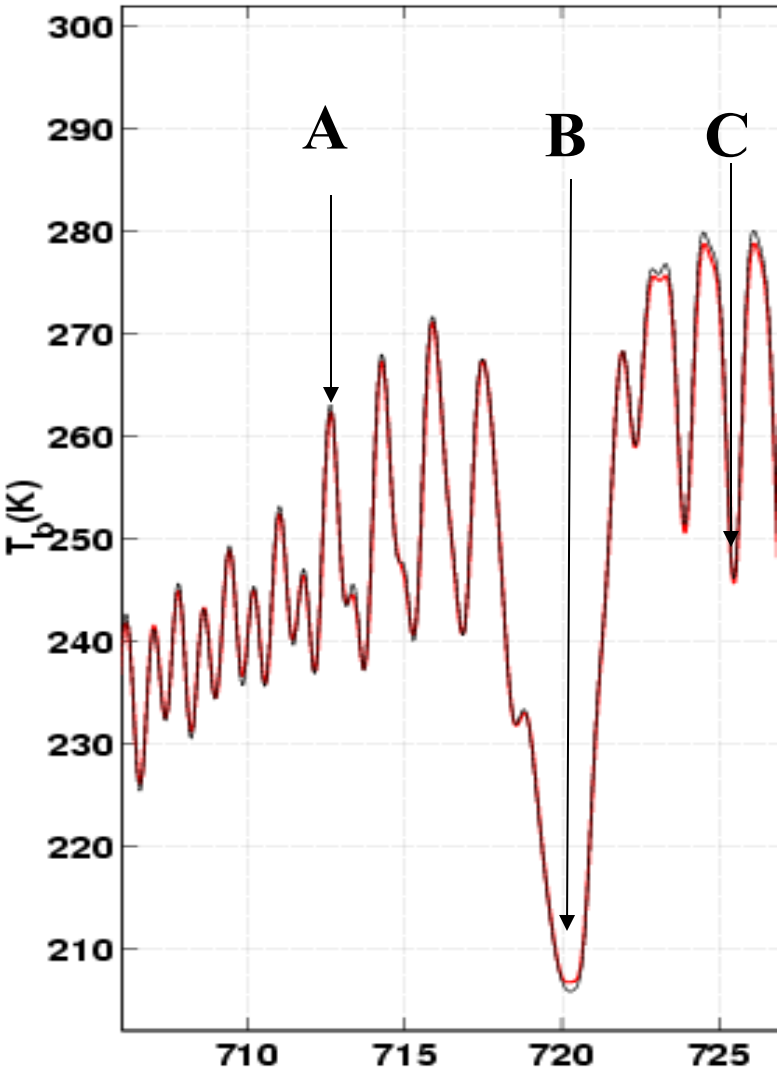

Wavenumber

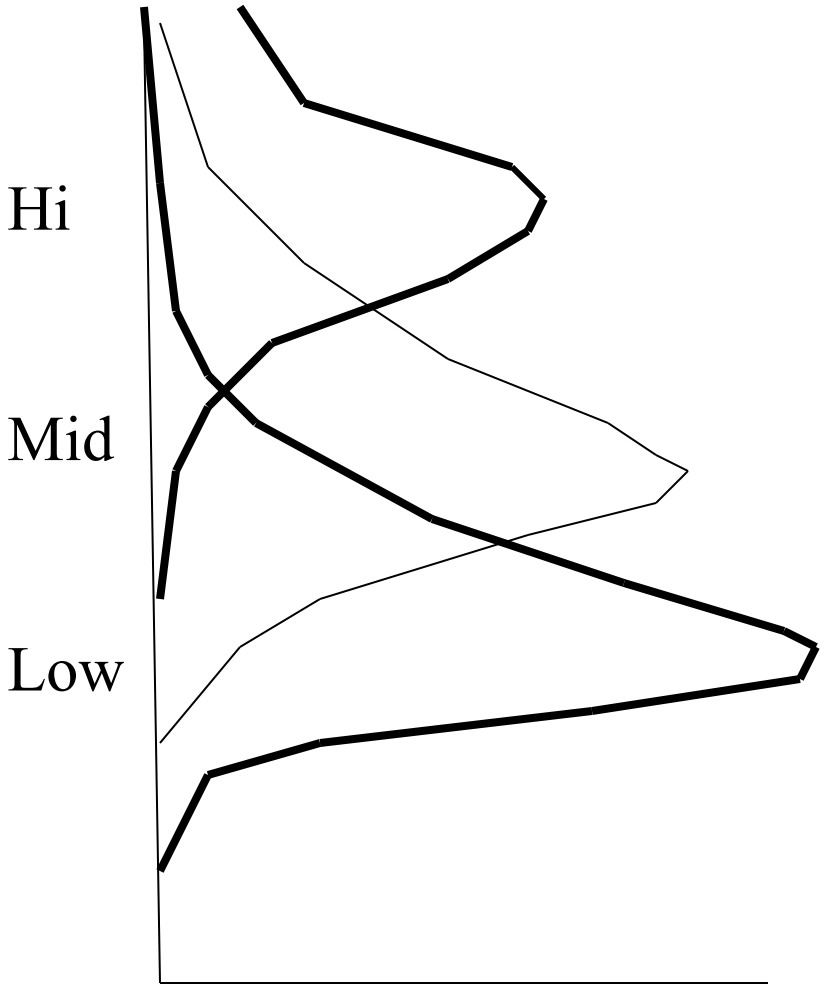

Weighting Function

Select

5

Selected Channel:

multi

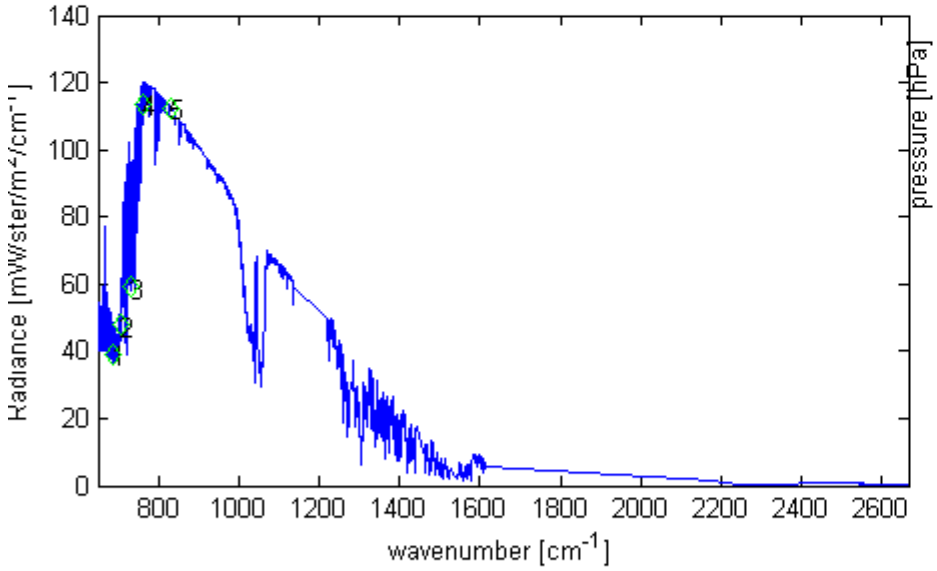

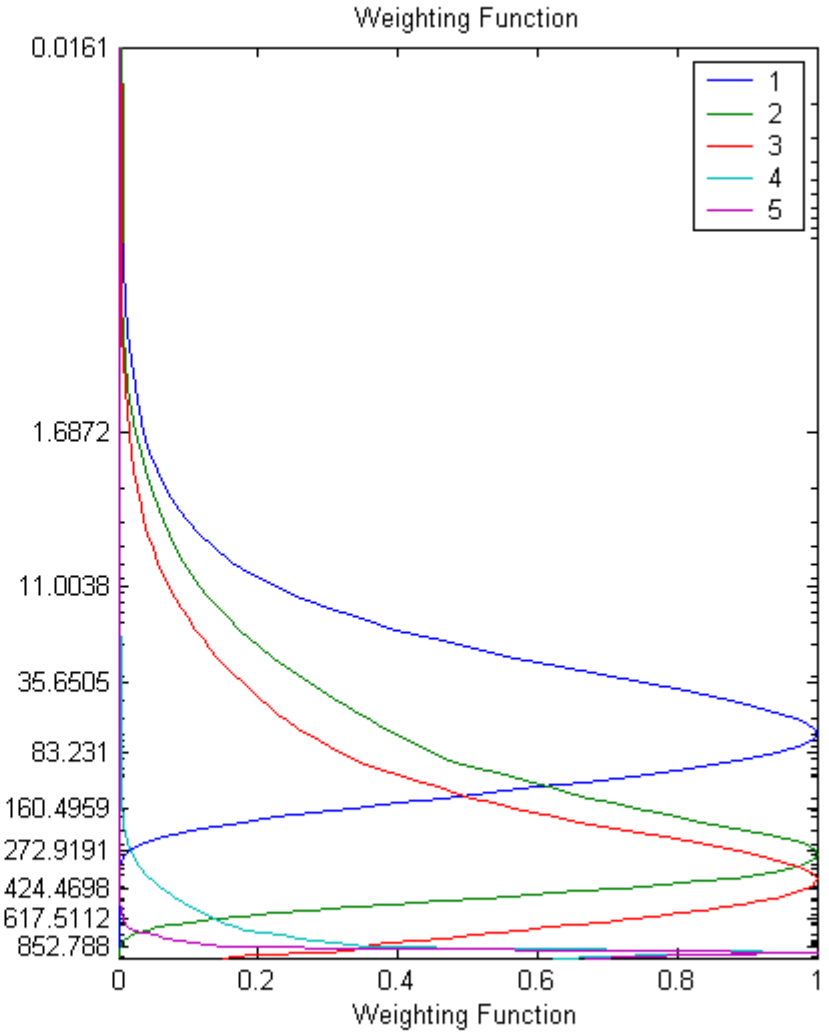

On-line off-line at 735 cm-1

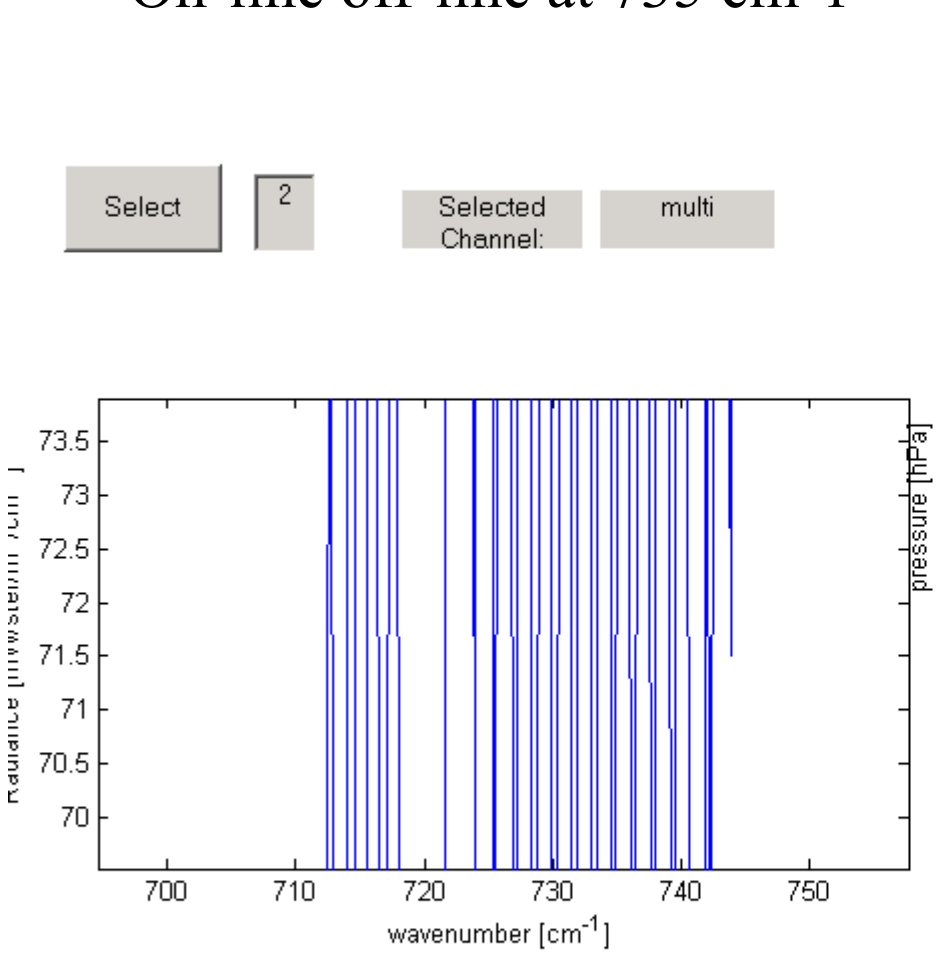

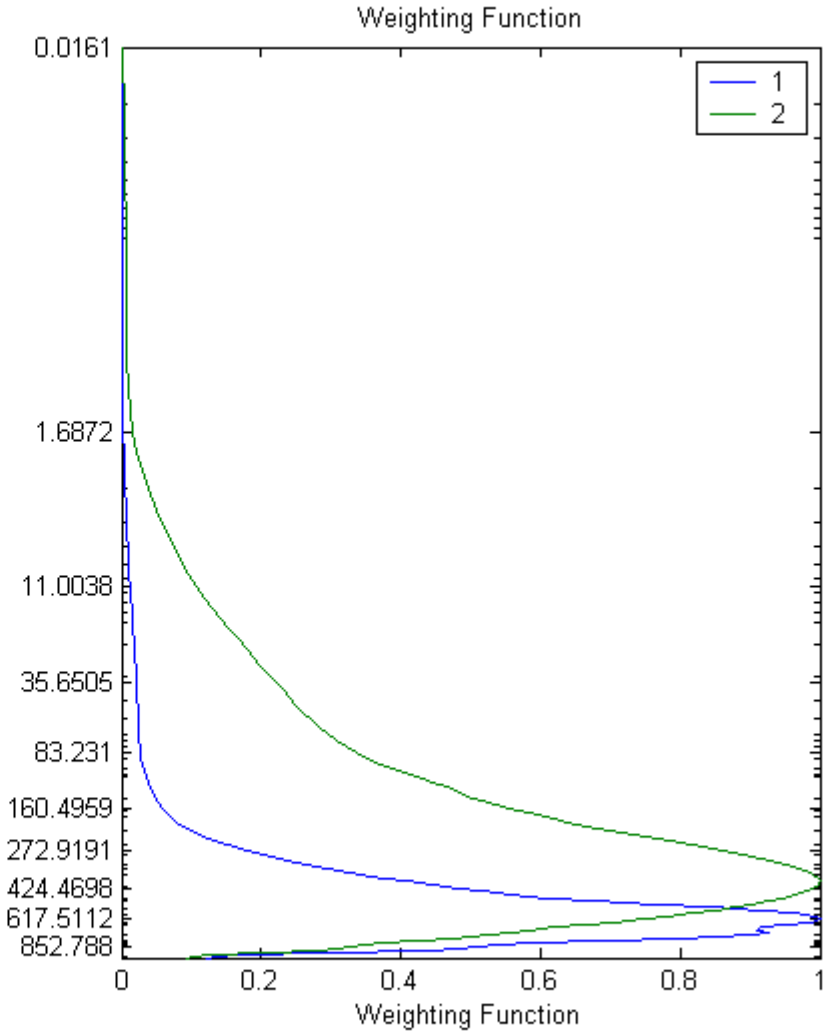

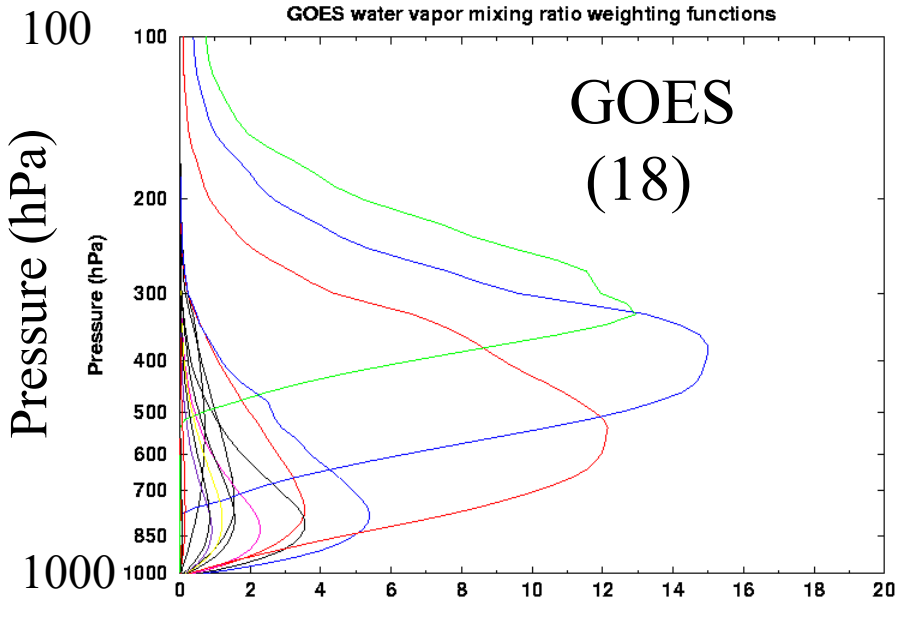

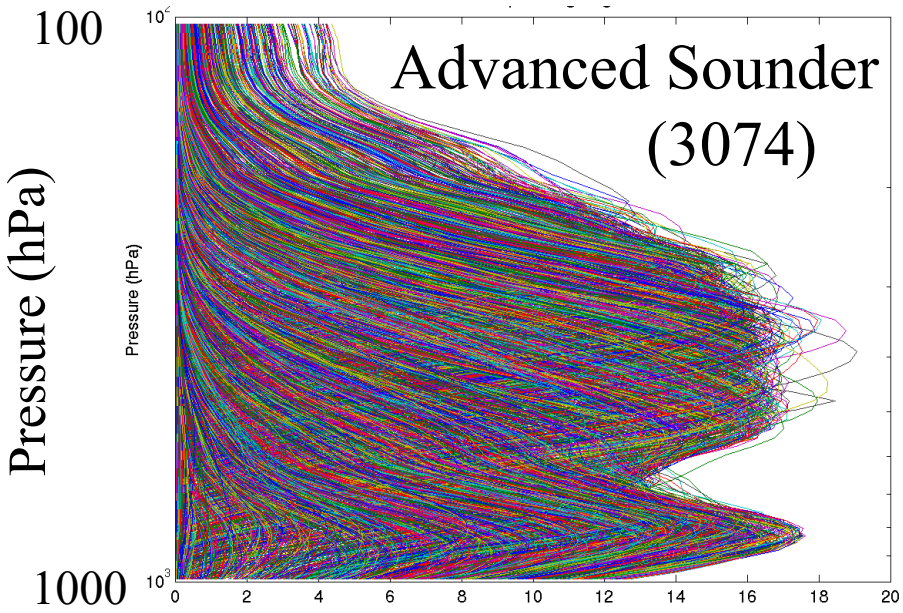

Moisture Weighting Functions

High spectral resolution advanced sounder will have more and sharper weighting functions compared to current GOES sounder. Retrievals will have better vertical resolution.

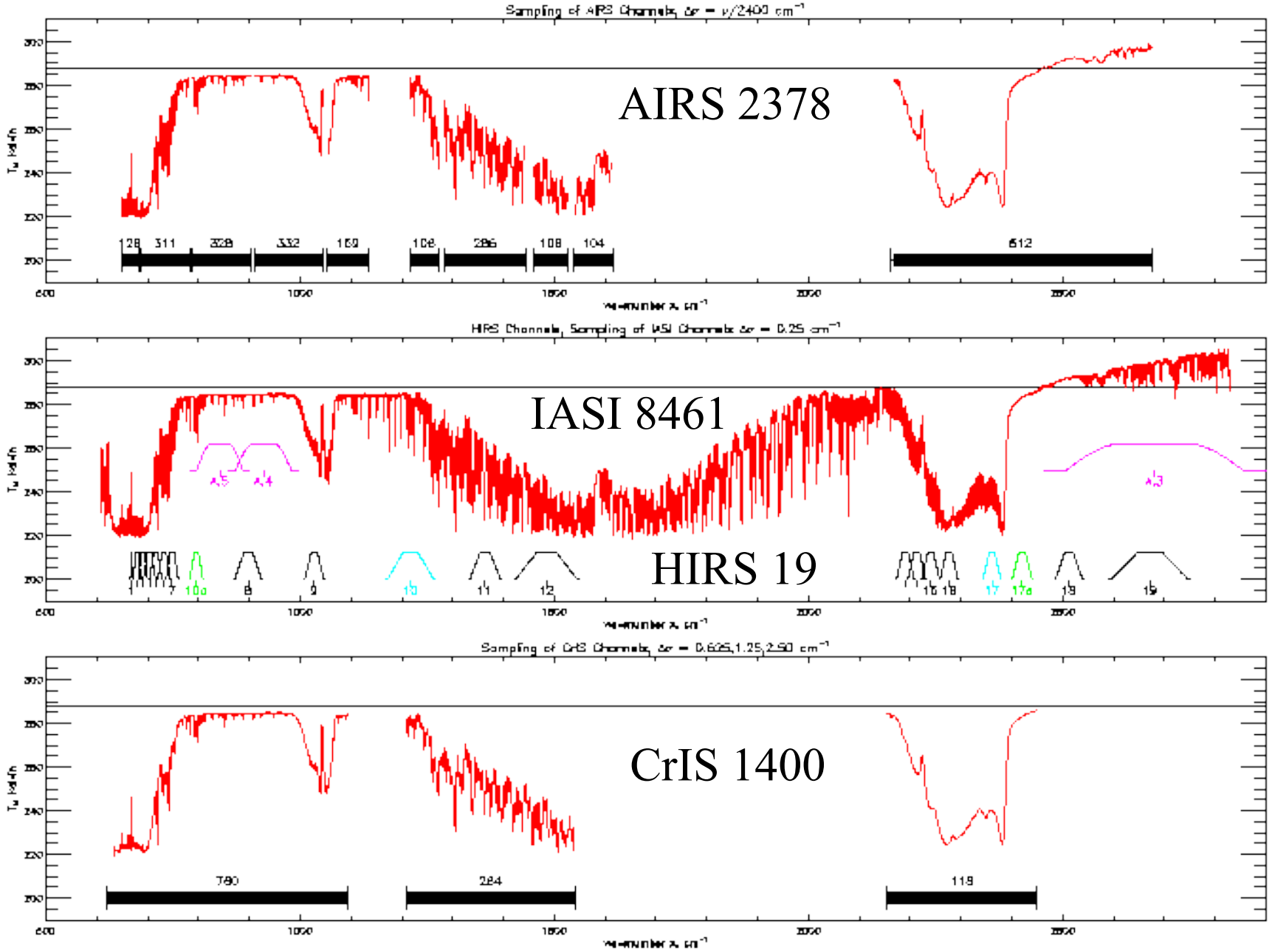
AIRS 2378
IASI 8461
HIRS 19
CrIS 1400

AIRS movie

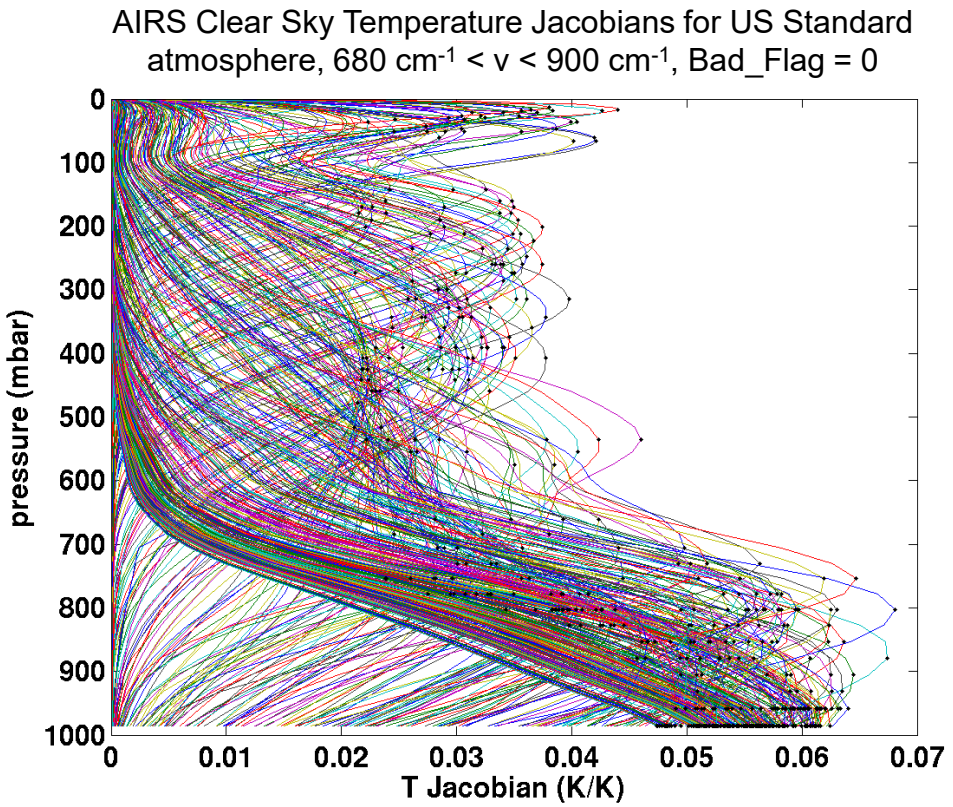

↙ Sort channels by pressure of Jacobian peaks

AIRS nighttime granules over CONUS, 6 Sept 2002

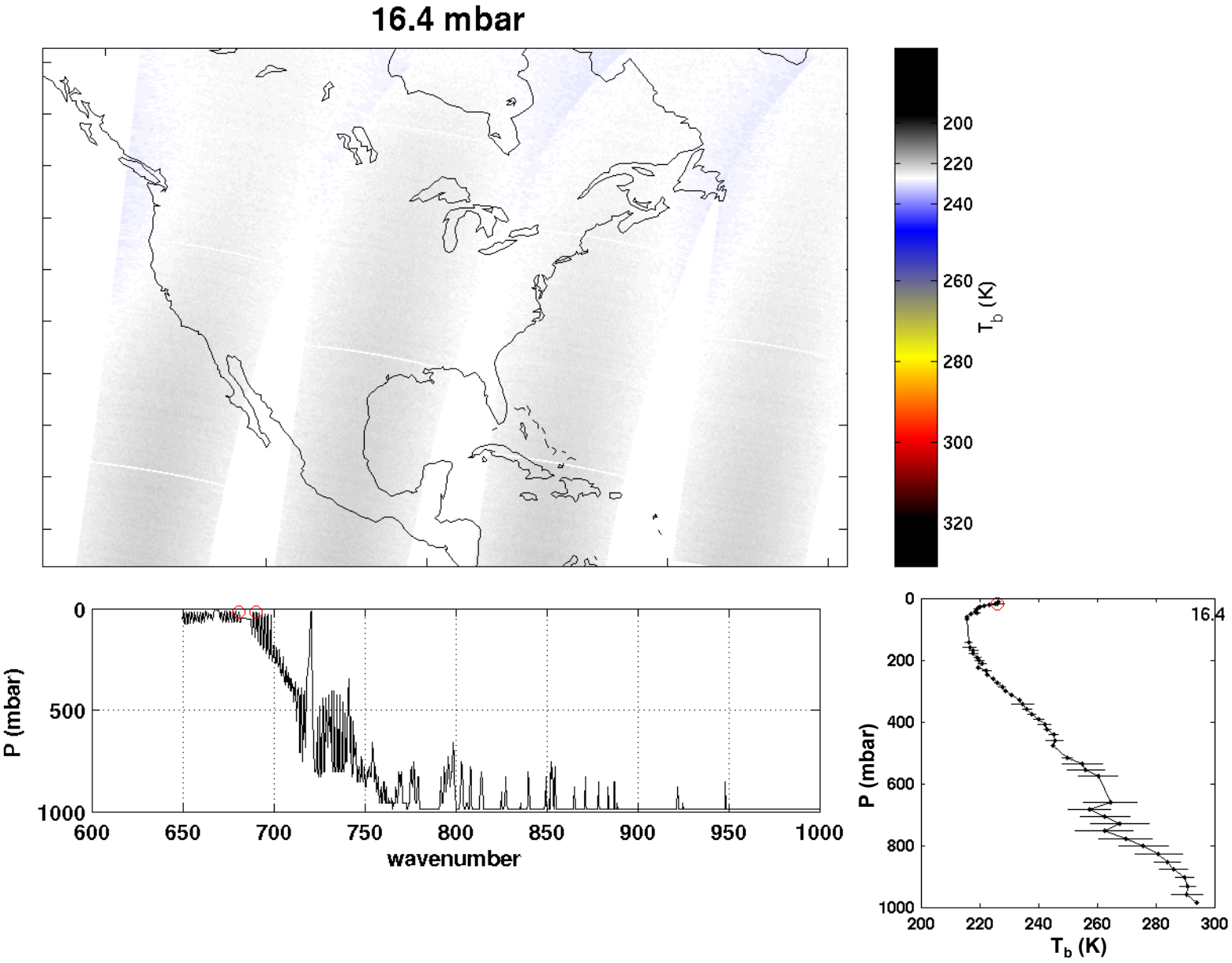

Mouse click or page down to start movie

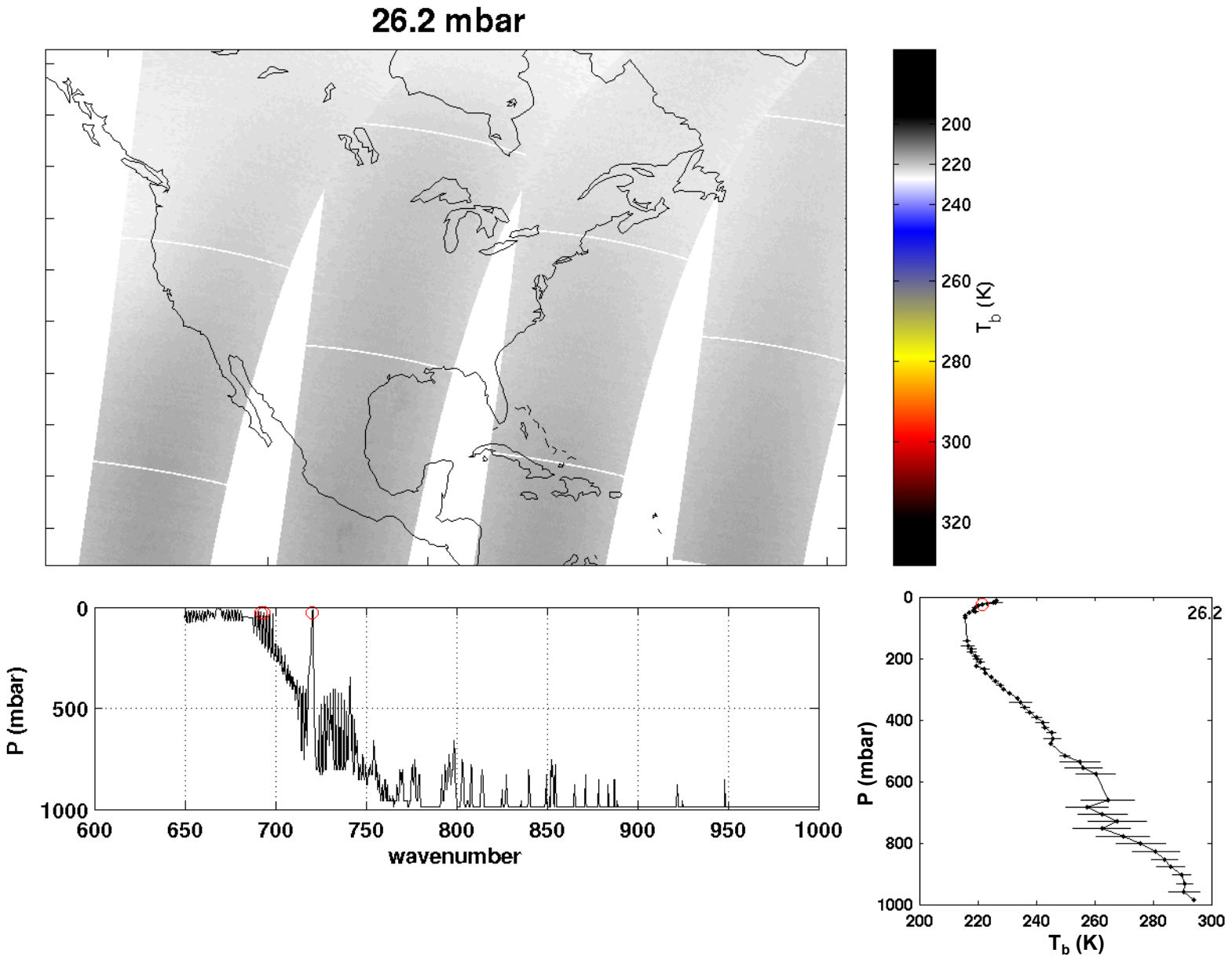
26.2 mbar
200
220
240
260
280
300
320
T_b (K)
P (mbar)
0
500
1000
600
650
700
750
800
850
900
950
1000
wavenumber
26.2
200
400
600
800
1000
220
240
260
280
300
T_b (K)

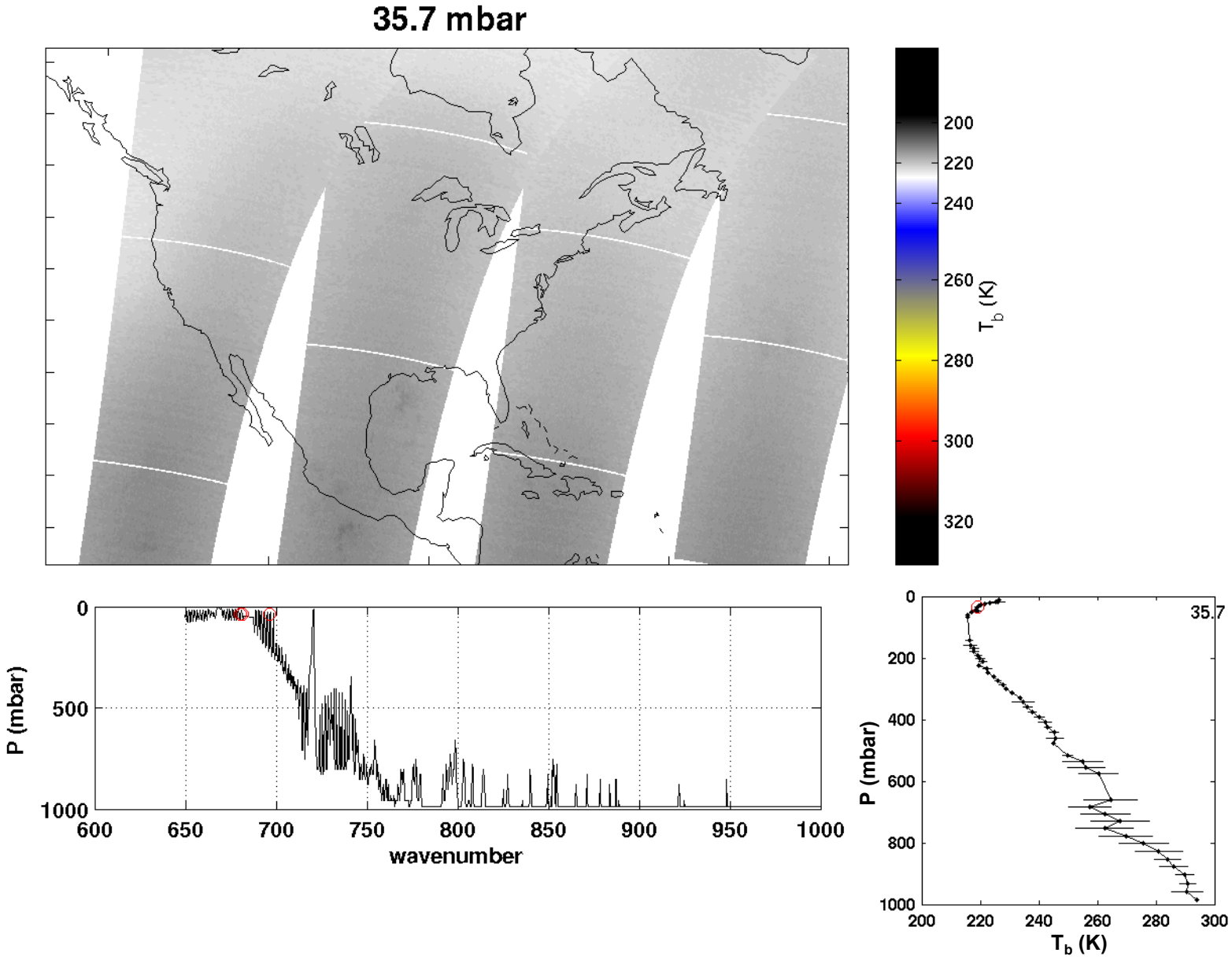
35.7 mbar
200
220
240
260
280
300
320
T_b (K)
P (mbar)
0
500
1000
600
650
700
750
800
850
900
950
1000
wavenumber
35.7
200
400
600
800
1000
220
240
260
280
300
T_b (K)

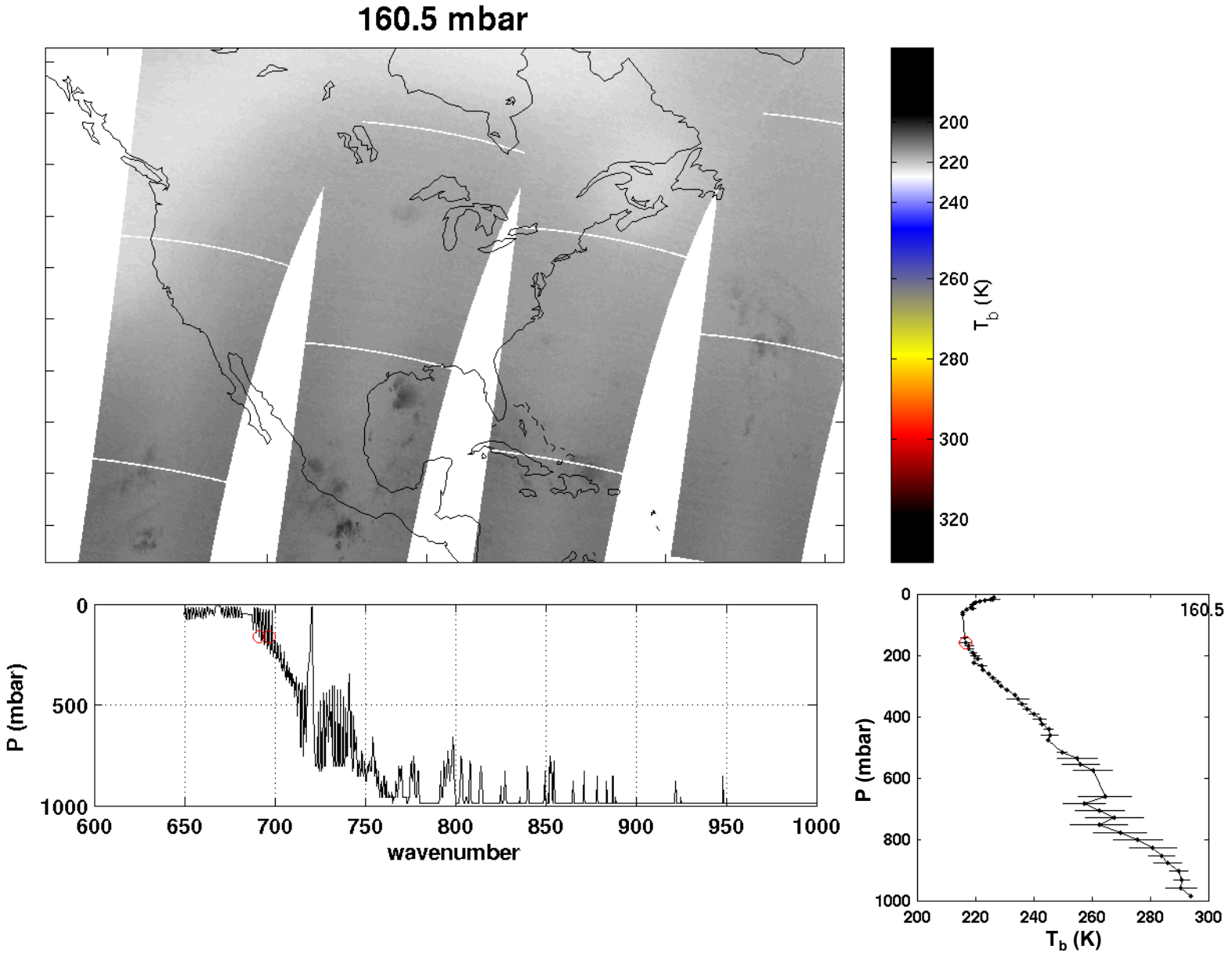
160.5 mbar
200
220
240
260
280
300
320
T_b (K)
P (mbar)
0
500
1000
600
650
700
750
800
850
900
950
1000
wavenumber
160.5
P (mbar)
0
200
400
600
800
1000
200
220
240
260
280
300
T_b (K)

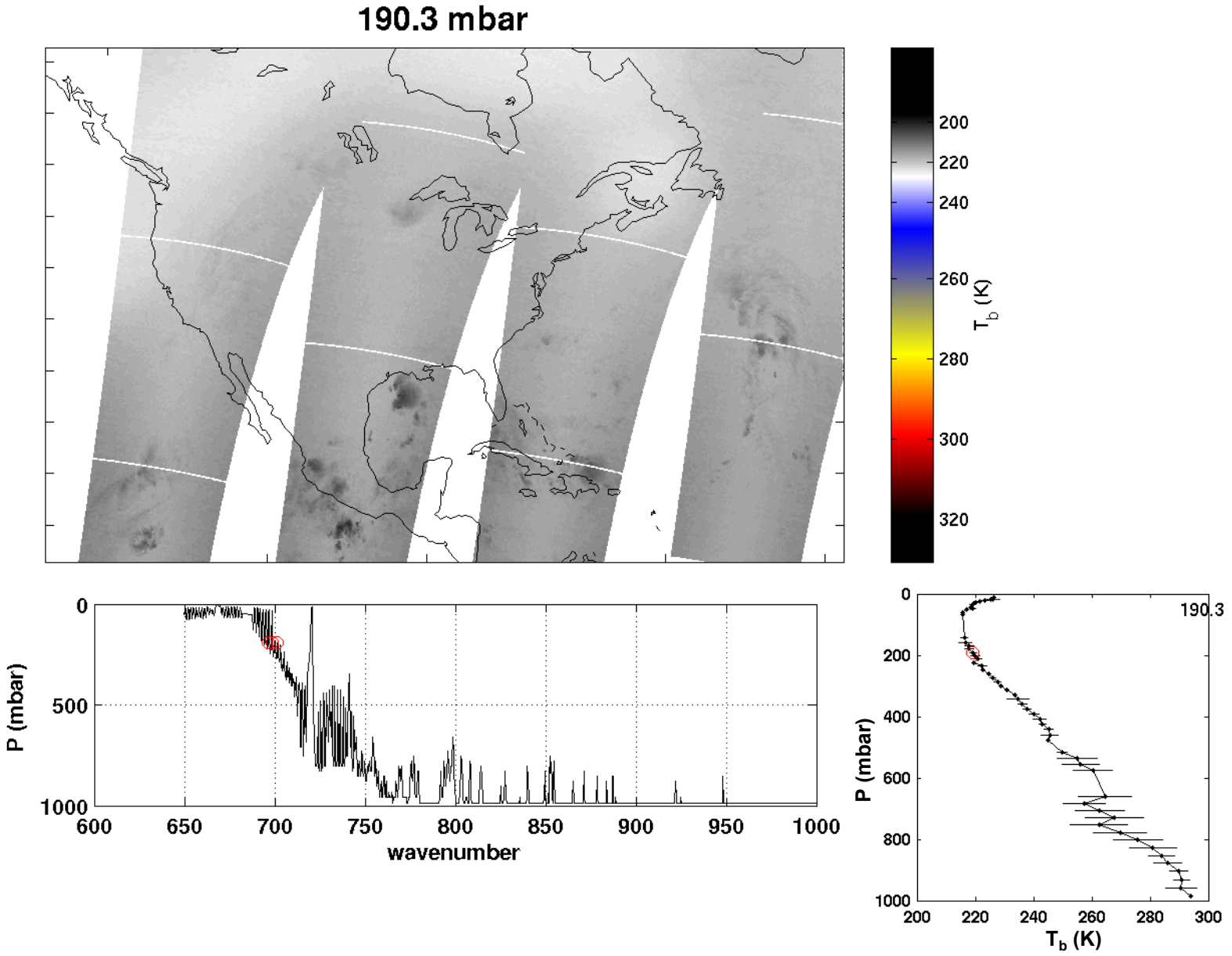
190.3 mbar
200
220
240
260
280
300
320
T_b (K)
0
500
1000
P (mbar)
600
650
700
750
800
850
900
950
1000
wavenumber
190.3
0
200
400
600
800
1000
P (mbar)
200
220
240
260
280
300
T_b (K)

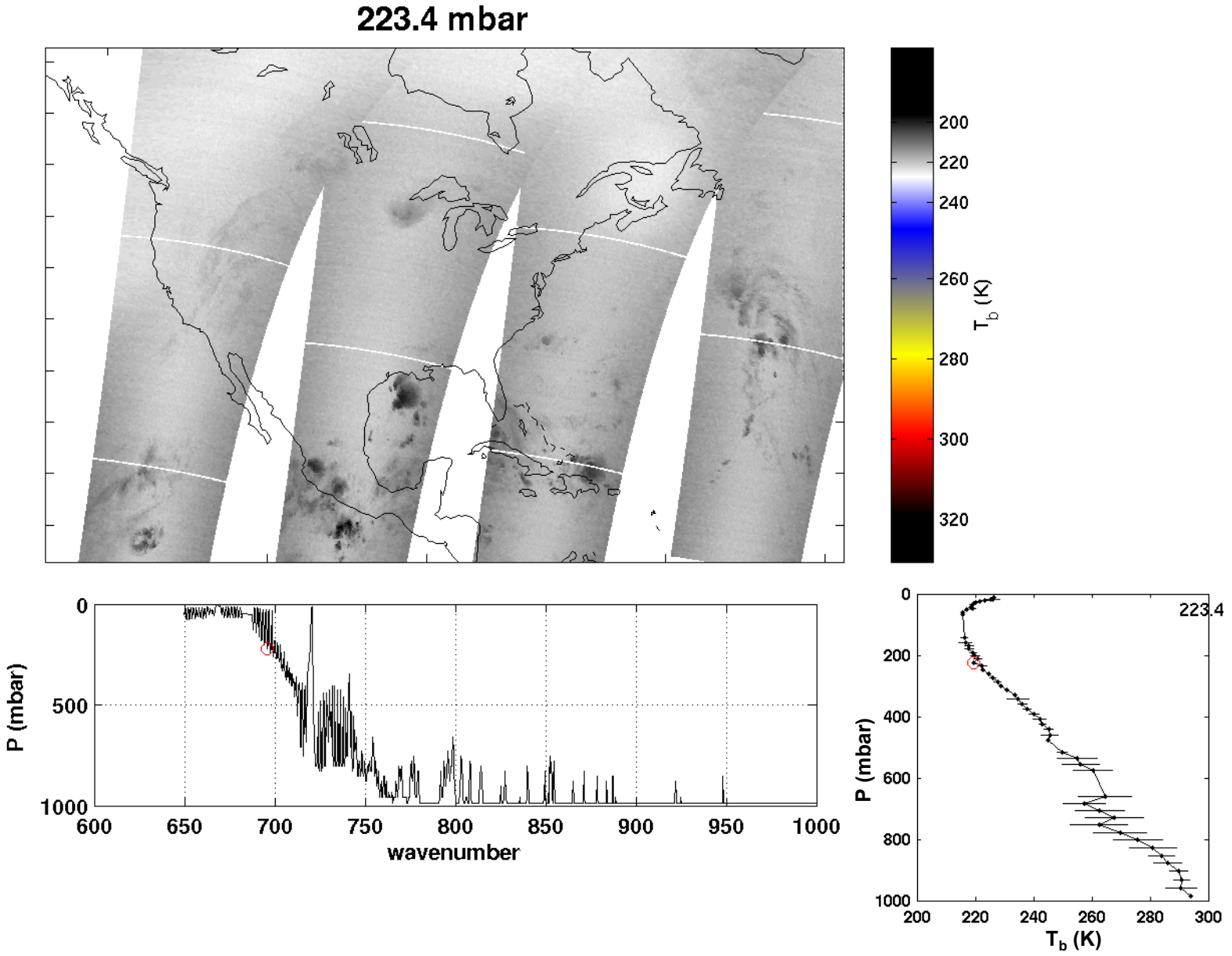
223.4 mbar
200
220
240
260
280
300
320
T_b (K)
0
500
1000
P (mbar)
600
650
700
750
800
850
900
950
1000
wavenumber
223.4
0
200
400
600
800
1000
P (mbar)
200
220
240
260
280
300
T_b (K)

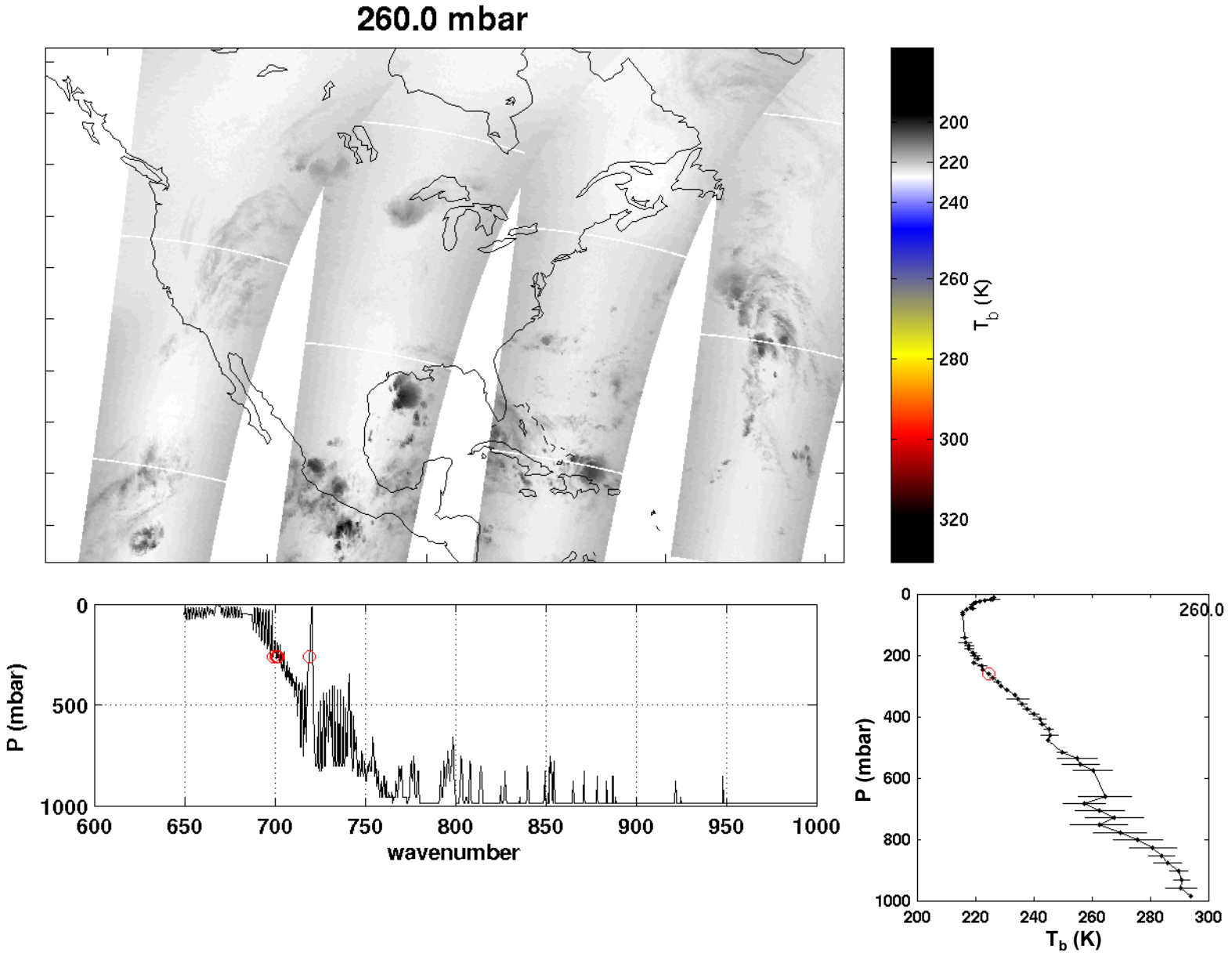
260.0 mbar
200
220
240
260
280
300
320
T_b (K)
P (mbar)
0
500
1000
600
650
700
750
800
850
900
950
1000
wavenumber
260.0
P (mbar)
0
200
400
600
800
1000
200
220
240
260
280
300
T_b (K)

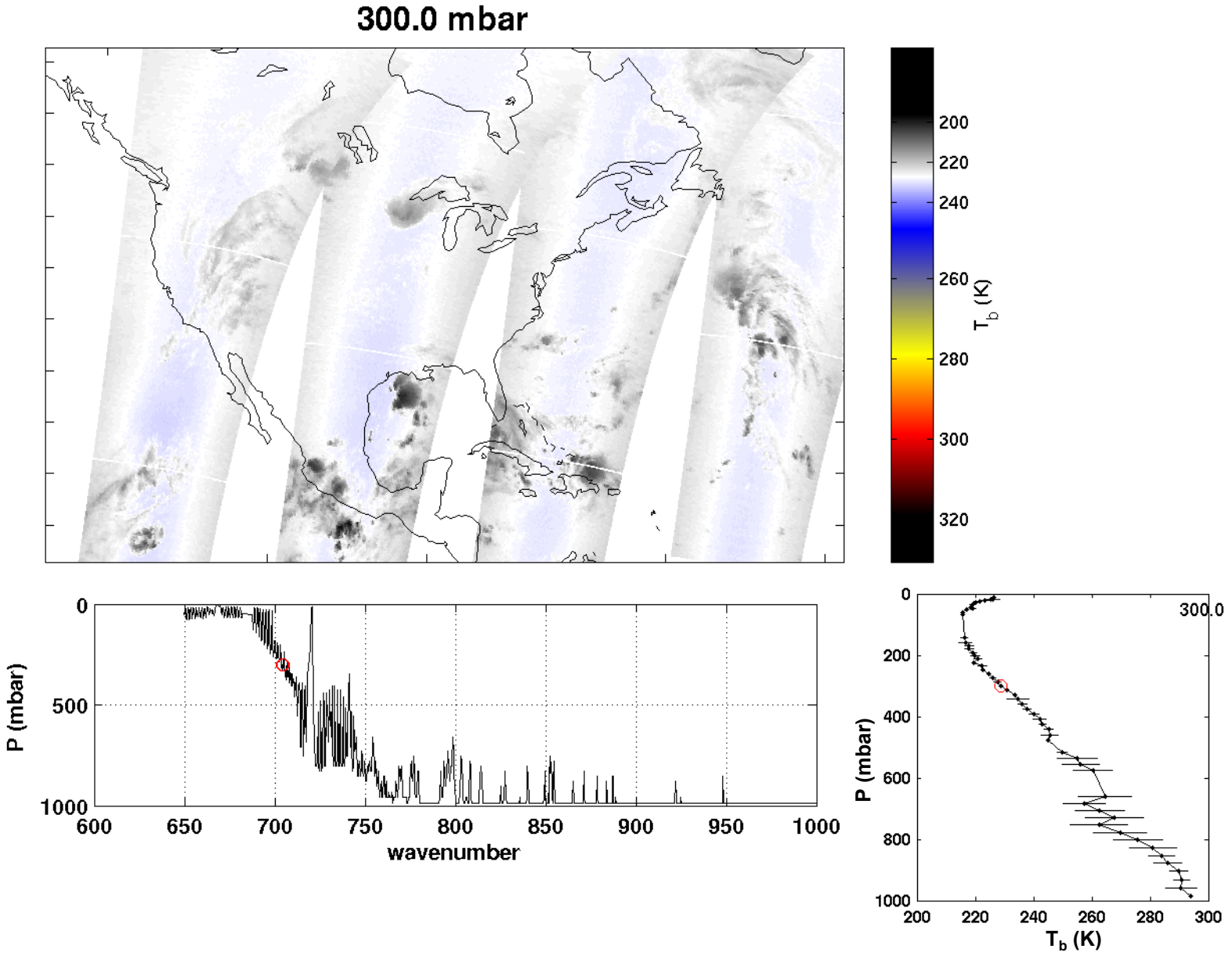
300.0 mbar
200
220
240
260
280
300
320
T_b (K)
P (mbar)
0
500
1000
600
650
700
750
800
850
900
950
1000
wavenumber
300.0
200
400
600
800
1000
200
220
240
260
280
300
P (mbar)
T_b (K)

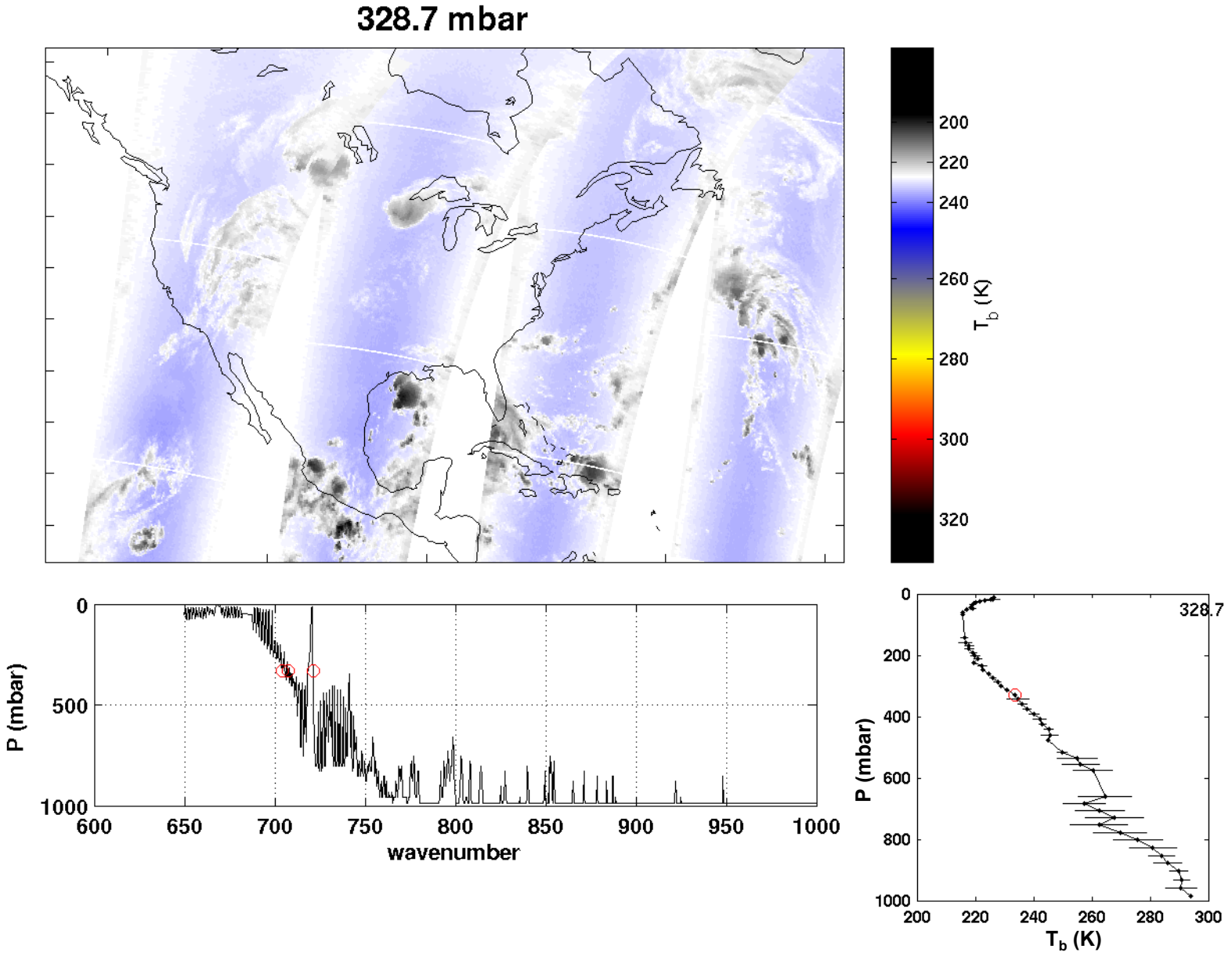
328.7 mbar
200
220
240
260
280
300
320
T_b (K)
P (mbar)
0
500
1000
600
650
700
750
800
850
900
950
1000
wavenumber
328.7
P (mbar)
0
200
400
600
800
1000
200
220
240
260
280
300
T_b (K)

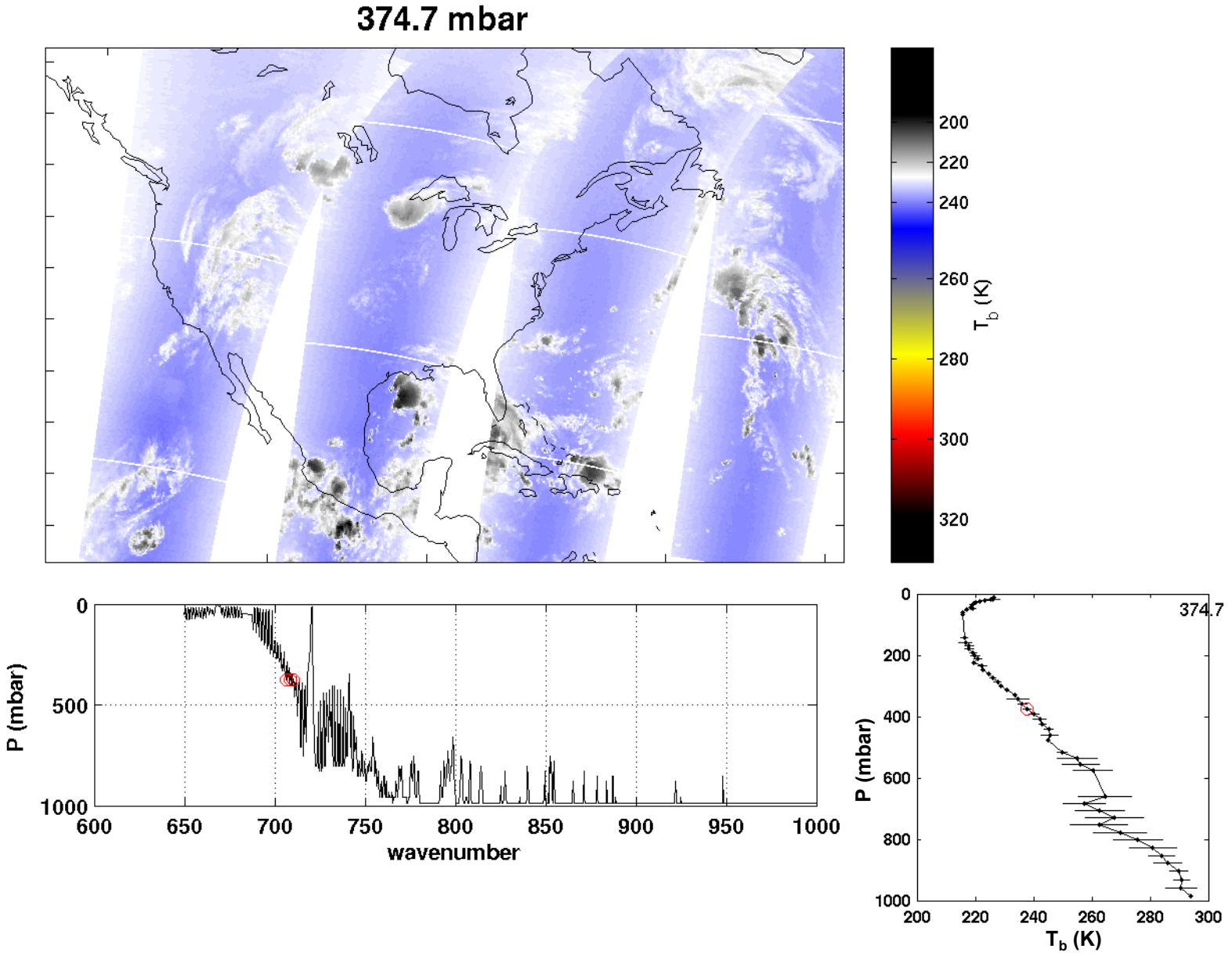
374.7 mbar
200
220
240
260
280
300
320
T_b (K)
P (mbar)
0
500
1000
600
650
700
750
800
850
900
950
1000
wavenumber
374.7
P (mbar)
0
200
400
600
800
1000
200
220
240
260
280
300
T_b (K)

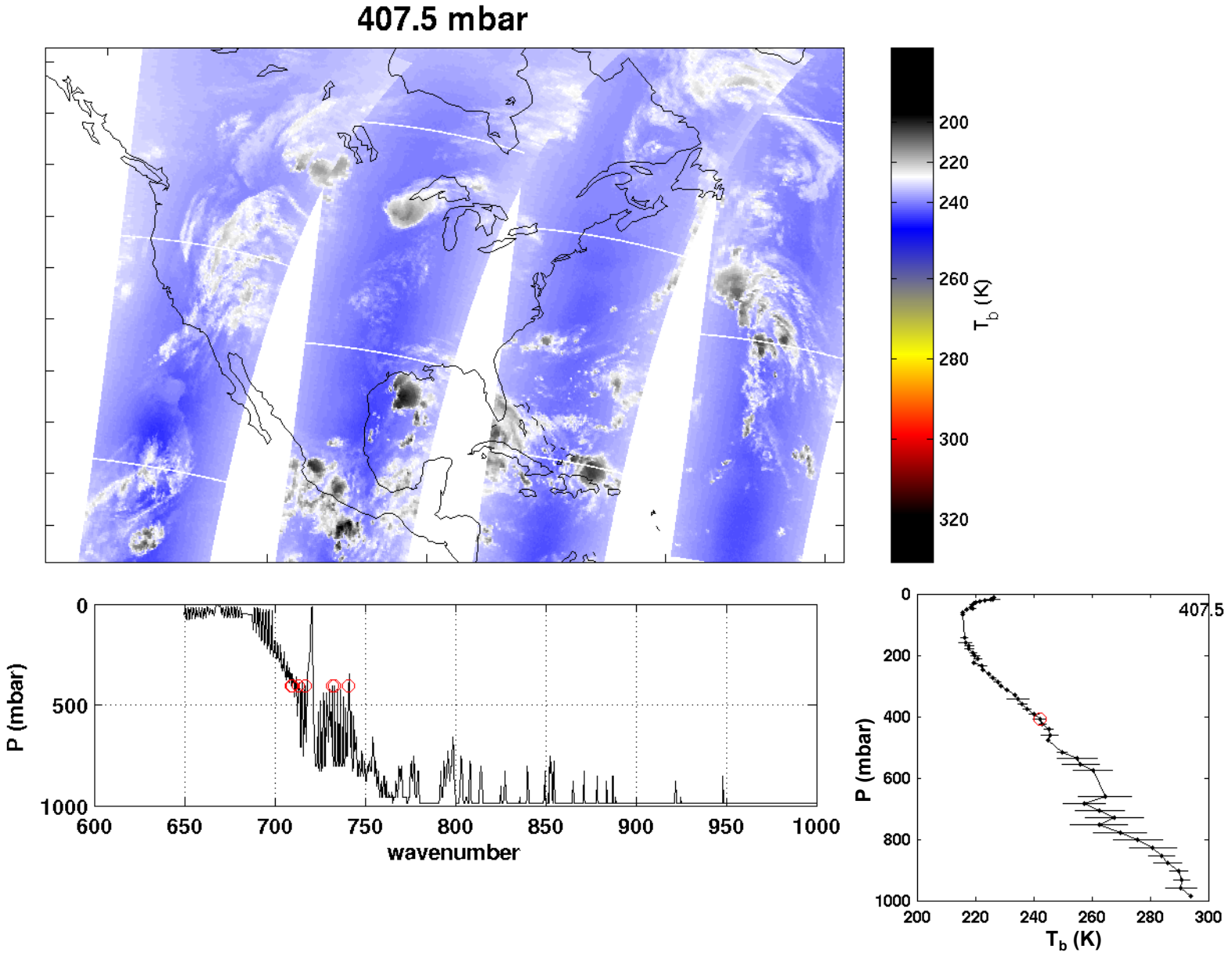
407.5 mbar
200
220
240
260
280
300
320
T_b (K)
P (mbar)
0
500
1000
600
650
700
750
800
850
900
950
1000
wavenumber
407.5
P (mbar)
0
200
400
600
800
1000
200
220
240
260
280
300
T_b (K)

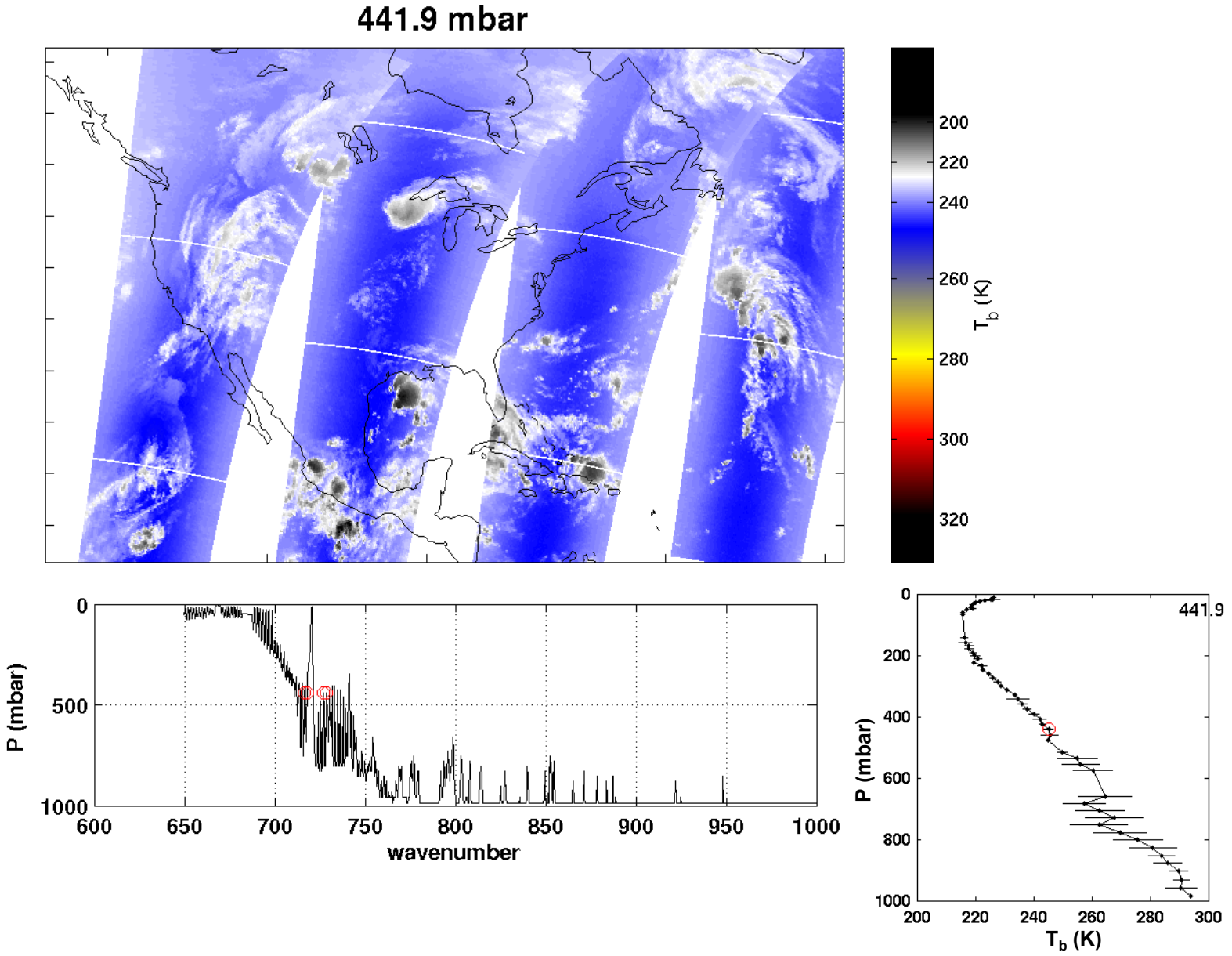
441.9 mbar
200
220
240
260
280
300
320
T_b (K)
P (mbar)
0
500
1000
600
650
700
750
800
850
900
950
1000
wavenumber
441.9
P (mbar)
0
200
400
600
800
1000
200
220
240
260
280
300
T_b (K)

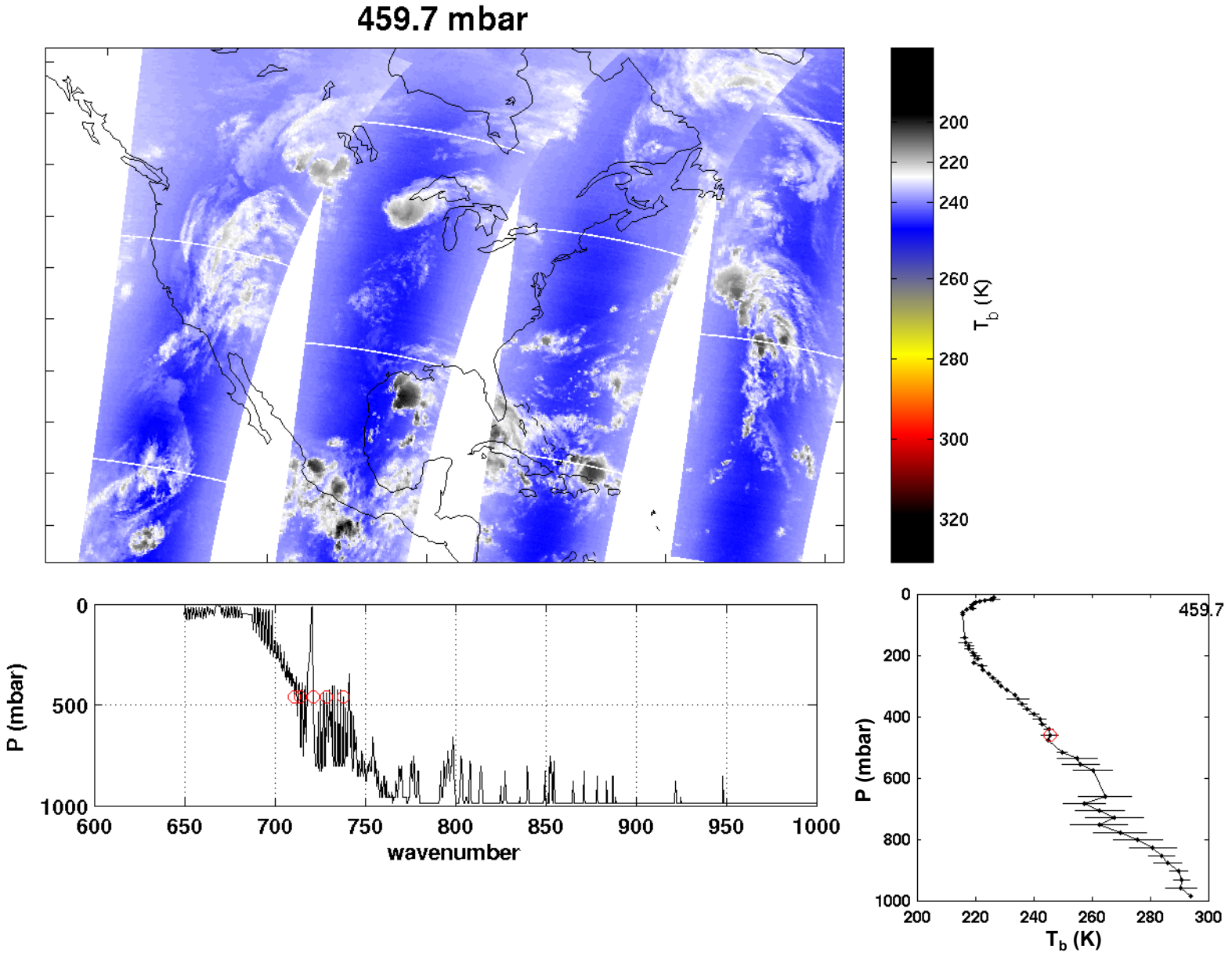
459.7 mbar
200
220
240
260
280
300
320
T_b (K)
0
500
1000
P (mbar)
600
650
700
750
800
850
900
950
1000
wavenumber
459.7
0
200
400
600
800
1000
P (mbar)
200
220
240
260
280
300
T_b (K)

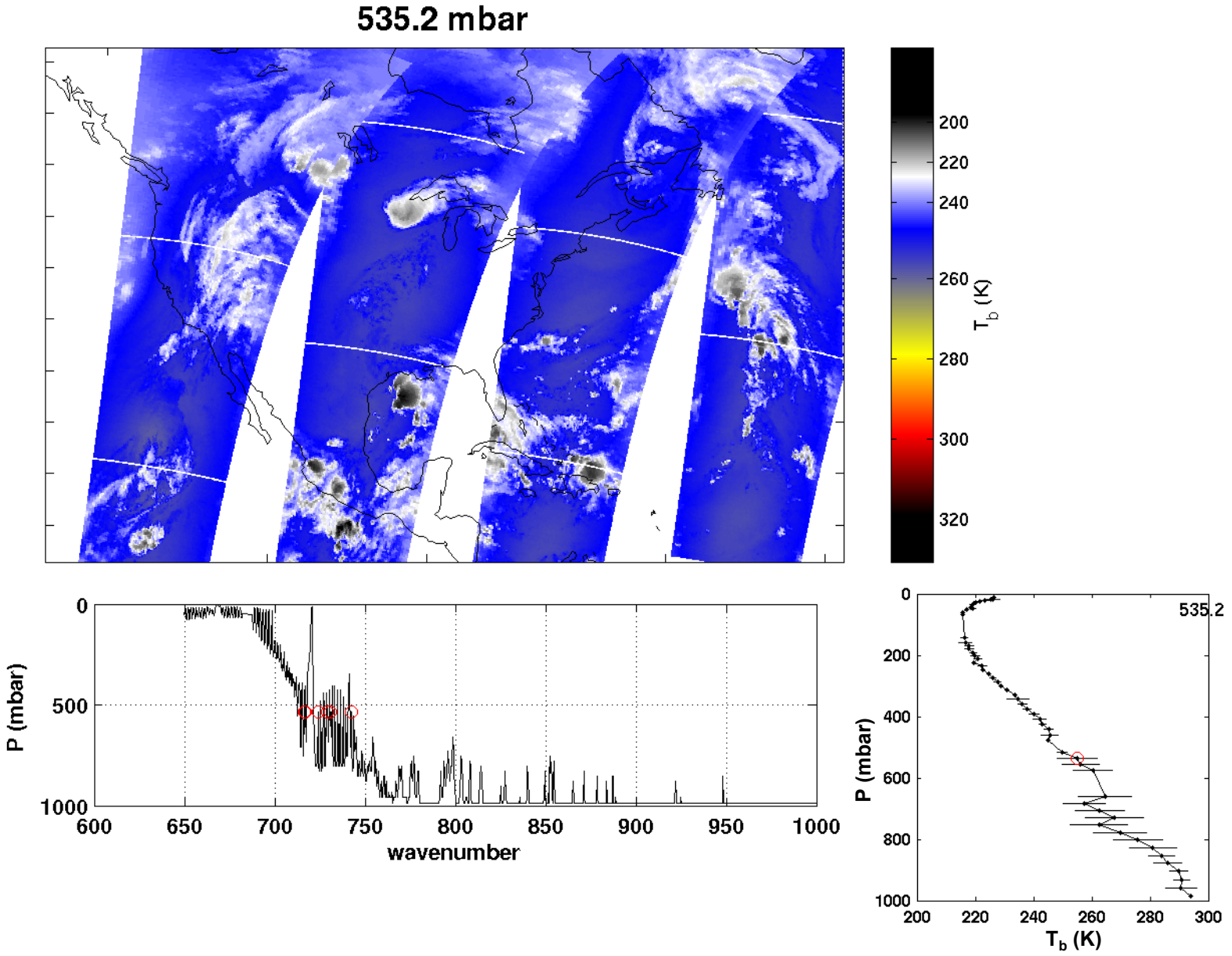
535.2 mbar
200
220
240
260
280
300
320
T_b (K)
0
500
1000
P (mbar)
600
650
700
750
800
850
900
950
1000
wavenumber
535.2
0
200
400
600
800
1000
P (mbar)
200
220
240
260
280
300
T_b (K)

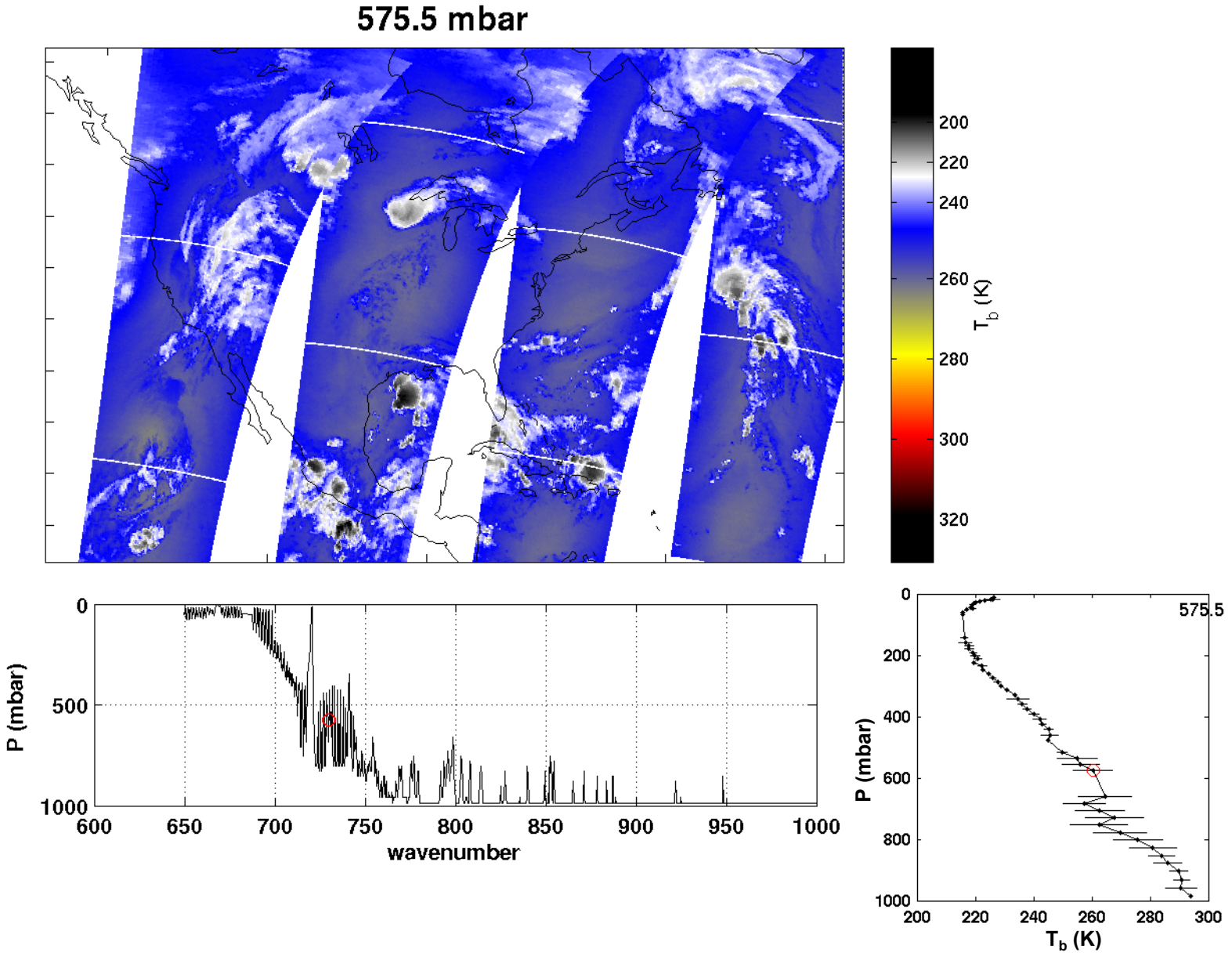
575.5 mbar
200
220
240
260
280
300
320
T_b (K)
0
500
1000
P (mbar)
600
650
700
750
800
850
900
950
1000
wavenumber
575.5
0
200
400
600
800
1000
P (mbar)
200
220
240
260
280
300
T_b (K)

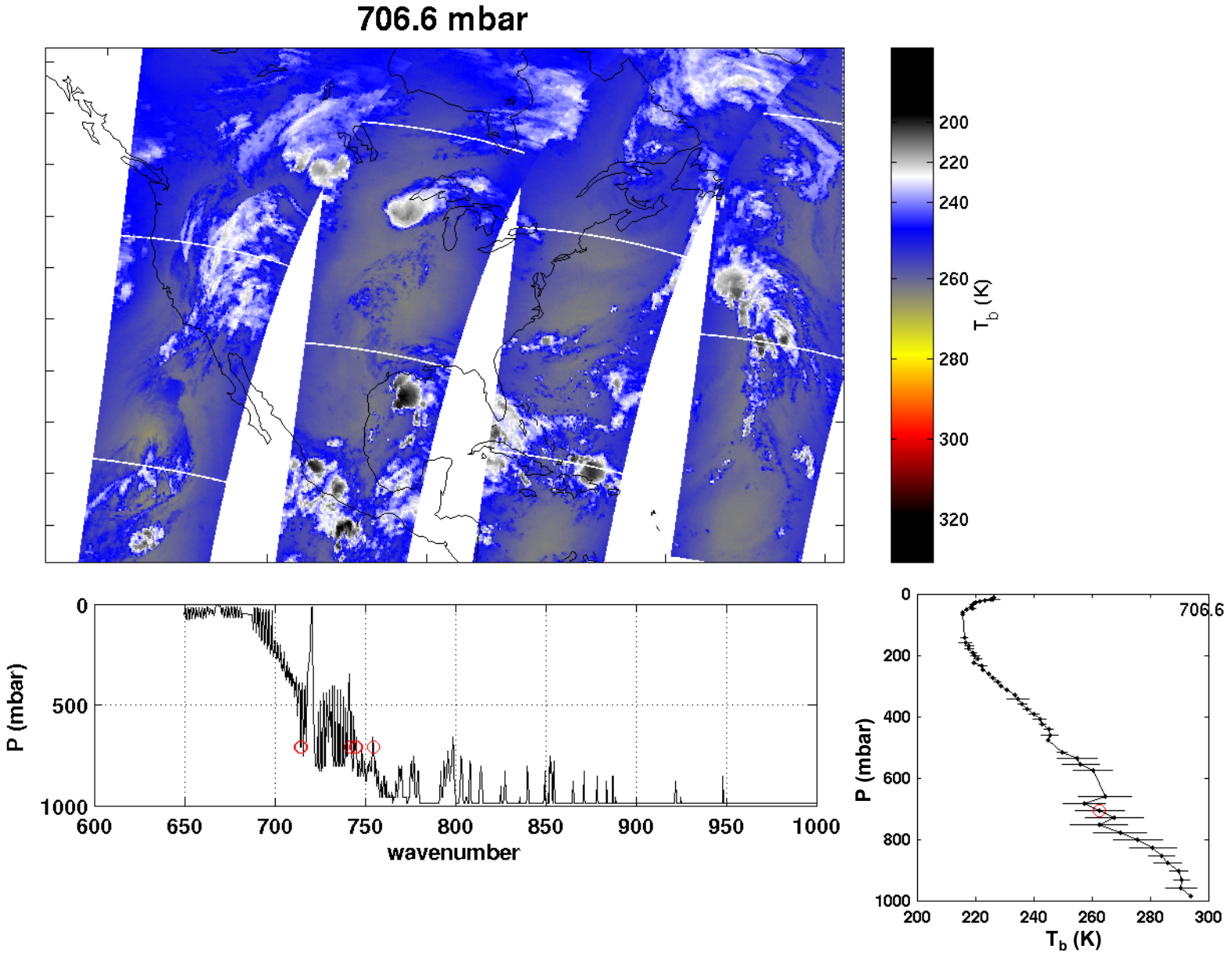
706.6 mbar
200
220
240
260
280
300
320
T_b (K)
0
500
1000
P (mbar)
600
650
700
750
800
850
900
950
1000
wavenumber
706.6
0
200
400
600
800
1000
P (mbar)
200
220
240
260
280
300
T_b (K)

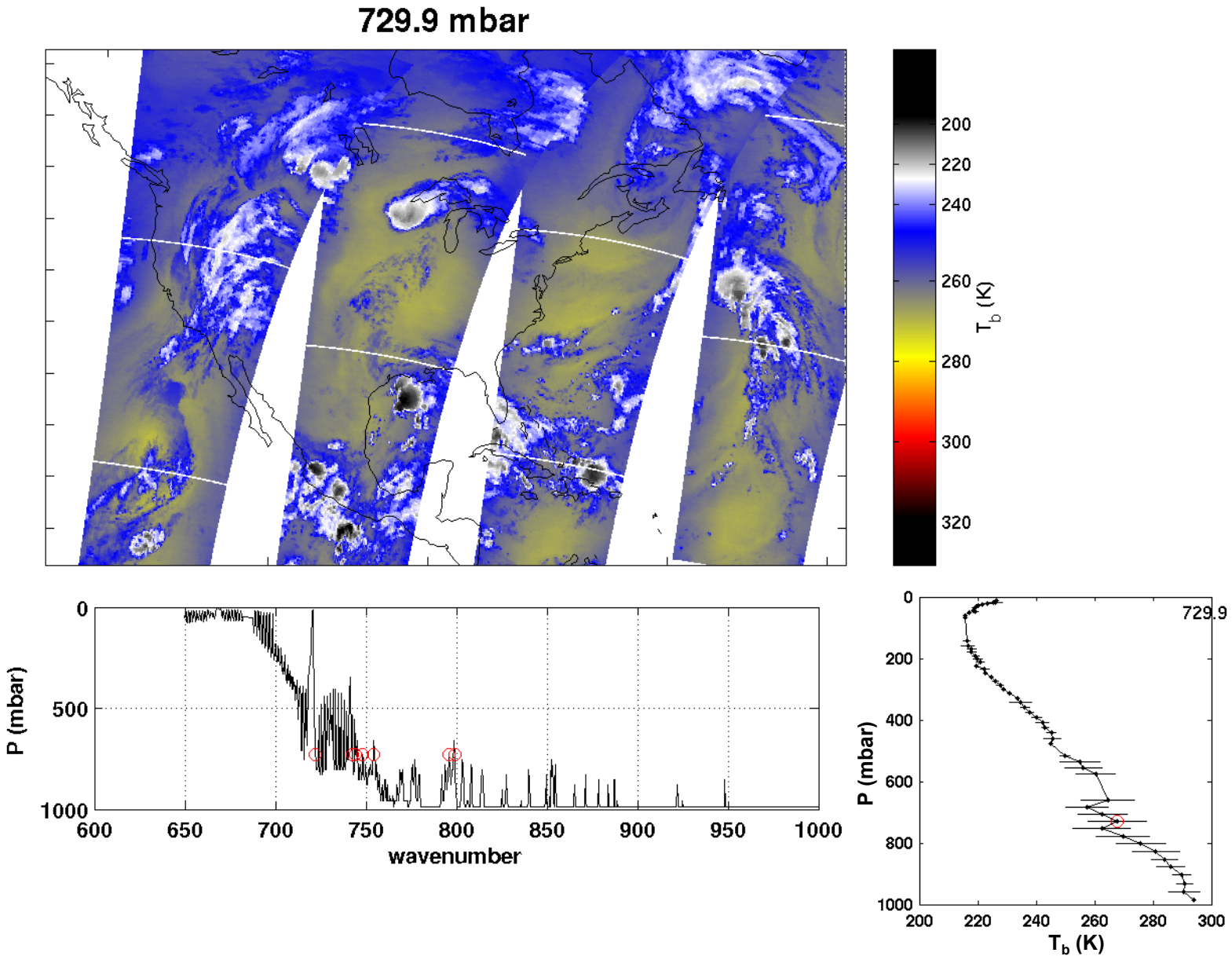
729.9 mbar
200
220
240
260
280
300
320
T_b (K)
P (mbar)
0
500
1000
600
650
700
750
800
850
900
950
1000
wavenumber
729.9
200
400
600
800
1000
220
240
260
280
300
T_b (K)

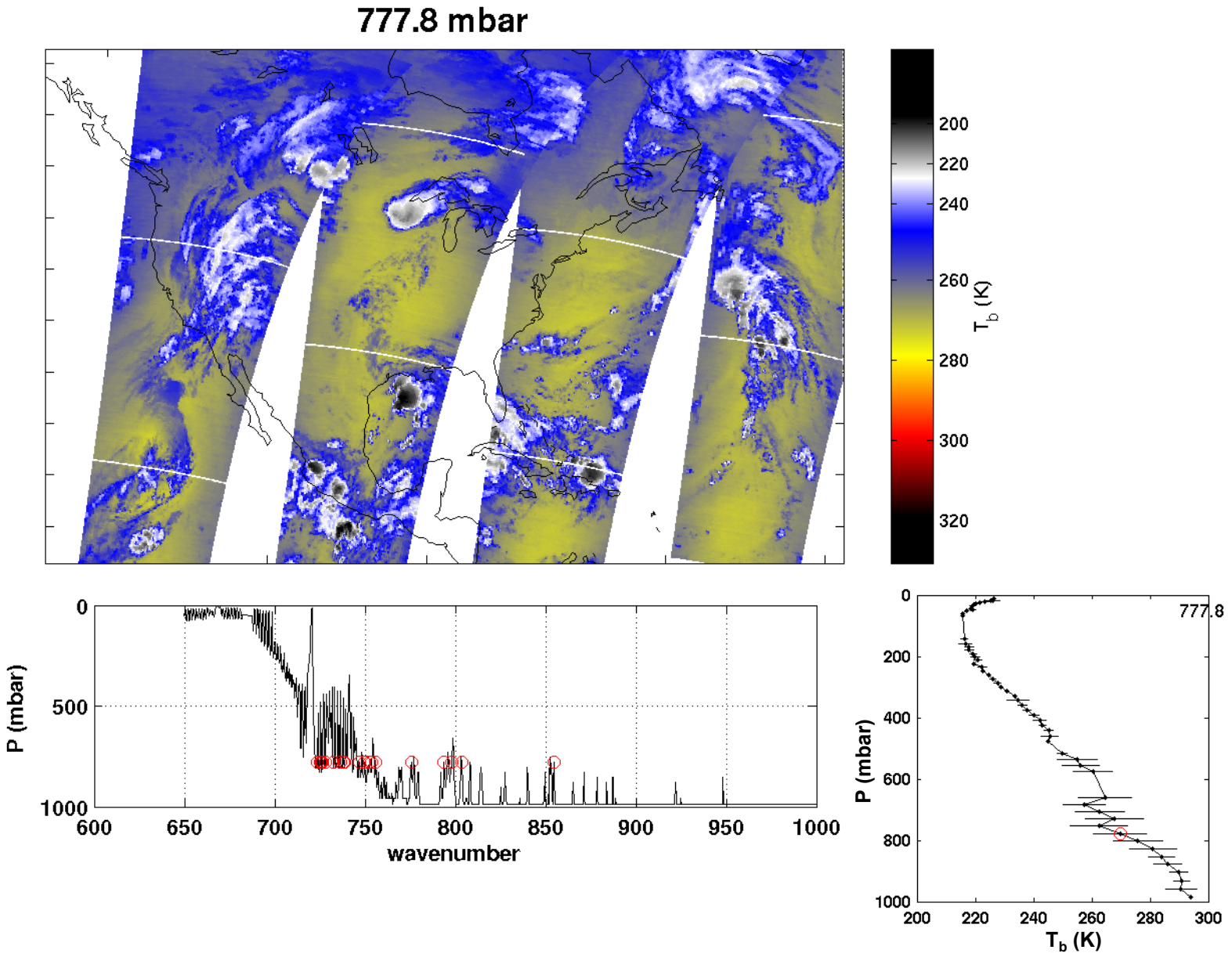
777.8 mbar
200
220
240
260
280
300
320
T_b (K)
0
500
1000
P (mbar)
600
650
700
750
800
850
900
950
1000
wavenumber
777.8
0
200
400
600
800
1000
P (mbar)
200
220
240
260
280
300
T_b (K)

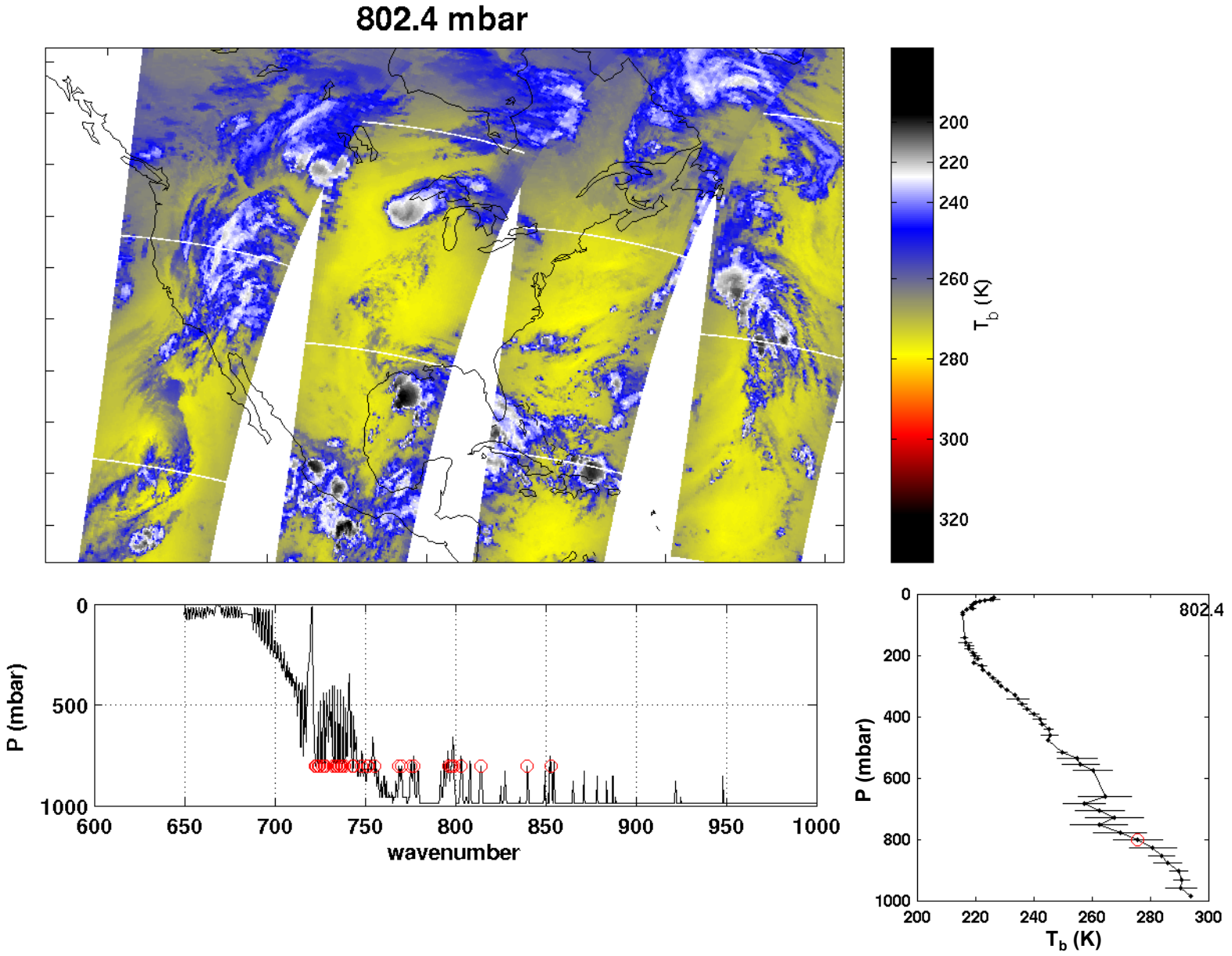
802.4 mbar
200
220
240
260
280
300
320
T_b (K)
0
500
1000
P (mbar)
600
650
700
750
800
850
900
950
1000
wavenumber
802.4
0
200
400
600
800
1000
P (mbar)
200
220
240
260
280
300
T_b (K)

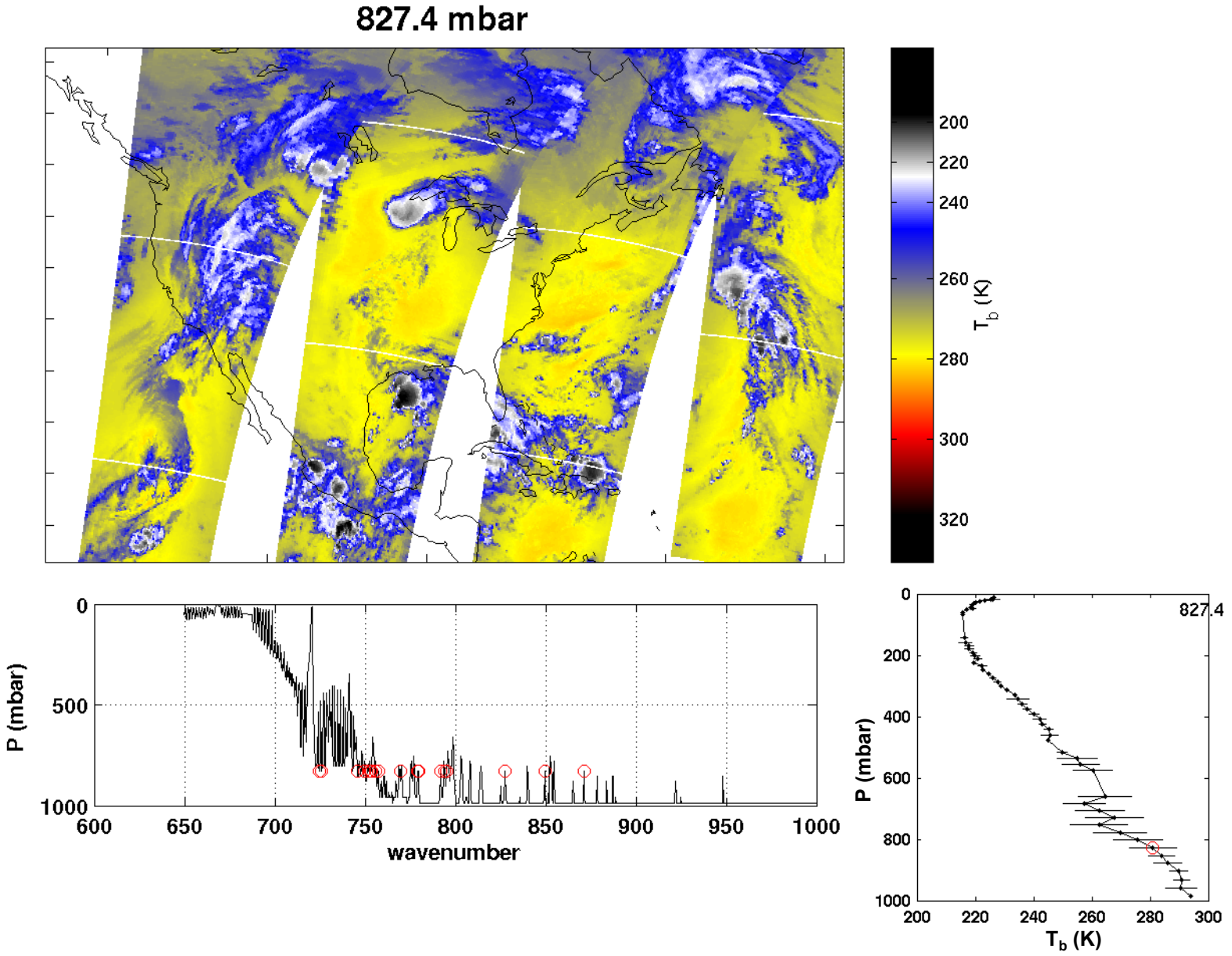
827.4 mbar
200
220
240
260
280
300
320
T_b (K)
0
500
1000
P (mbar)
600
650
700
750
800
850
900
950
1000
wavenumber
827.4
0
200
400
600
800
1000
P (mbar)
200
220
240
260
280
300
T_b (K)

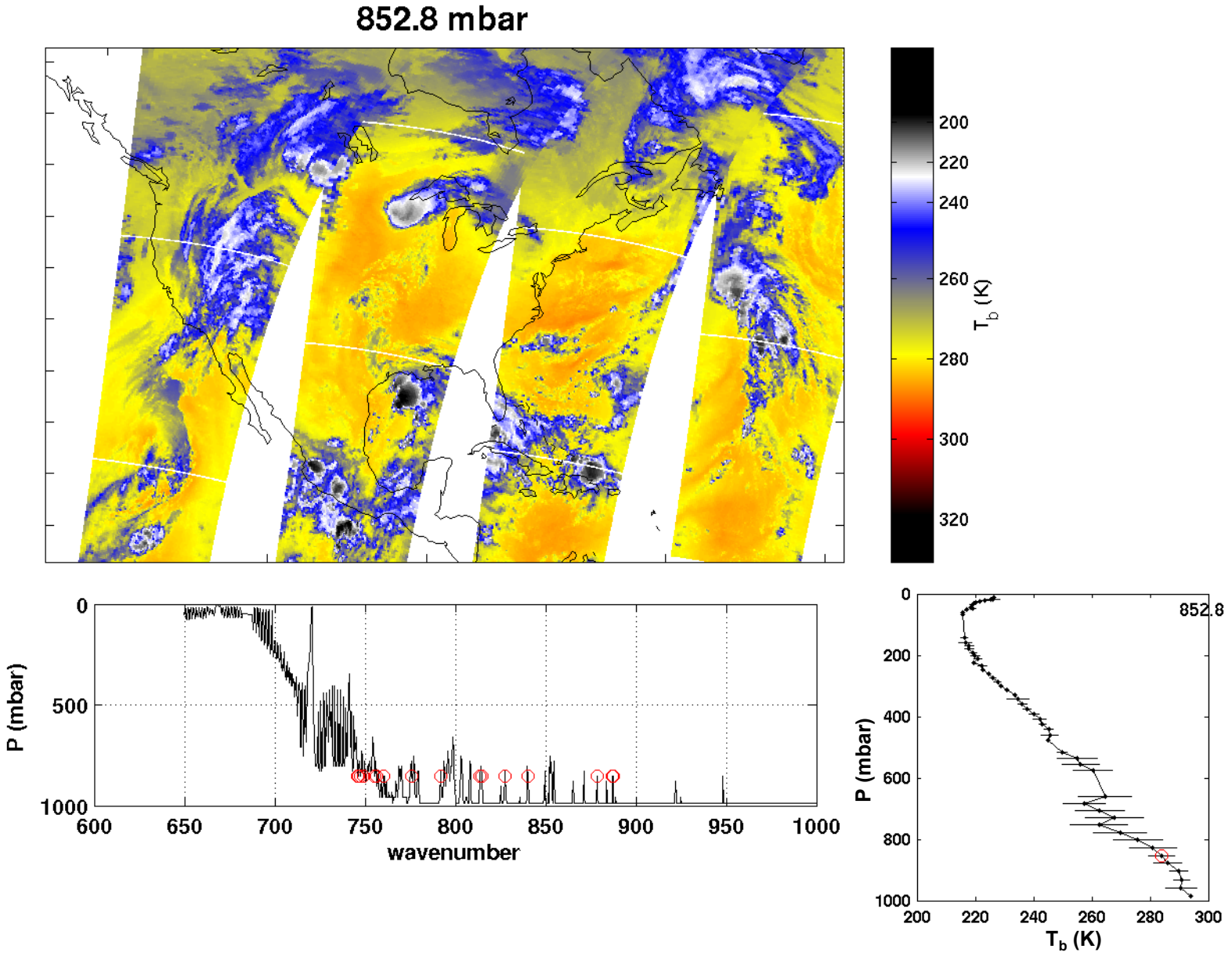
852.8 mbar
200
220
240
260
280
300
320
T_b (K)
0
500
1000
P (mbar)
600
650
700
750
800
850
900
950
1000
wavenumber
852.8
0
200
400
600
800
1000
P (mbar)
200
220
240
260
280
300
T_b (K)

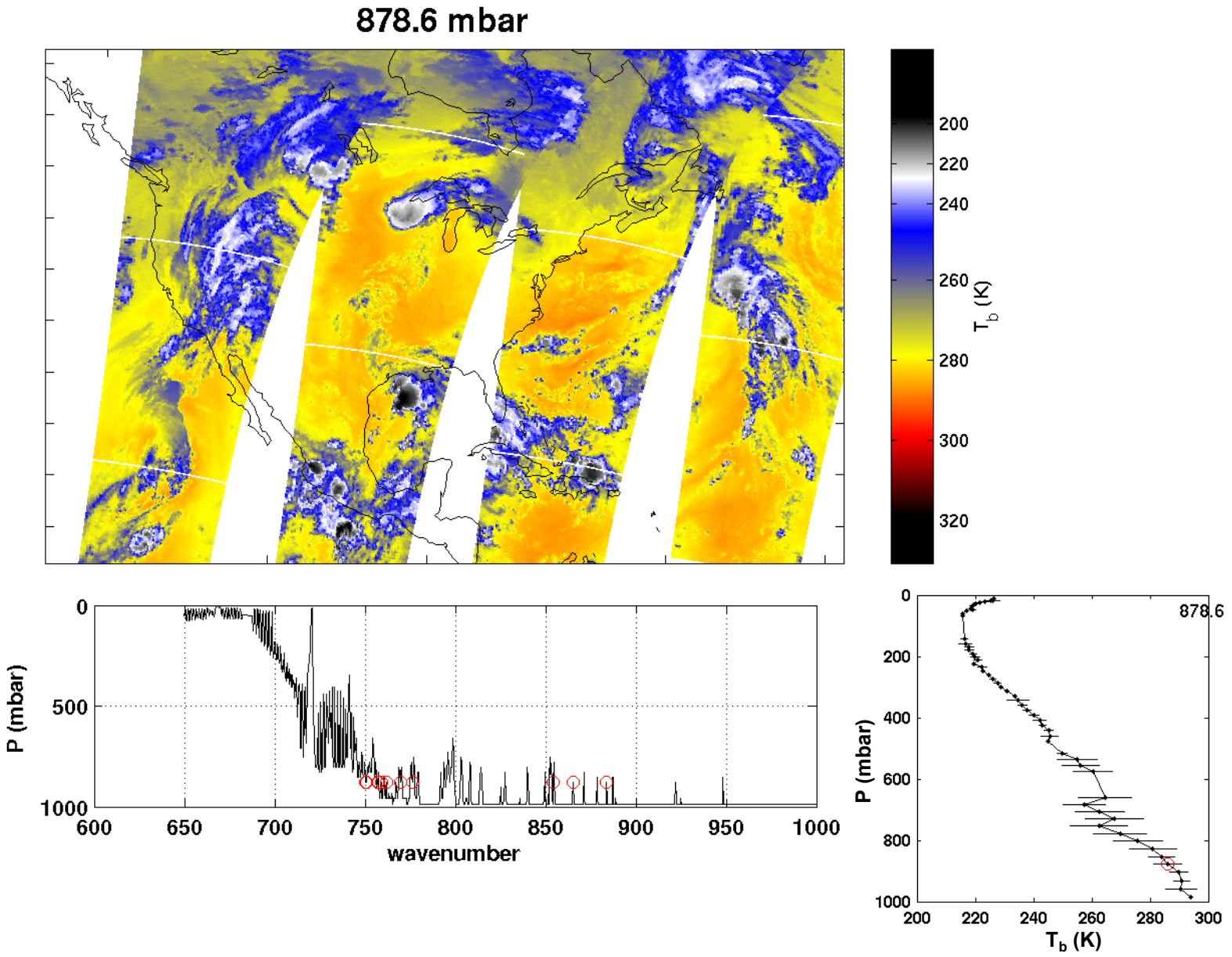
878.6 mbar
200
220
240
260
280
300
320
T_b (K)
P (mbar)
0
500
1000
600
650
700
750
800
850
900
950
1000
wavenumber
878.6
200
400
600
800
1000
200
220
240
260
280
300
T_b (K)

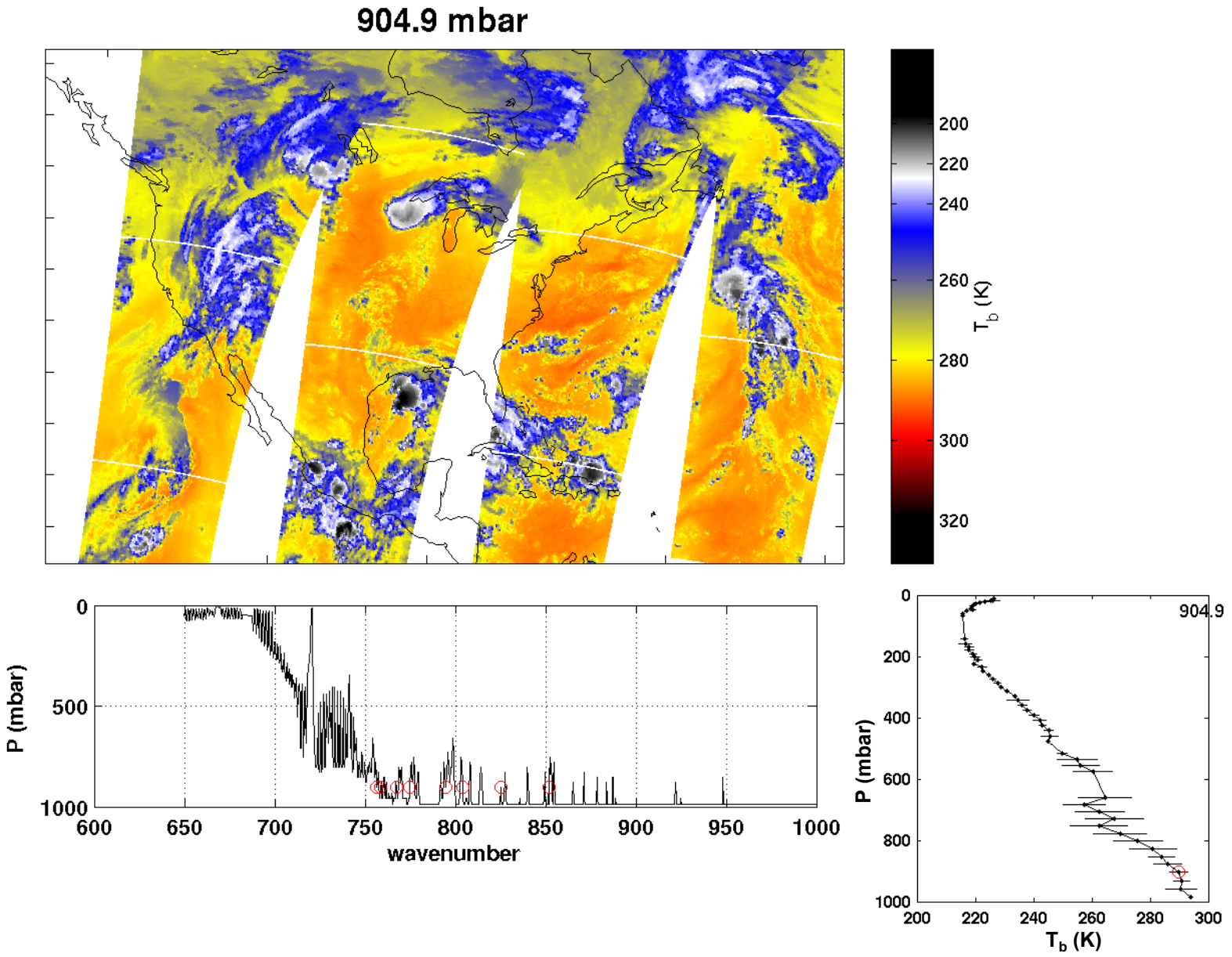
904.9 mbar
200
220
240
260
280
300
320
T_b (K)
P (mbar)
0
500
1000
600
650
700
750
800
850
900
950
1000
wavenumber
904.9
200
400
600
800
1000
220
240
260
280
300
T_b (K)

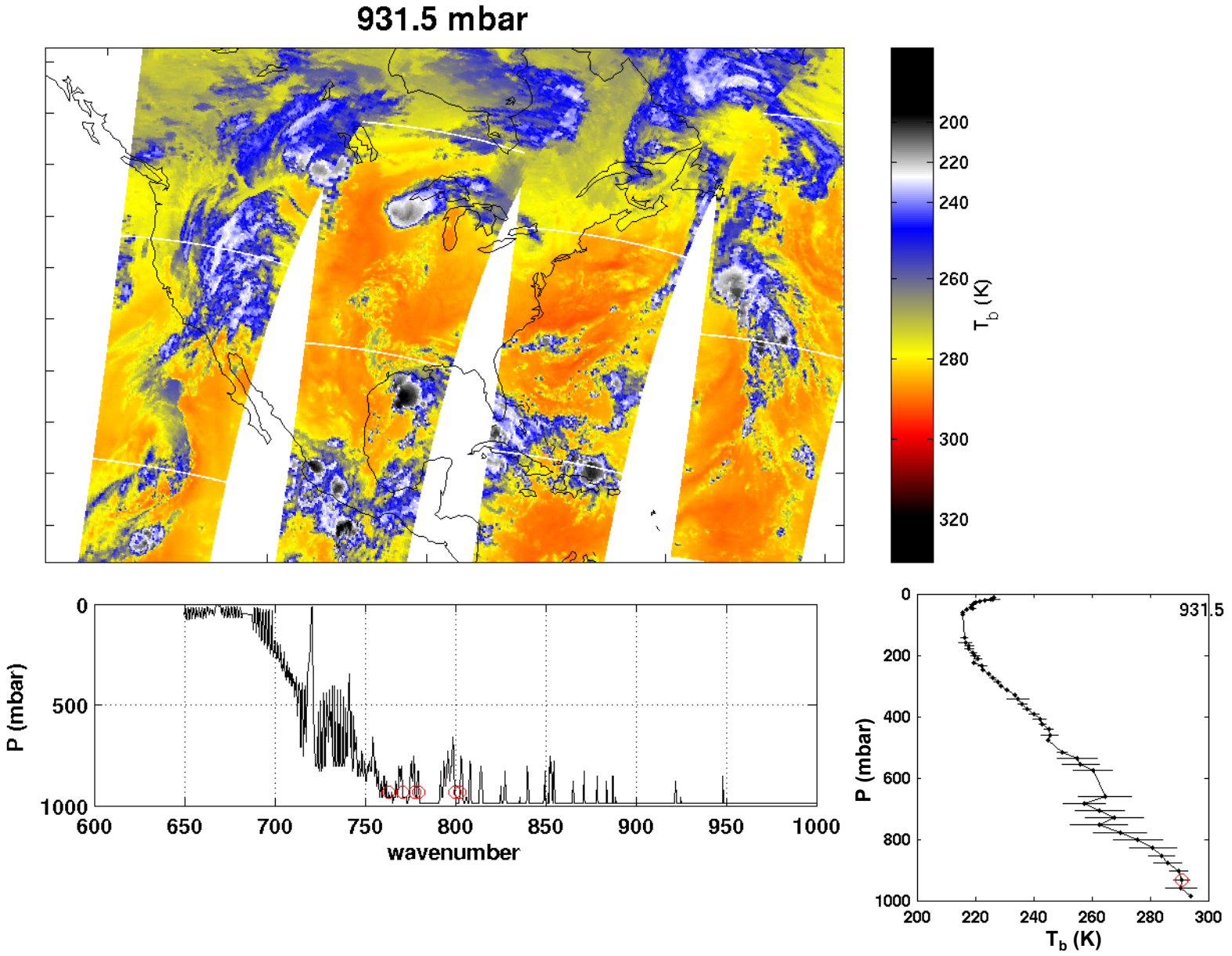
931.5 mbar
200
220
240
260
280
300
320
T_b (K)
0
500
1000
P (mbar)
600
650
700
750
800
850
900
950
1000
wavenumber
931.5
200
400
600
800
1000
P (mbar)
200
220
240
260
280
300
T_b (K)

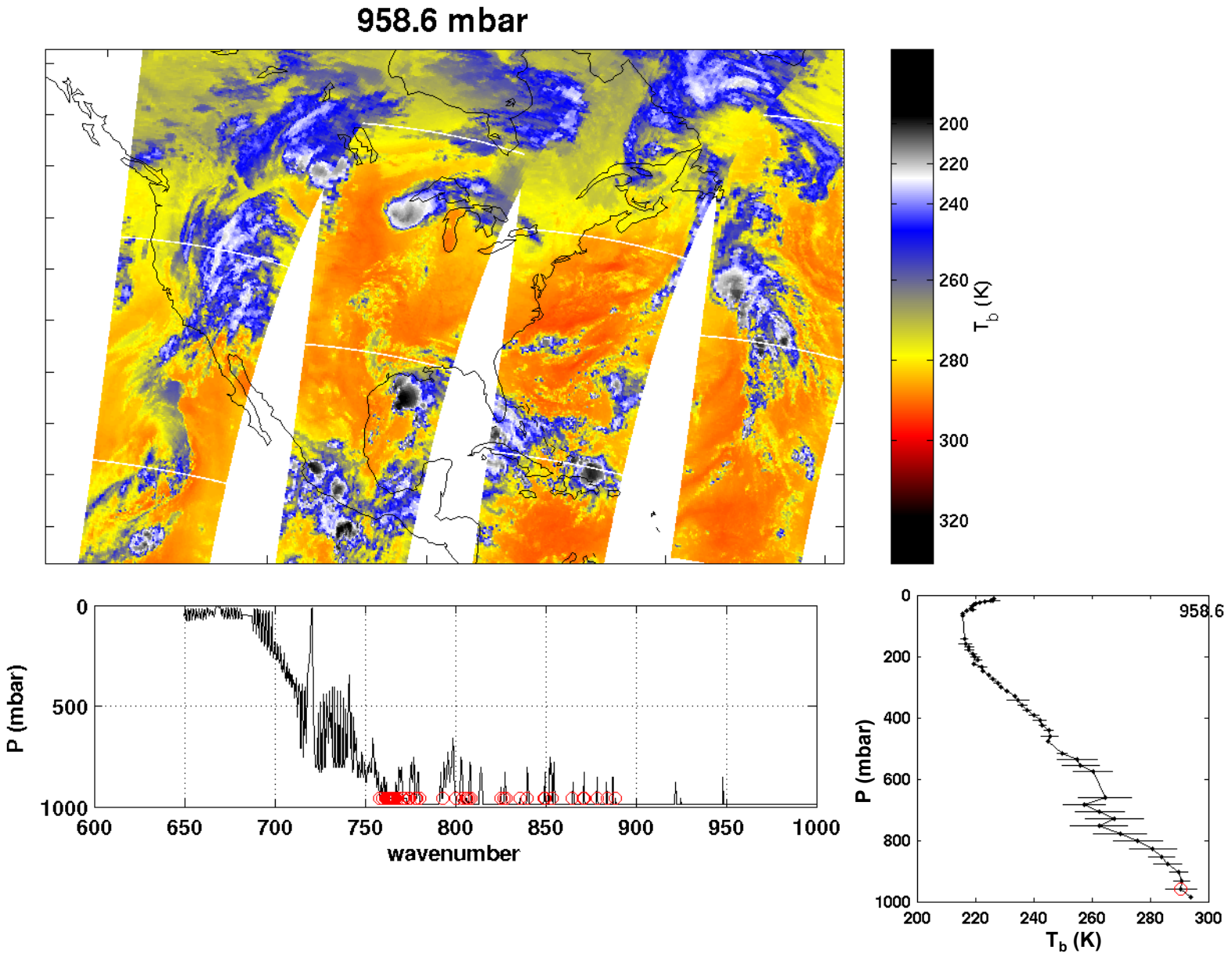
958.6 mbar
200
220
240
260
280
300
320
T_b (K)
0
500
1000
P (mbar)
600
650
700
750
800
850
900
950
1000
wavenumber
958.6
0
200
400
600
800
1000
P (mbar)
200
220
240
260
280
300
T_b (K)

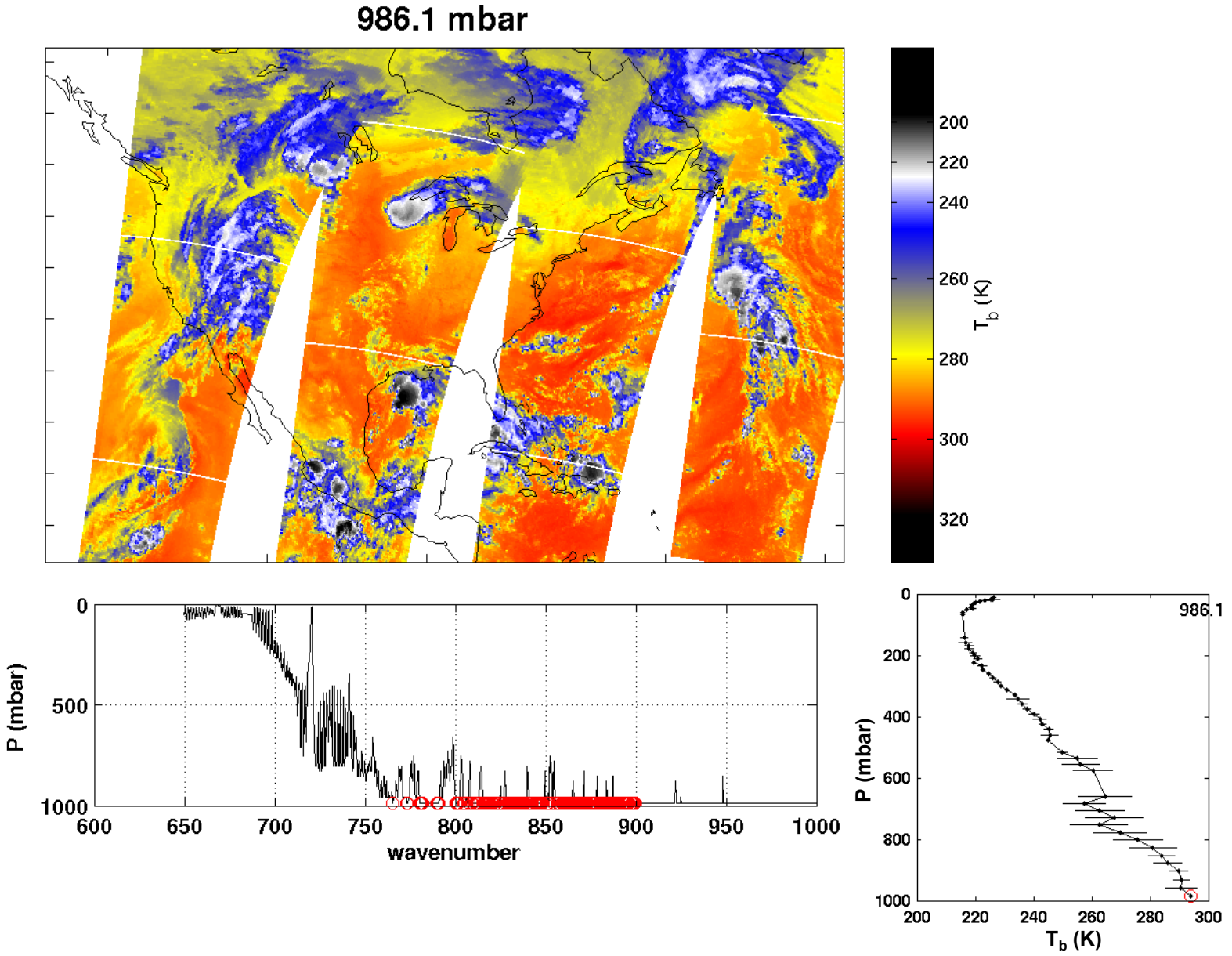
986.1 mbar
200
220
240
260
280
300
320
T_b (K)
0
500
1000
P (mbar)
600
650
700
750
800
850
900
950
1000
wavenumber
986.1
200
400
600
800
1000
P (mbar)
200
220
240
260
280
300
T_b (K)

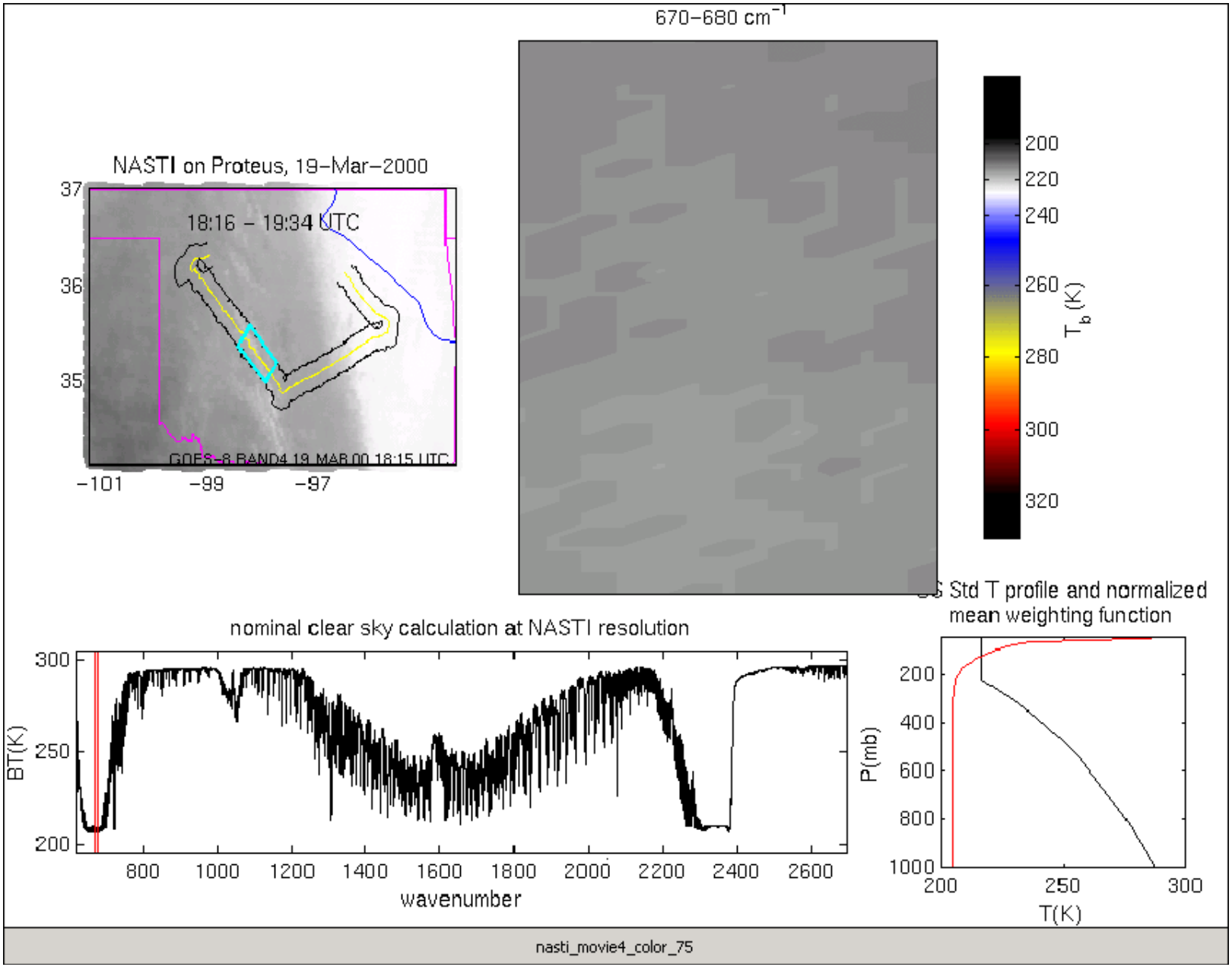
NASTI on Proteus, 19-Mar-2000
18:16 - 19:34 UTC
GOES-8 BAND4 19 MAR 00 18:15 UTC
37
36
35
-101
-99
-97
670-680 cm^{-1}
200
220
240
260
280
300
320
T_b (K)
Std T profile and normalized
mean weighting function
nominal clear sky calculation at NASTI resolution
BT(K)
300
250
200
800
1000
1200
1400
1600
1800
2000
2200
2400
2600
wavenumber
P(mb)
200
400
600
800
1000
200
250
300
T(K)
nasti_movie4_color_75

AIRS data and Level 2 Products are being processed at the GSFC DAAC and now available to the public!

The NASA GSFC Data Active Archive Center at

http://daac.gsfc.nasa.gov/

offers a menu driven selection of archived calibrated navigated radiances as well as derived products such as temperature and moisture soundings and total column concentrations of water vapor and ozone.

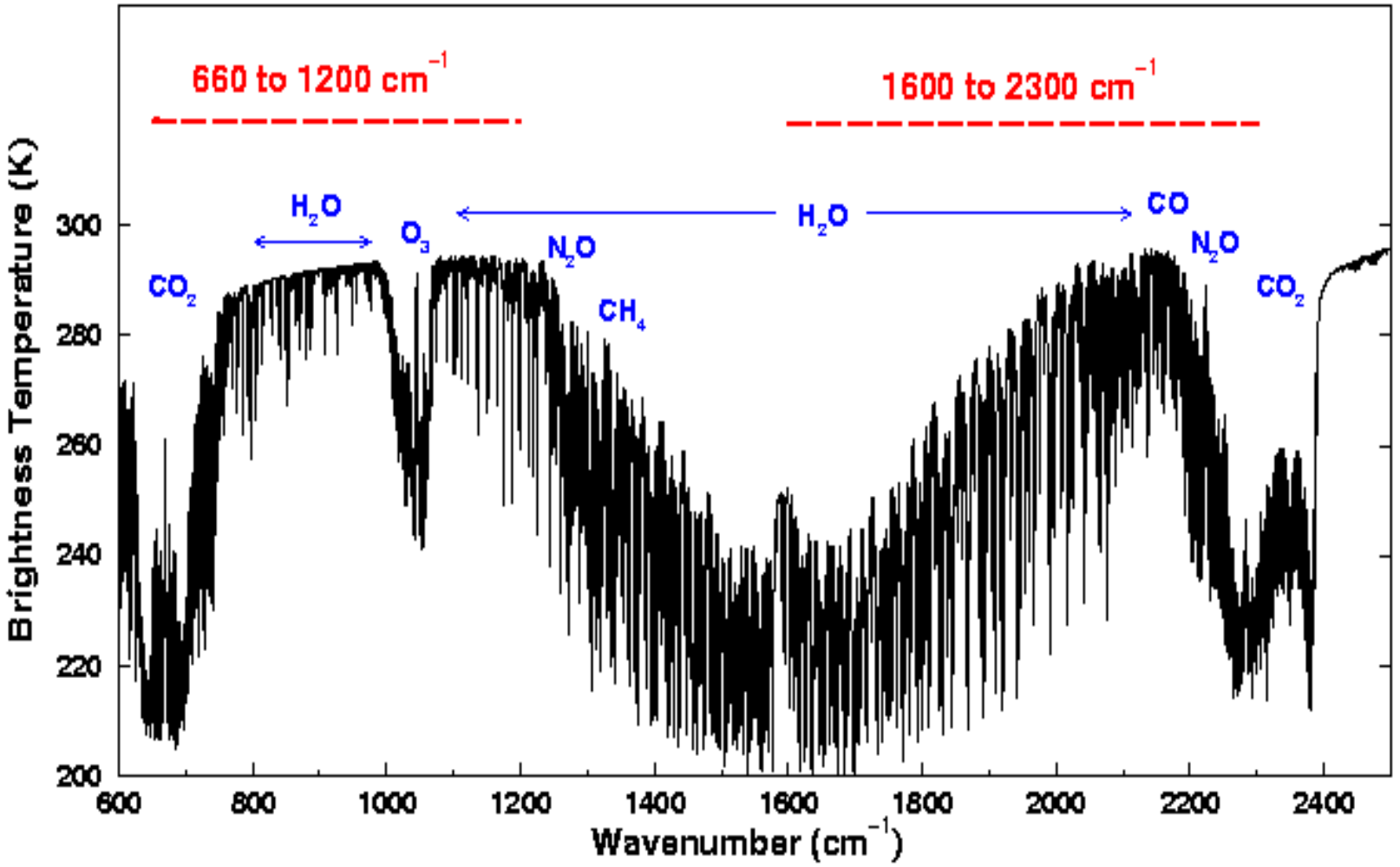
660 to 1200 cm^{-1}
1600 to 2300 cm^{-1}
H_2O
O_3
N_2O
CH_4
CO_2
H_2O
CO
N_2O
CO_2
Brightness Temperature (K)
300
280
260
240
220
200
600
800
1000
1200
1400
1600
1800
2000
2200
2400
Wavenumber (cm^{-1})

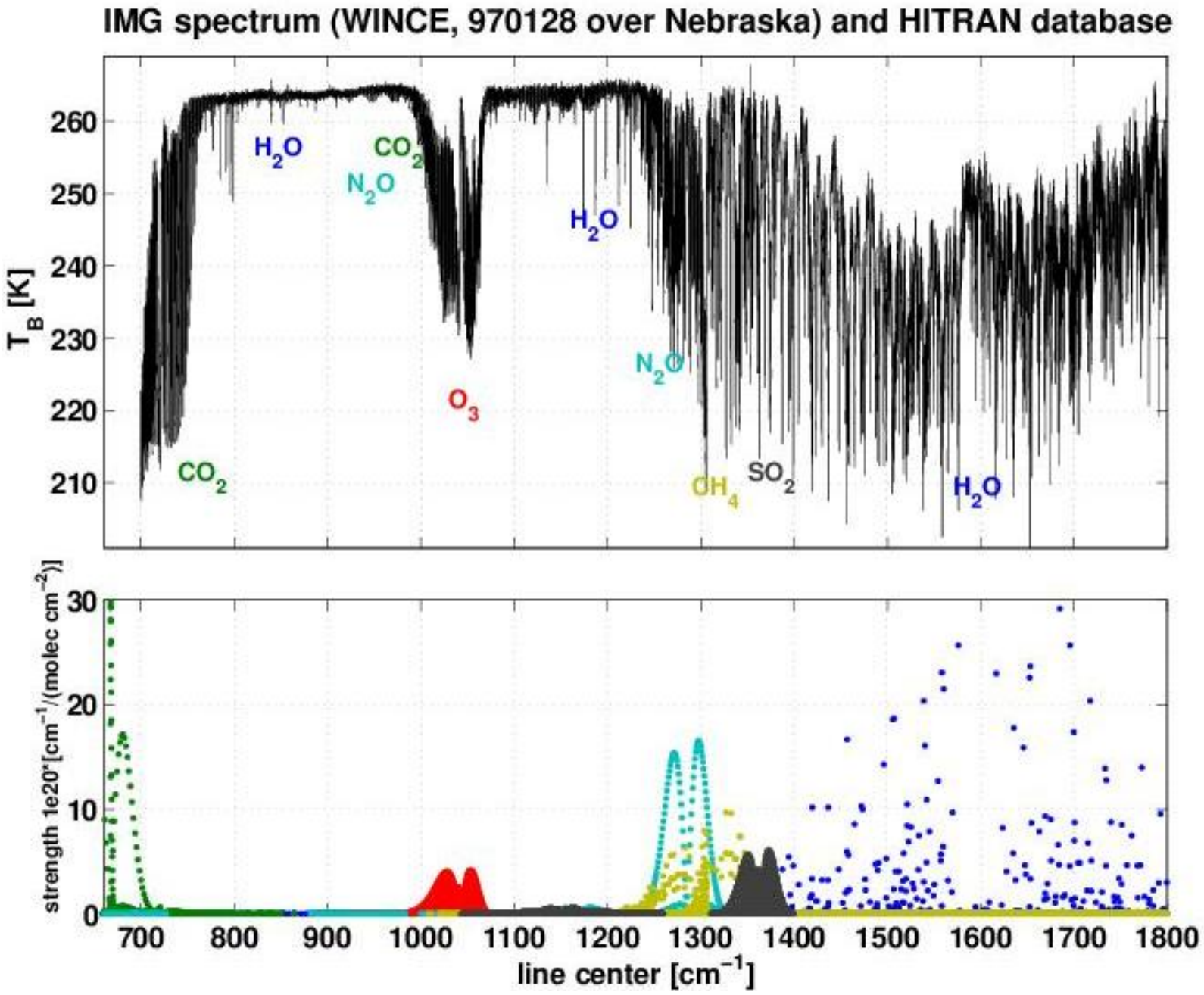
IMG spectrum (WINCE, 970128 over Nebraska) and HITRAN database
T_B [K]
260
250
240
230
220
210
H2O
CO2
N2O
H2O
N2O
O3
CO2
CH4
SO2
H2O
strength 1e20*[cm^-1/(molec cm^-2)]
30
20
10
0
700
800
900
1000
1100
1200
1300
1400
1500
1600
1700
1800
line center [cm^-1]

AIRS Spectra from around the Globe

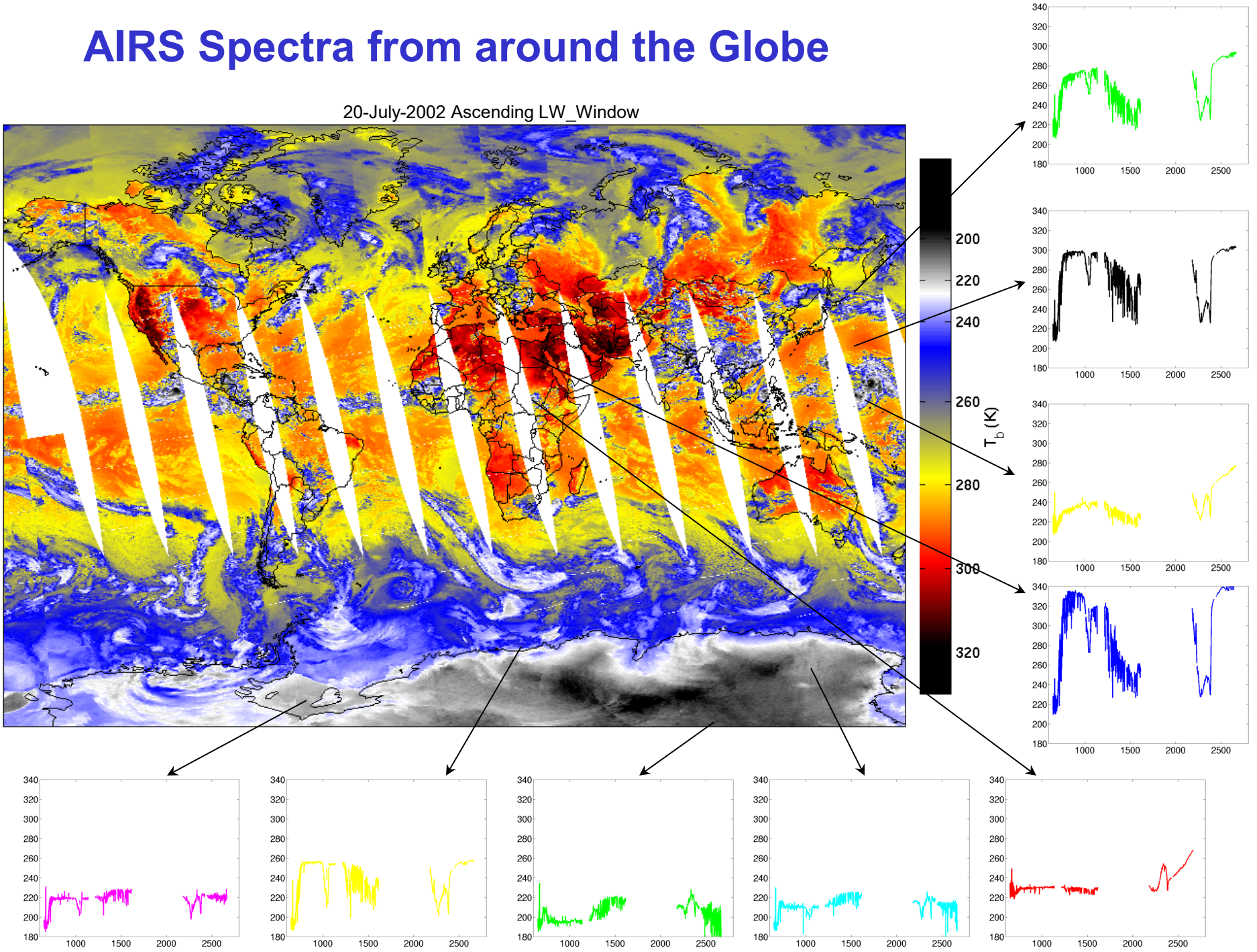

Resolving absorption features in atmospheric windows enables detection of temperature inversions

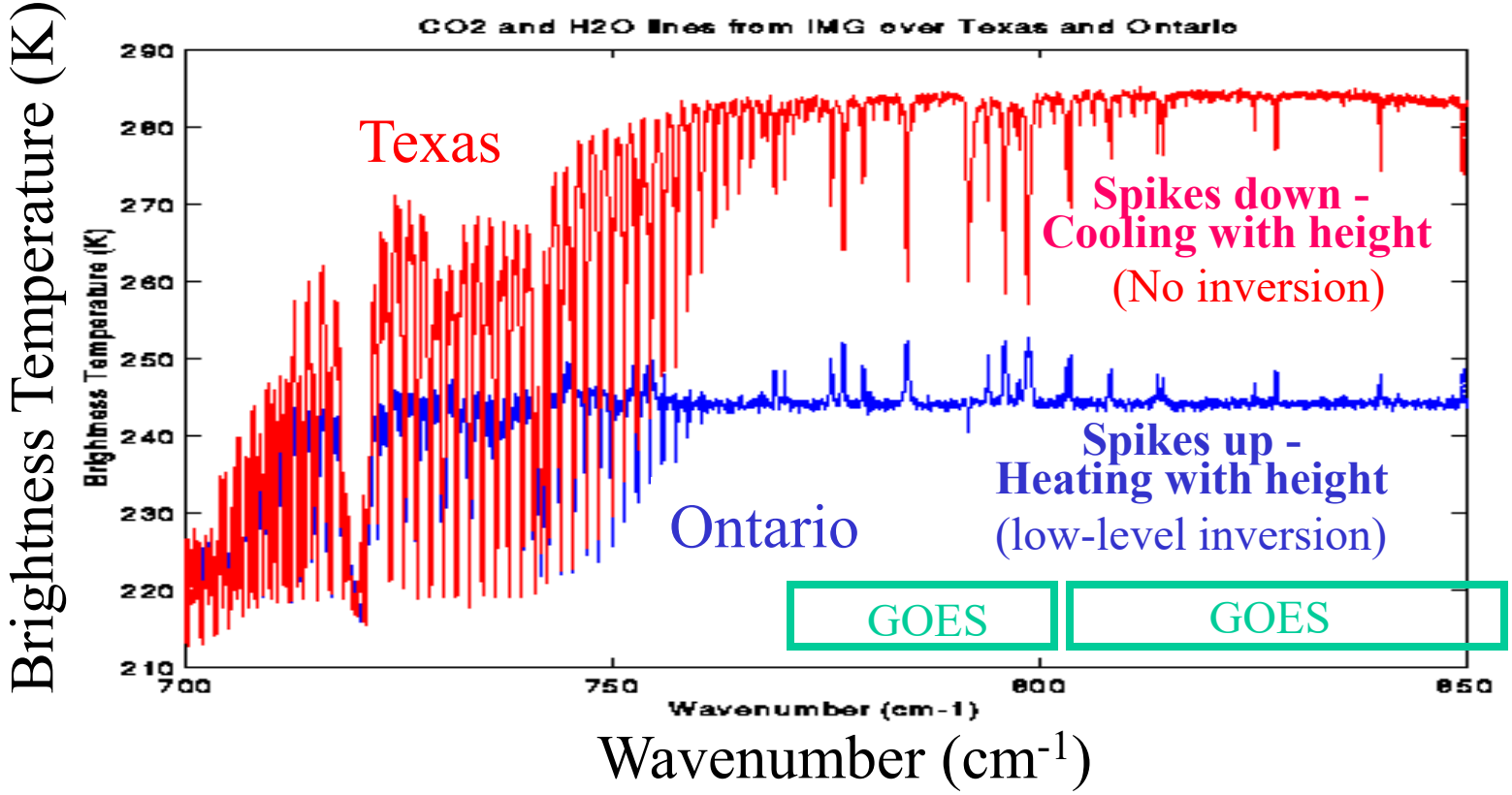

Detection of inversions is critical for severe weather forecasting. Combined with improved low-level moisture depiction, key ingredients for night-time severe storm development can be monitored.

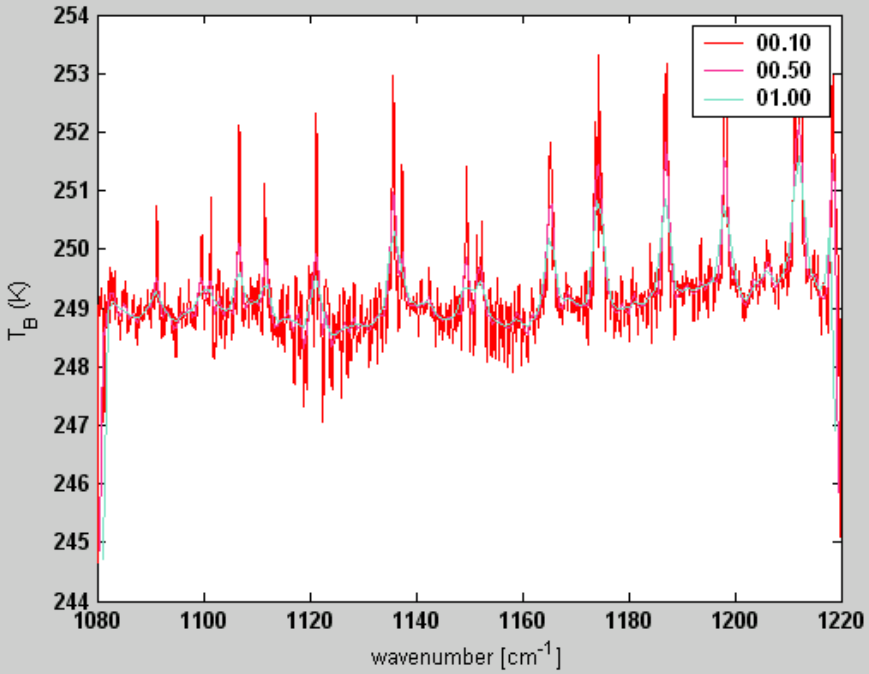

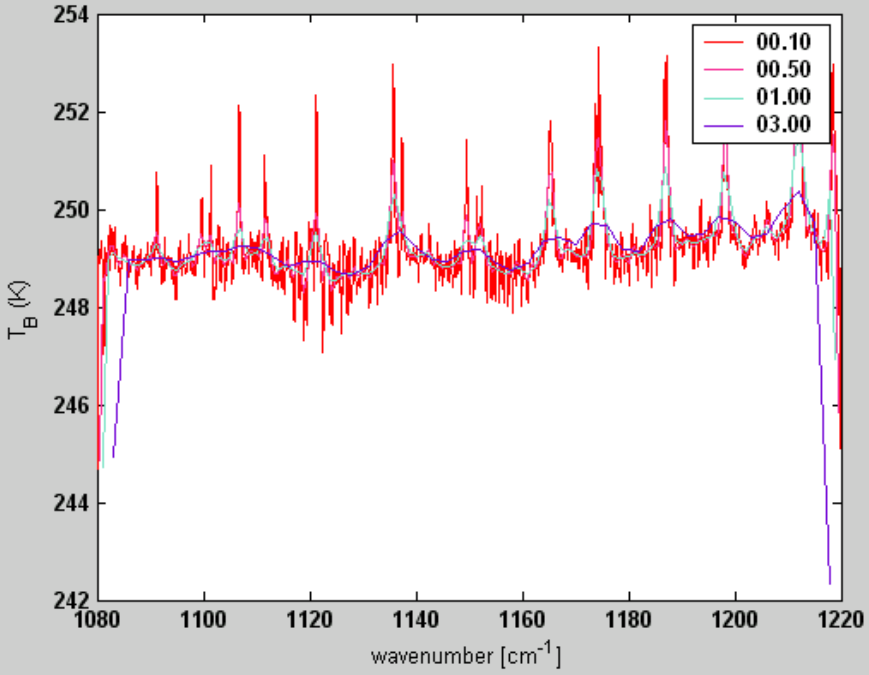

Ability to detect inversions disappears with broadband observations (> 3 cm-1)

Twisted Ribbon formed by CO_2 spectrum:

Tropopause inversion causes On-line & off-line patterns to cross

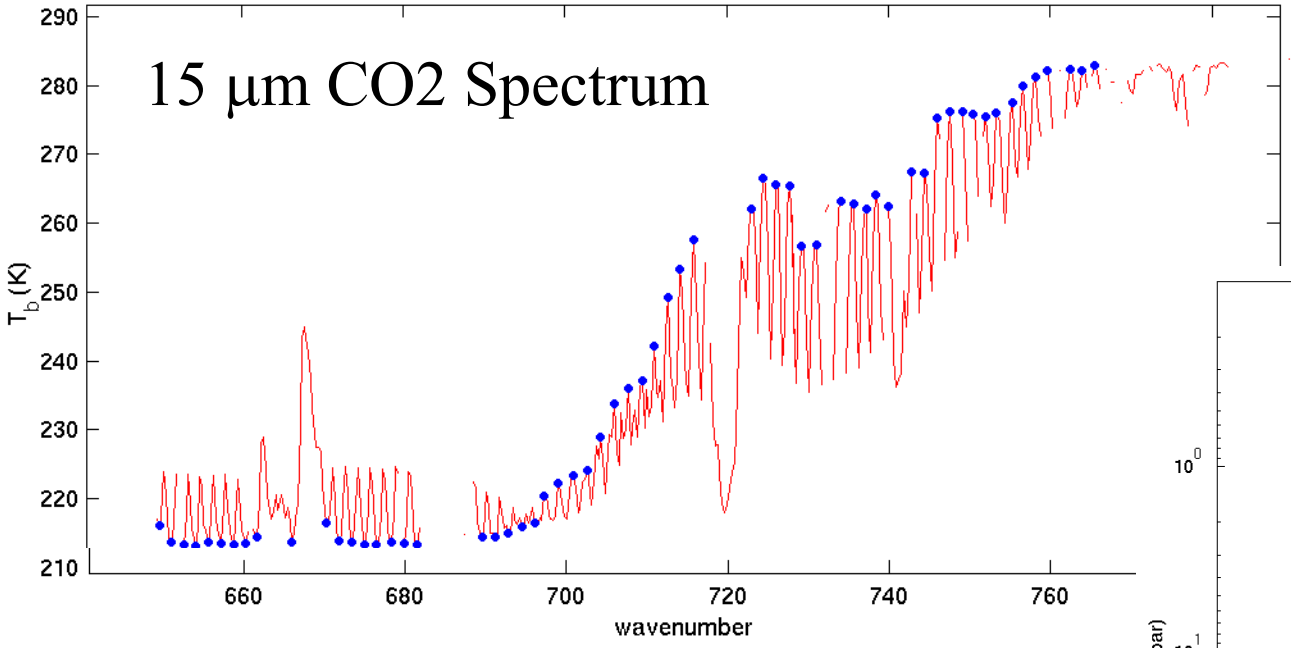

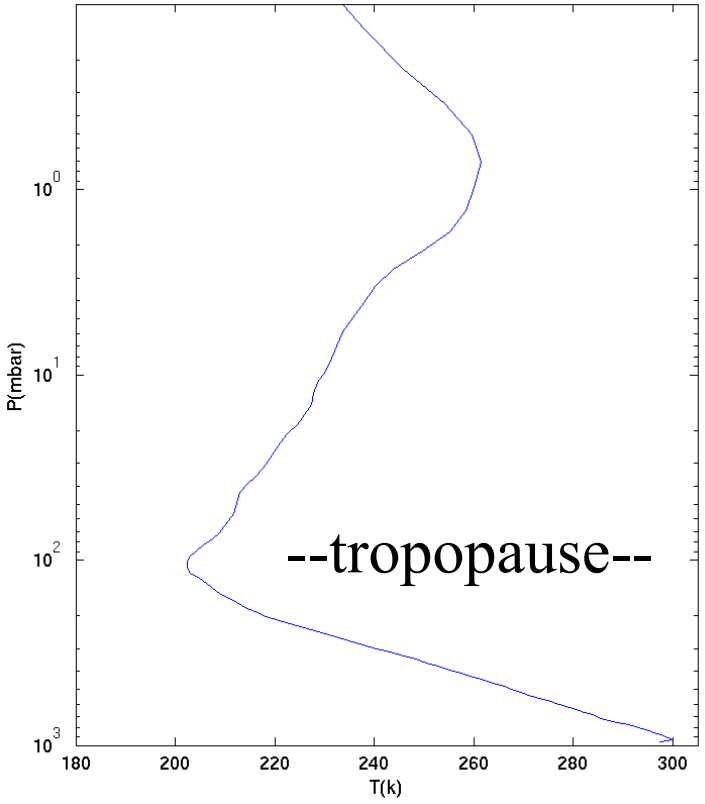

Blue between-line T_b
warmer for tropospheric channels,
colder for stratospheric channels

Signature not available at low resolution

AIRS obs in H2O band

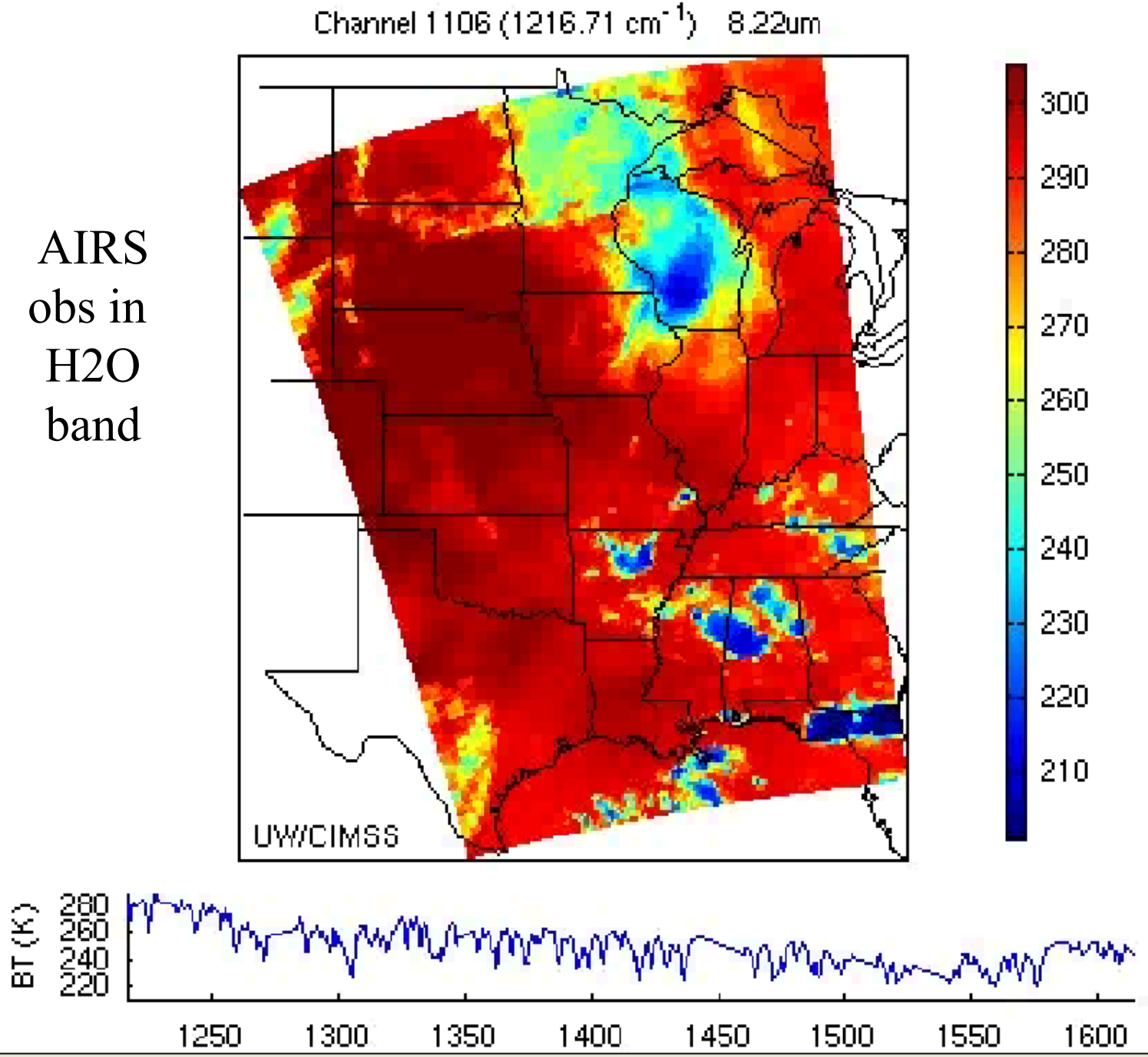

Spatial distribution of 944.1 [1/cm] measurements [K]

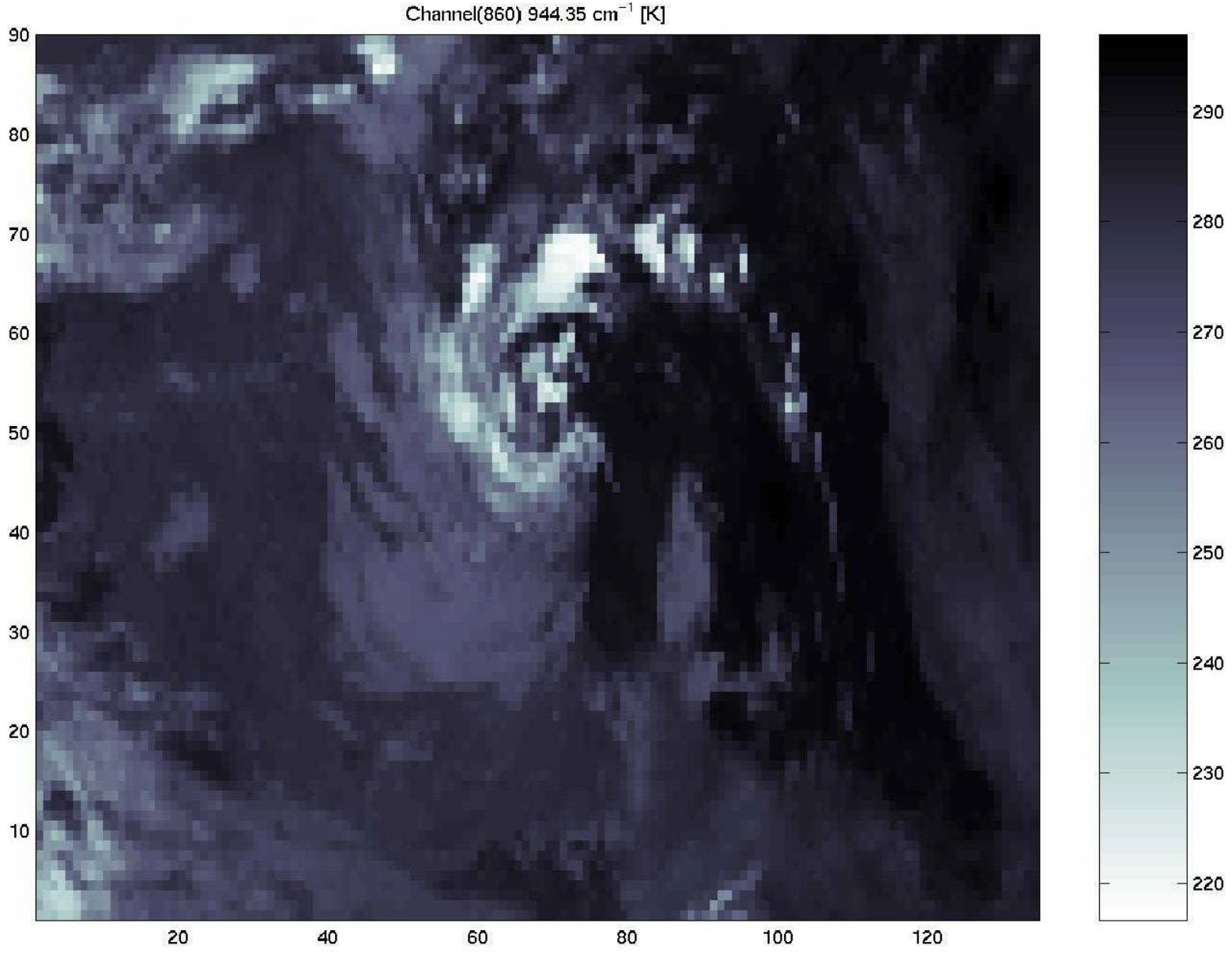

Spatial distribution of 944.1 [1/cm] measurements [K]

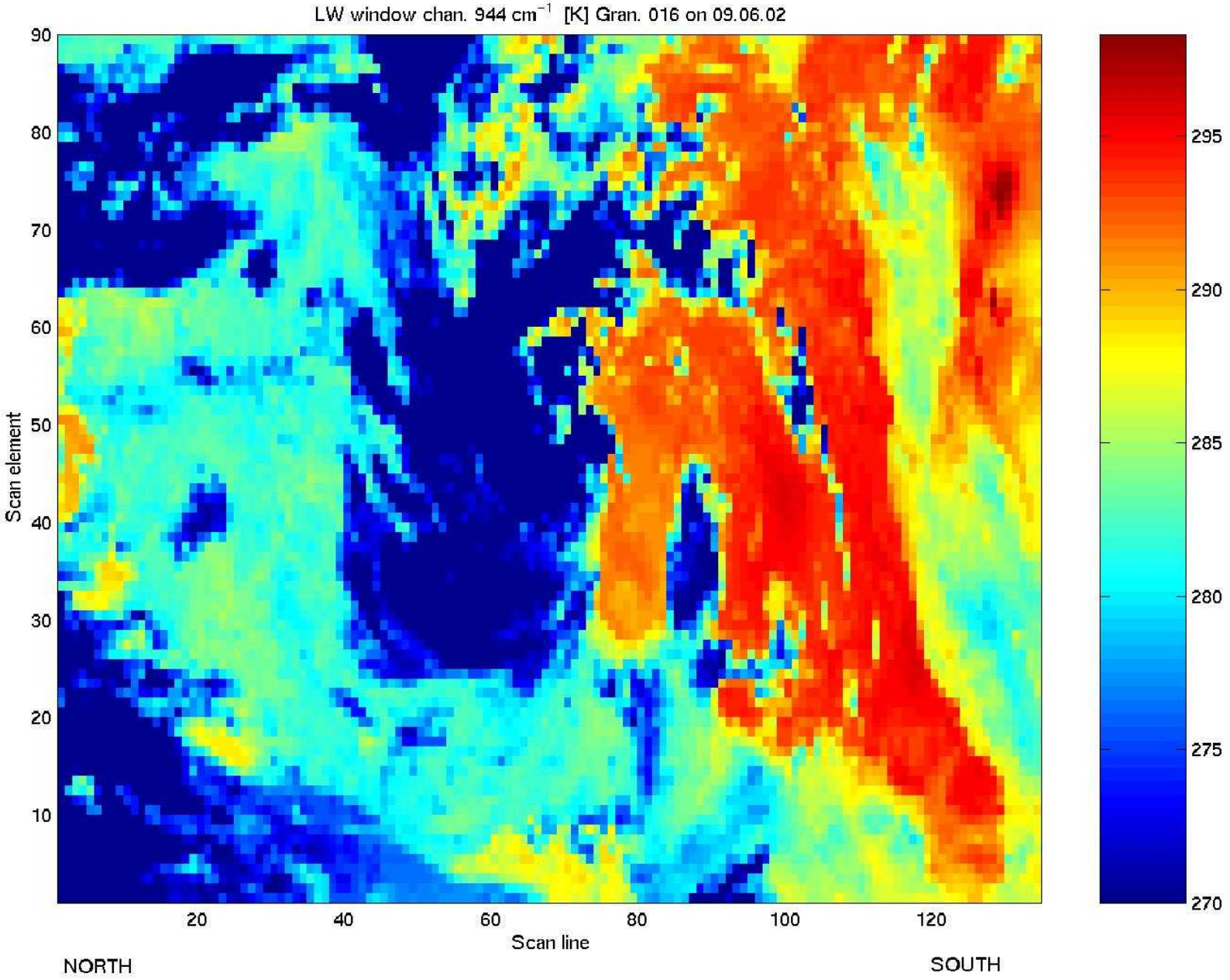

Spatial distribution of 2555 [1/cm] measurements [K]

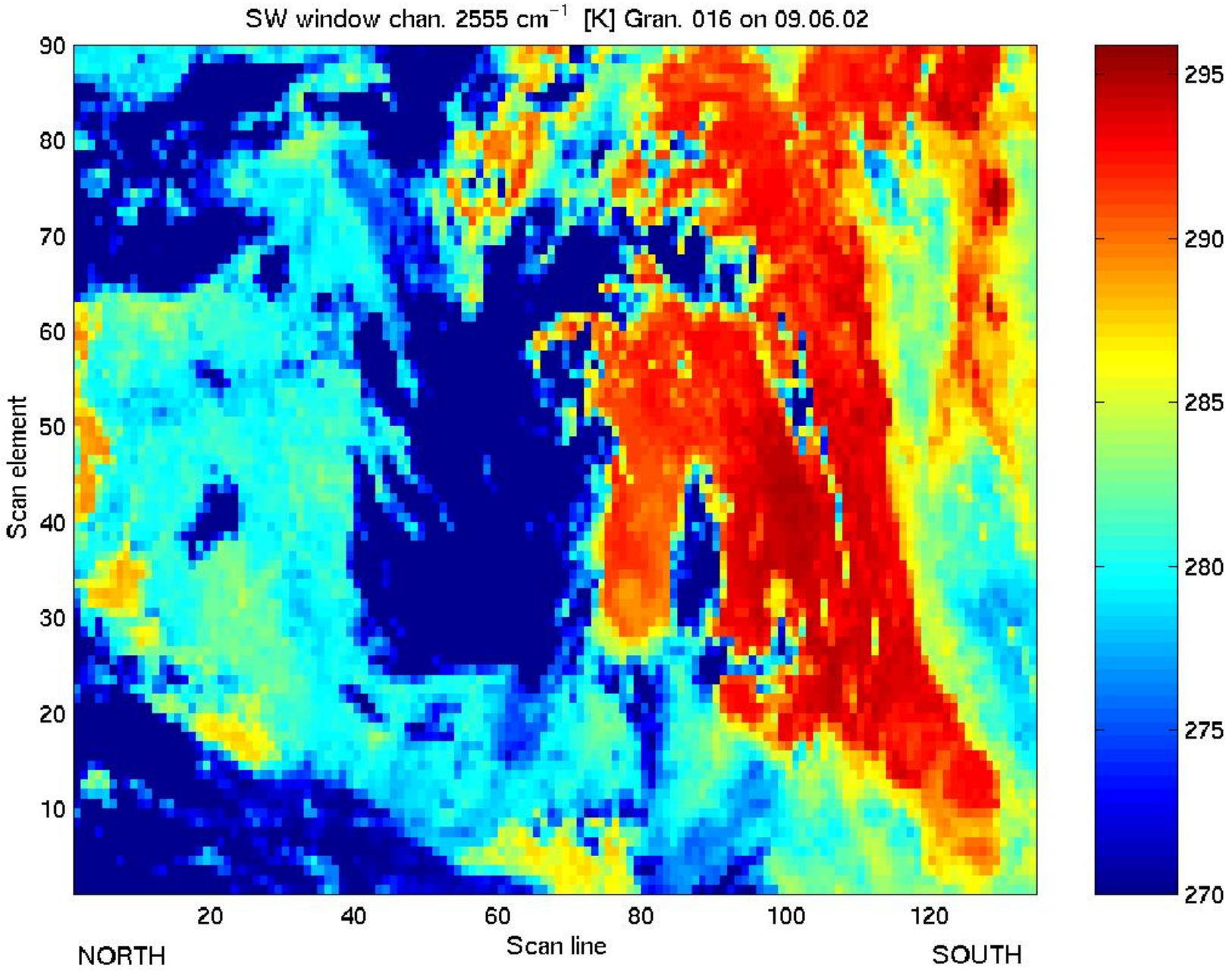

Spatial distribution of 2555 – 944.1 [1/cm] measurements [K]

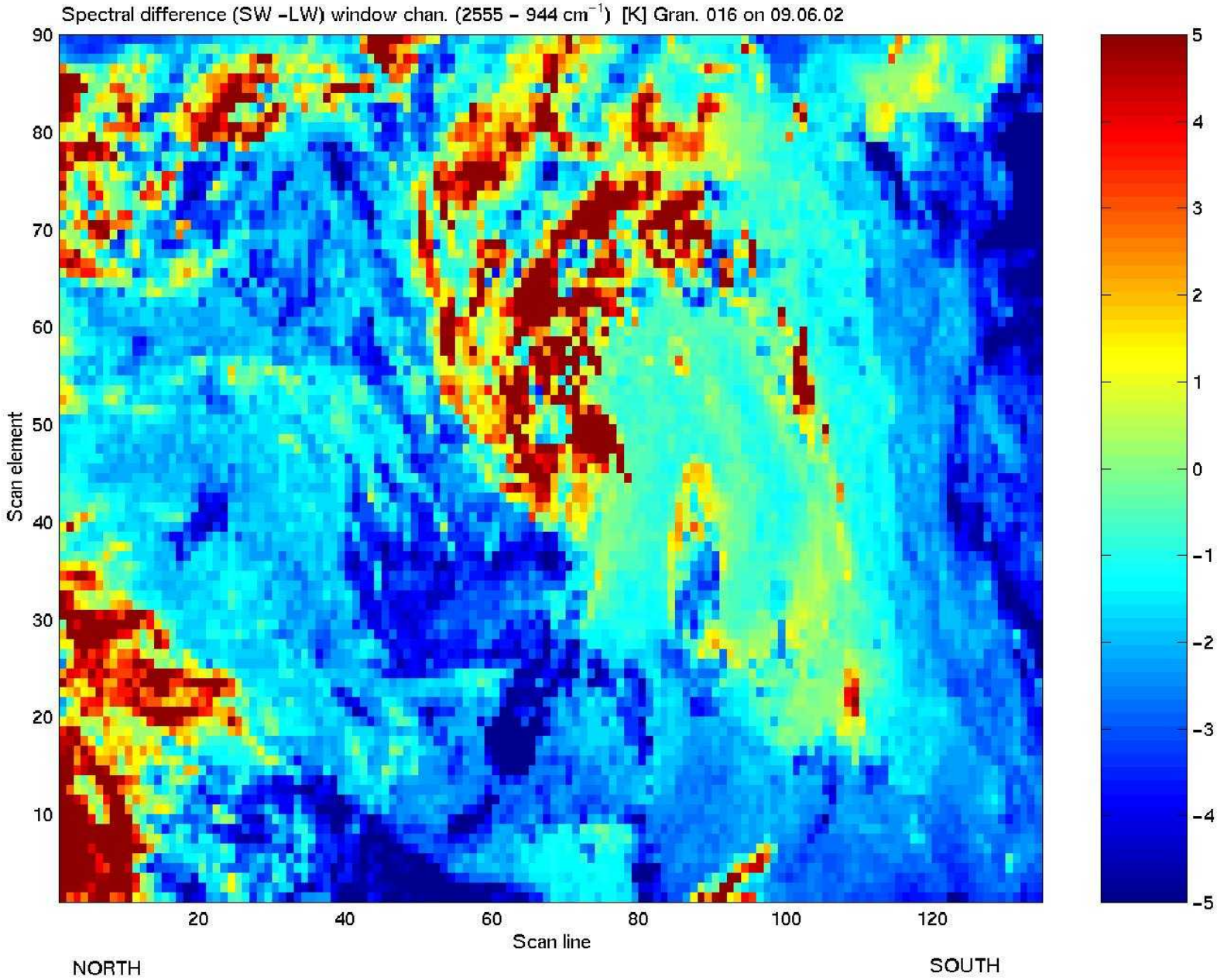

Optical properties of cloud particles: imaginary part of refraction index

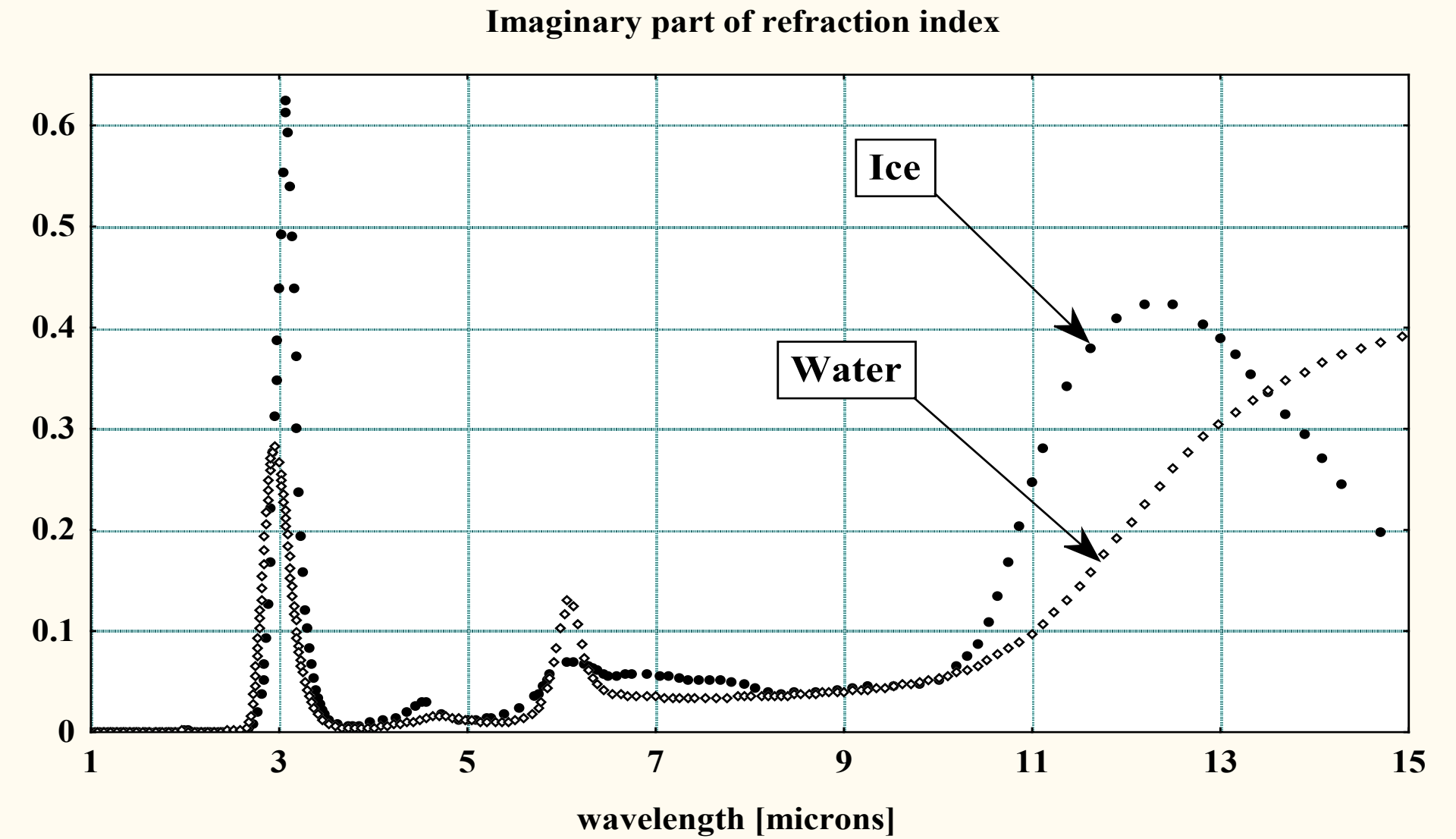

SW & LW channel differences are used for cloud identification
{4 μm - 11μm}, {4.13 μm - 12.6μm}, and {4.53 μm - 13.4μm}

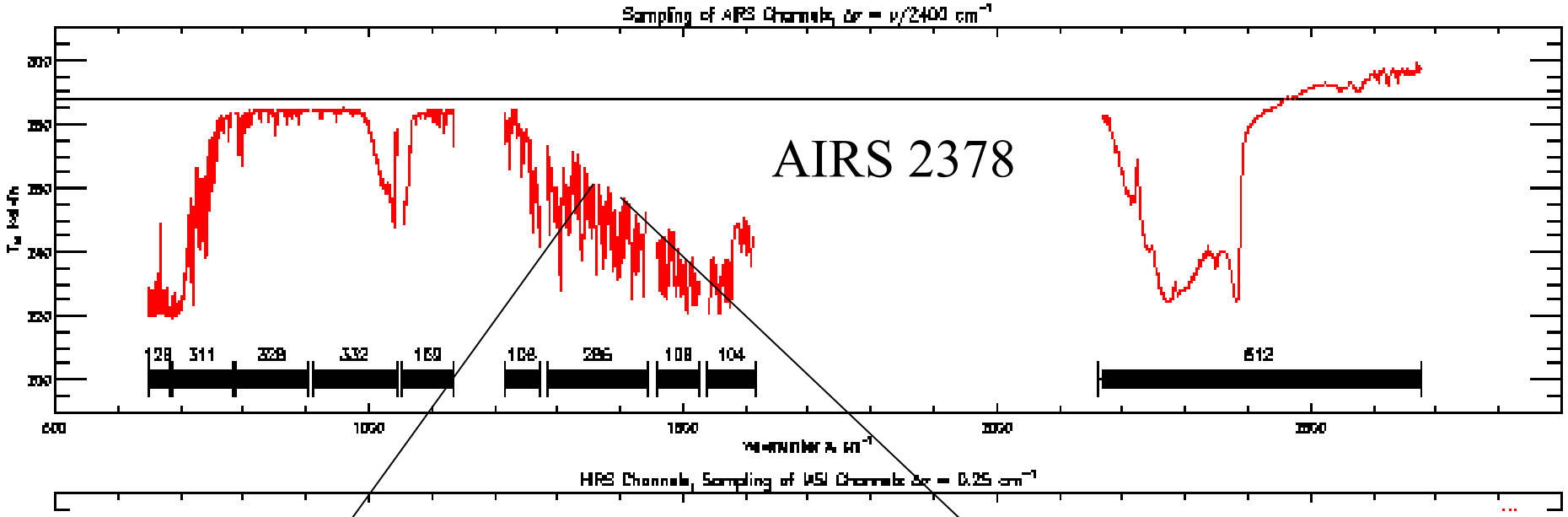

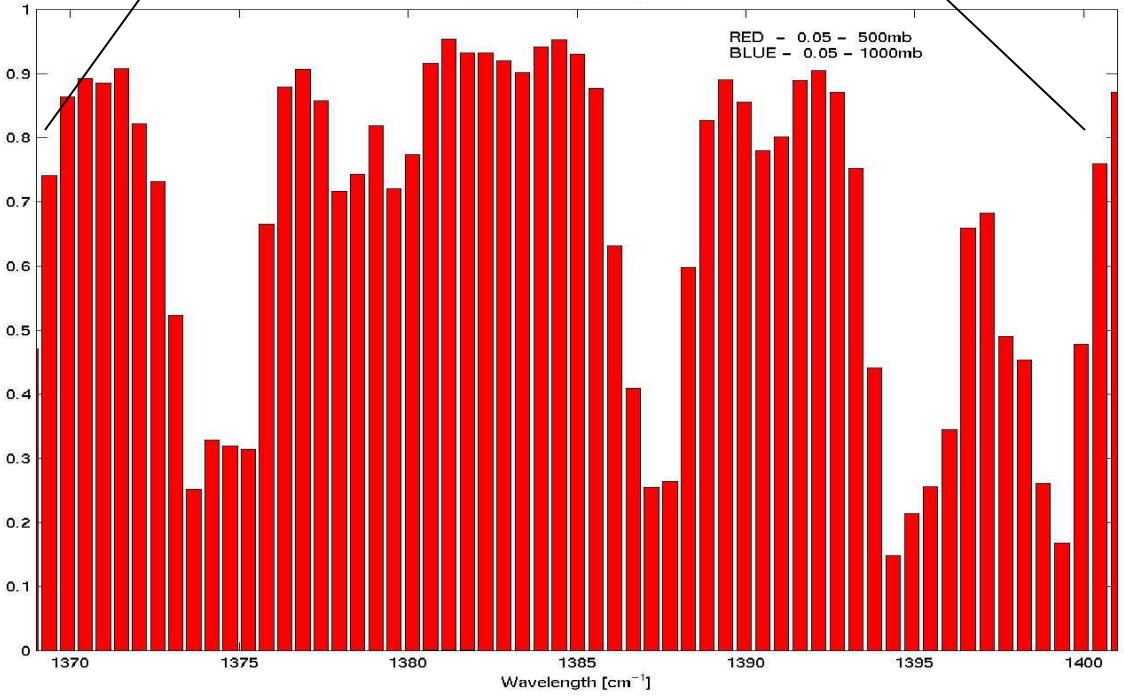

Transmittance within H20 absorption band

Atmospheric transmittance in H2O sensitive region of spectrum

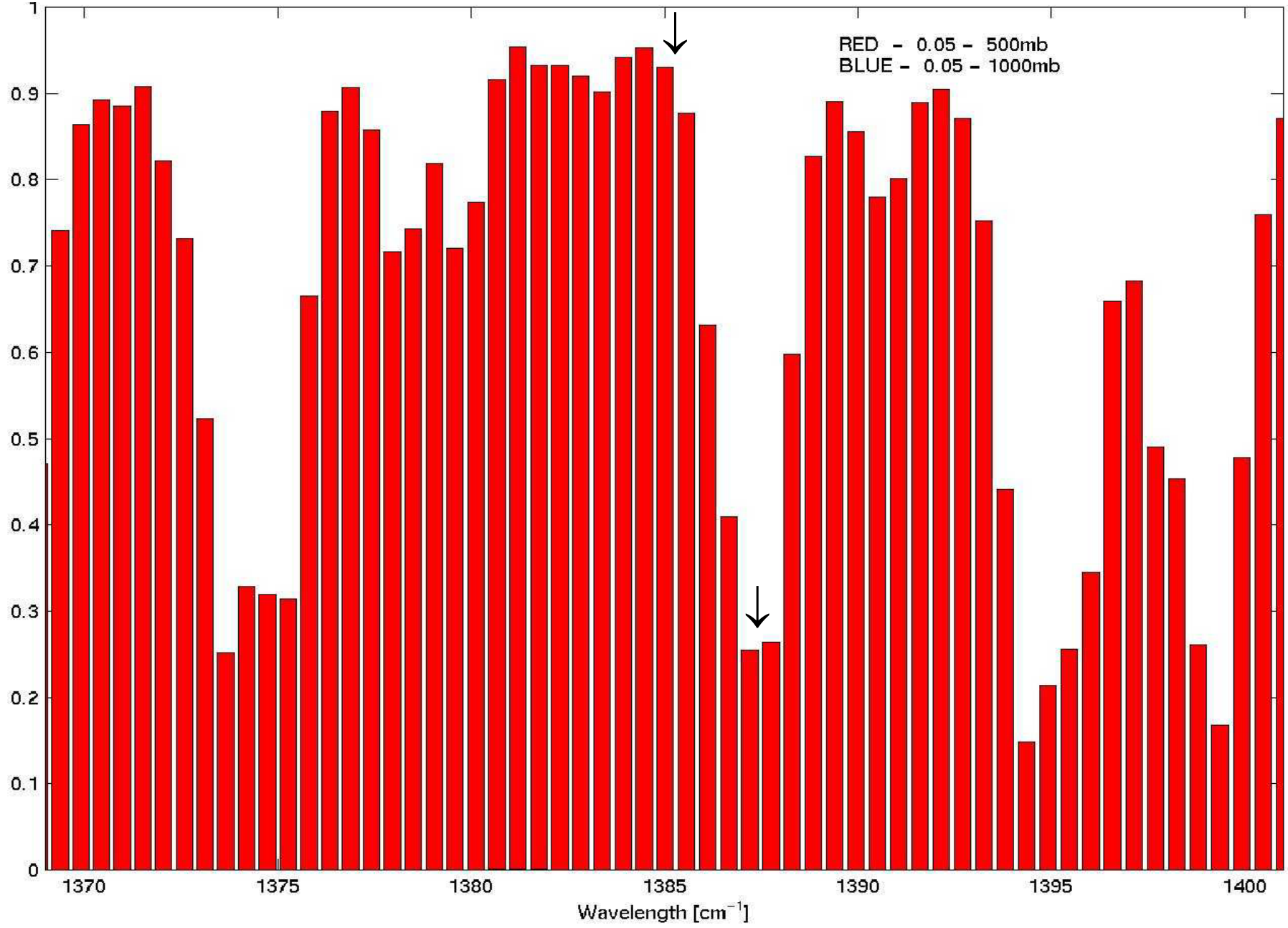

Spatial distribution of Ch 1552 at 1385.02 [1/cm] measurements [K]

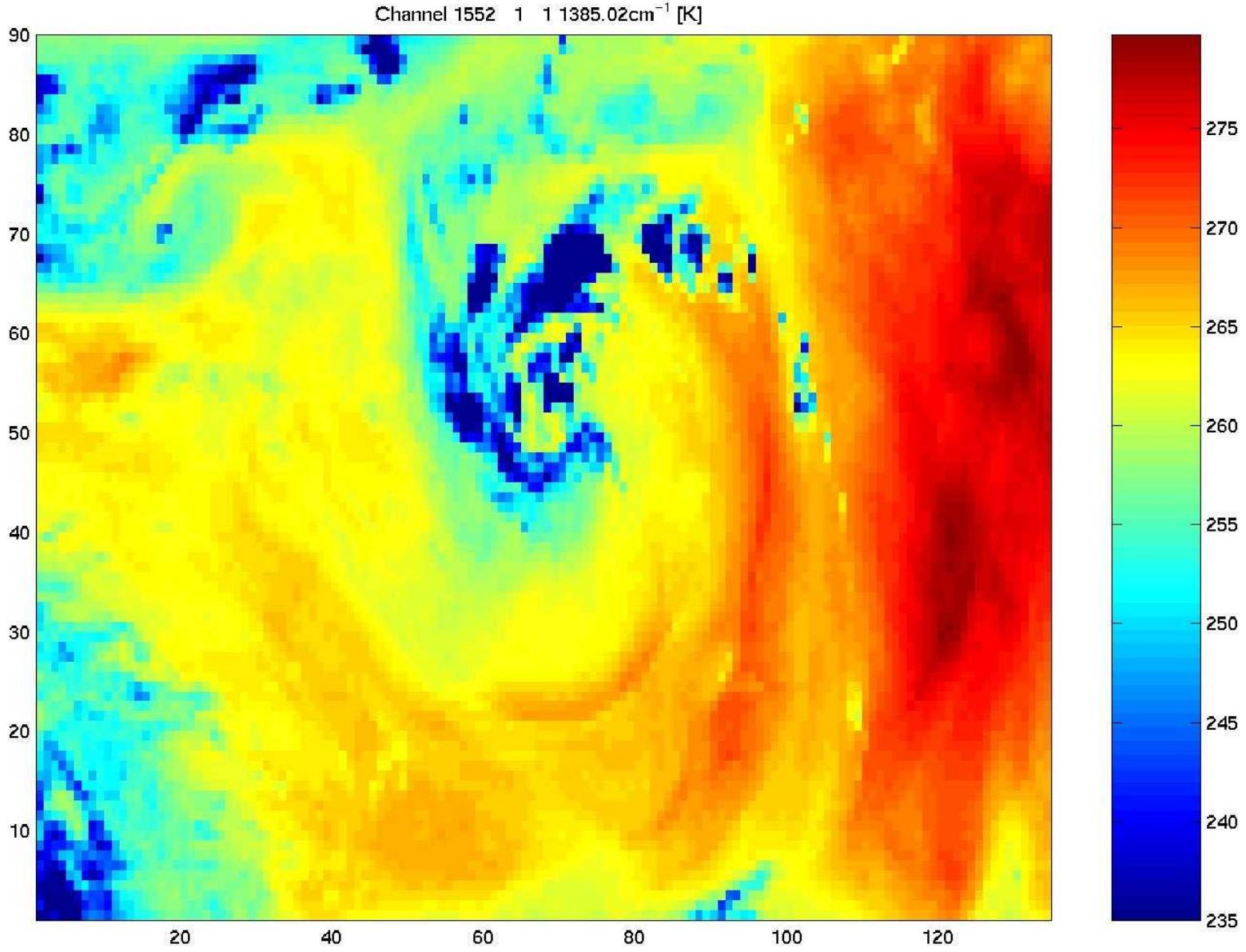

Spatial distribution of Ch 1553 at 1385.57 [1/cm] measurements [K]

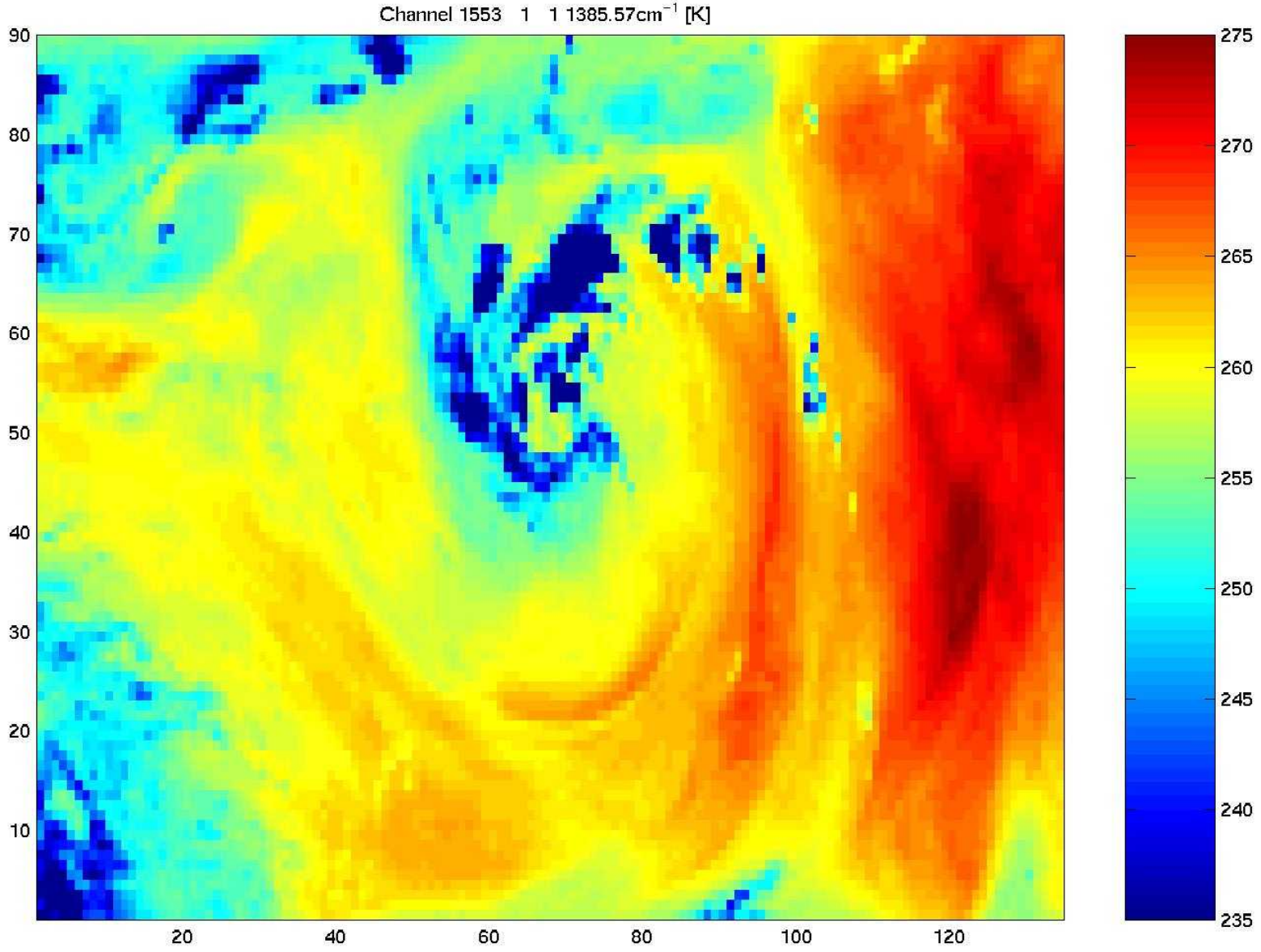

Spatial distribution of Ch 1554 at 1386.11 [1/cm] measurements [K]

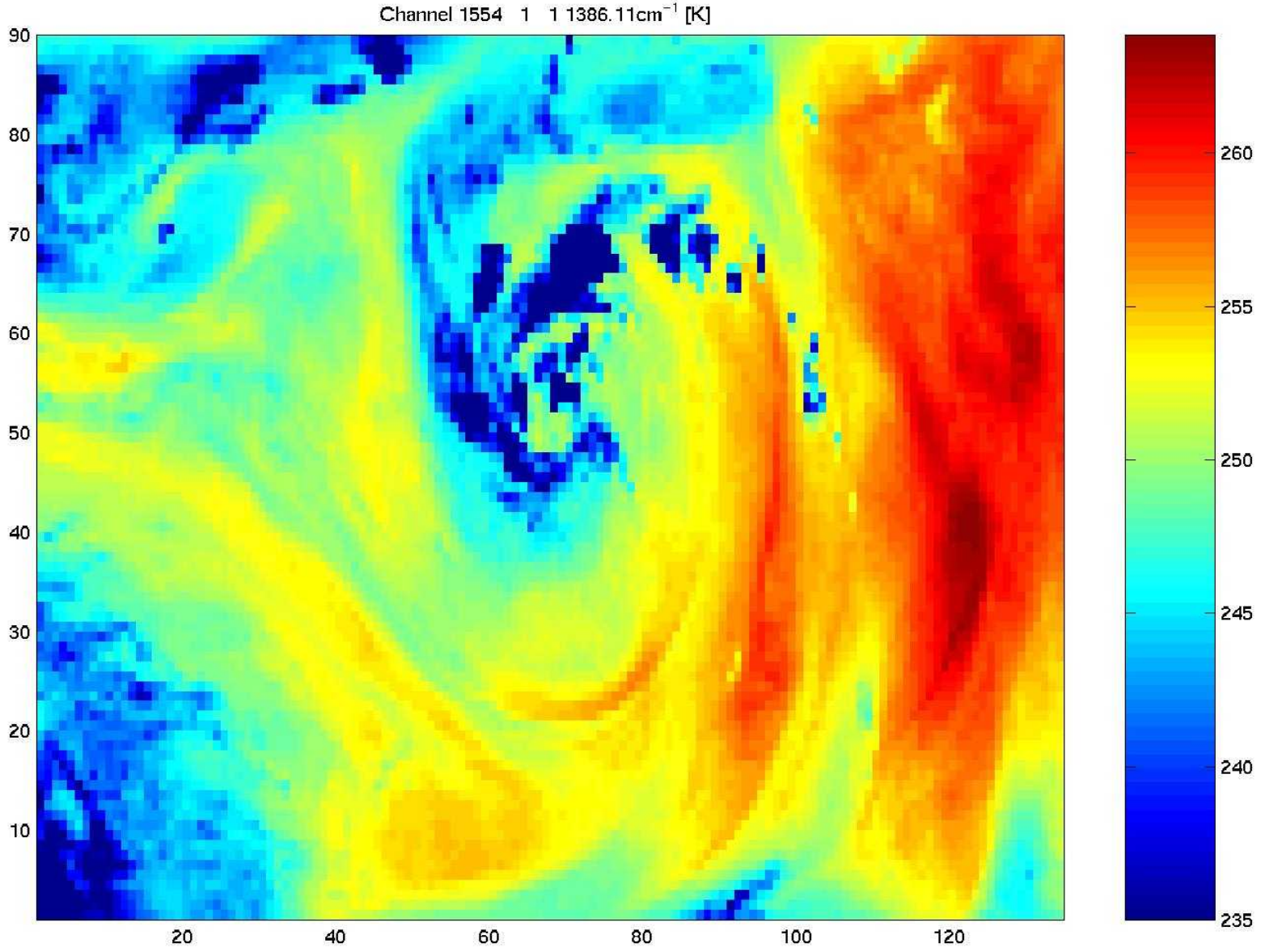

Spatial distribution of Ch 1555 at 1386.66 [1/cm] measurements [K]

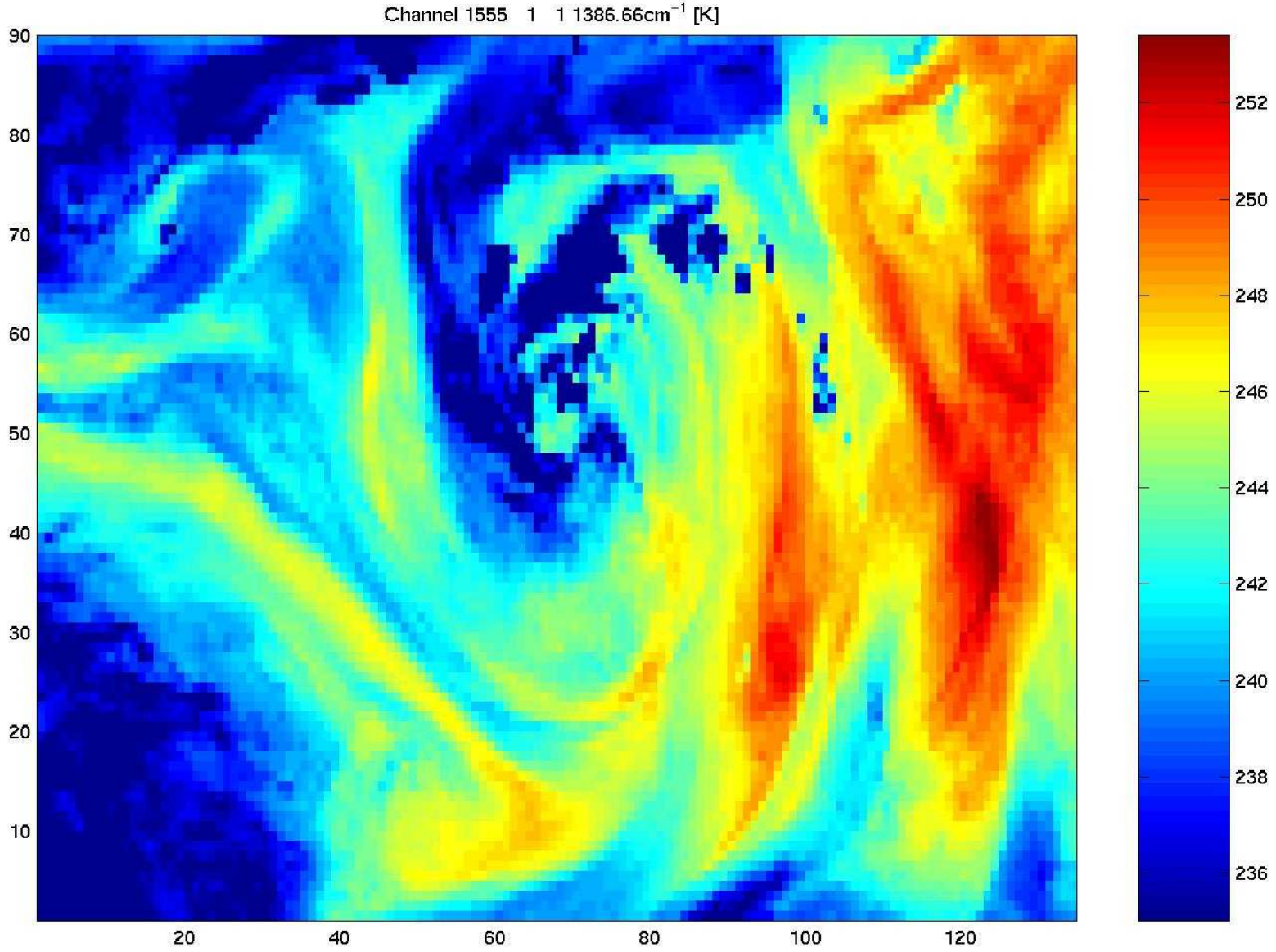

Spatial distribution of Ch 1556 at 1387.21 [1/cm] measurements [K]

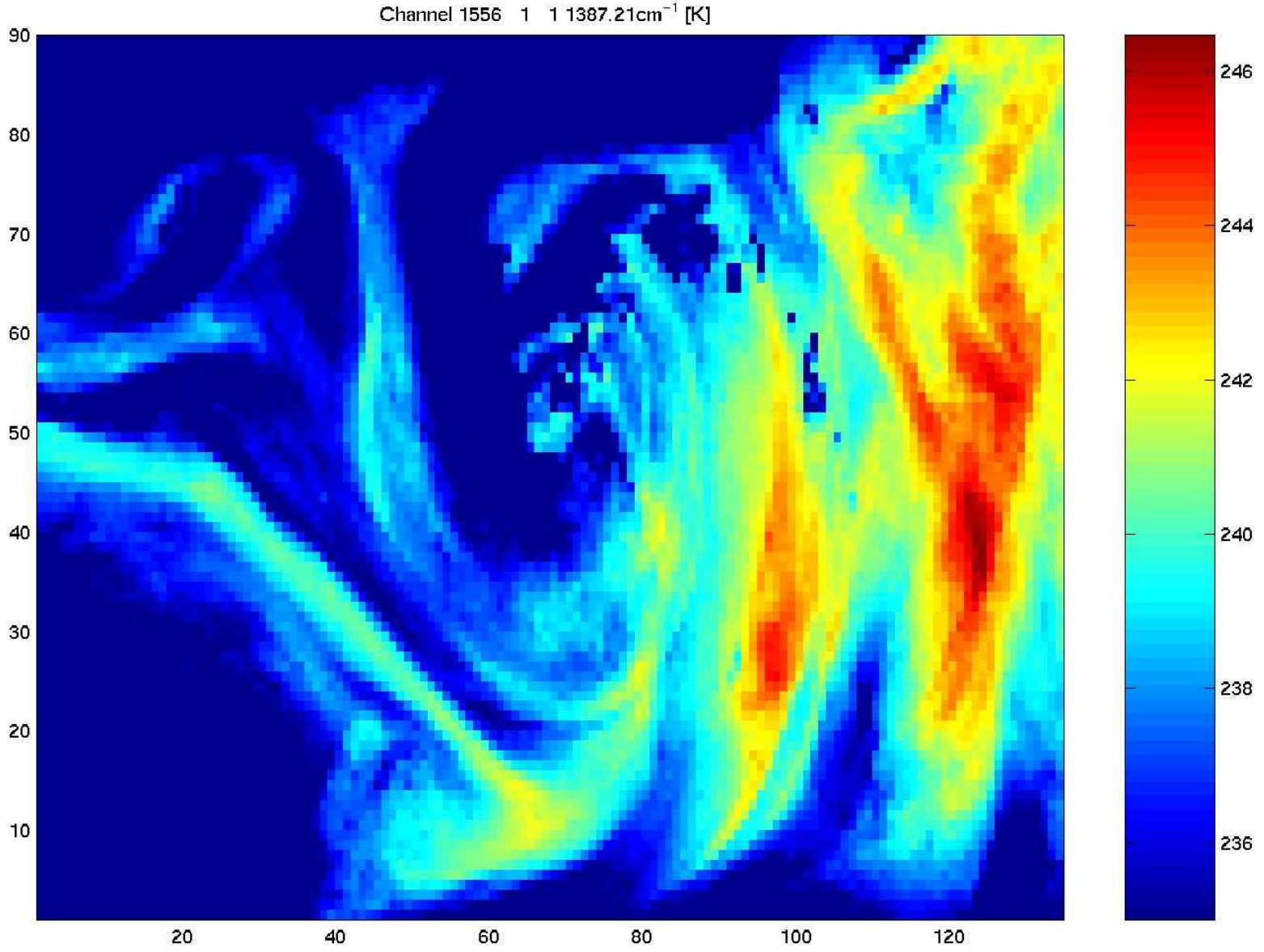

Atmospheric transmittance in H2O sensitive region of spectrum

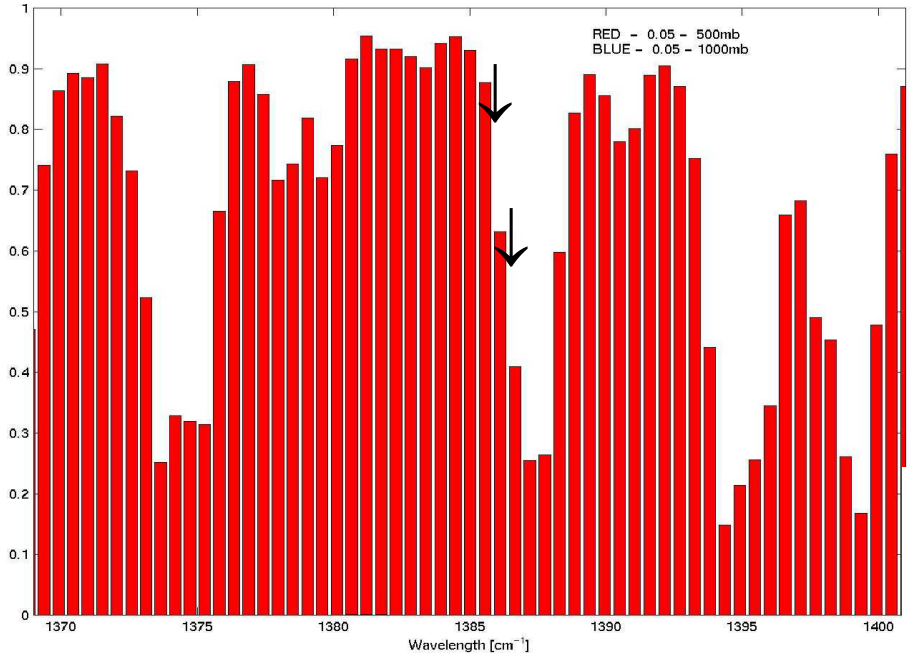

Studying spectral sensitivity with AIRS Data

AIRS BT[1386.11] – BT[1386.66]

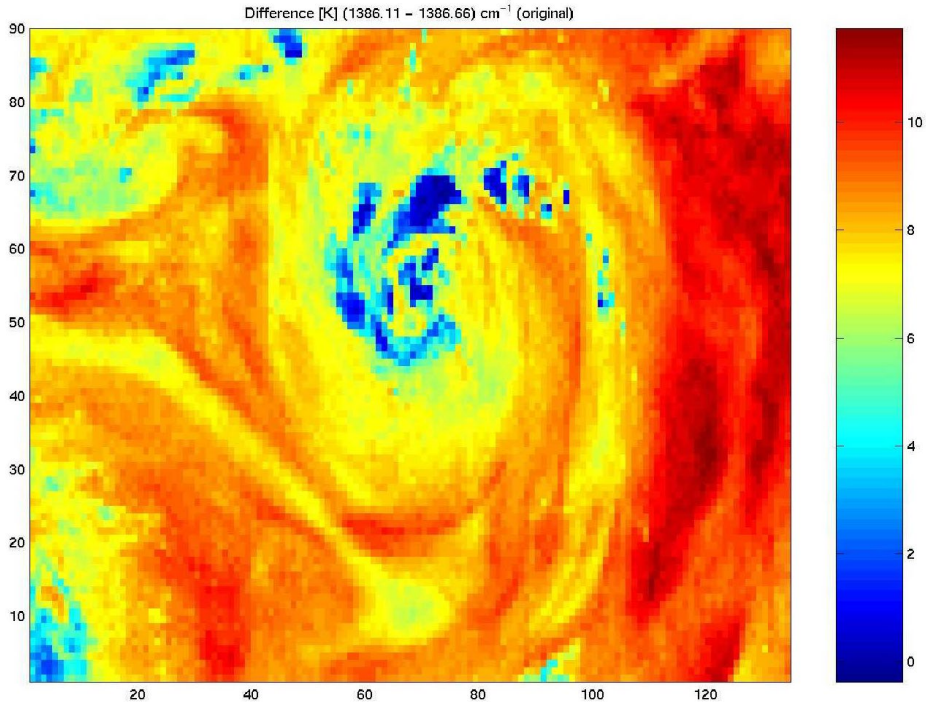

Spectral change of 0.5 cm-1 causes BT changes > 10 C

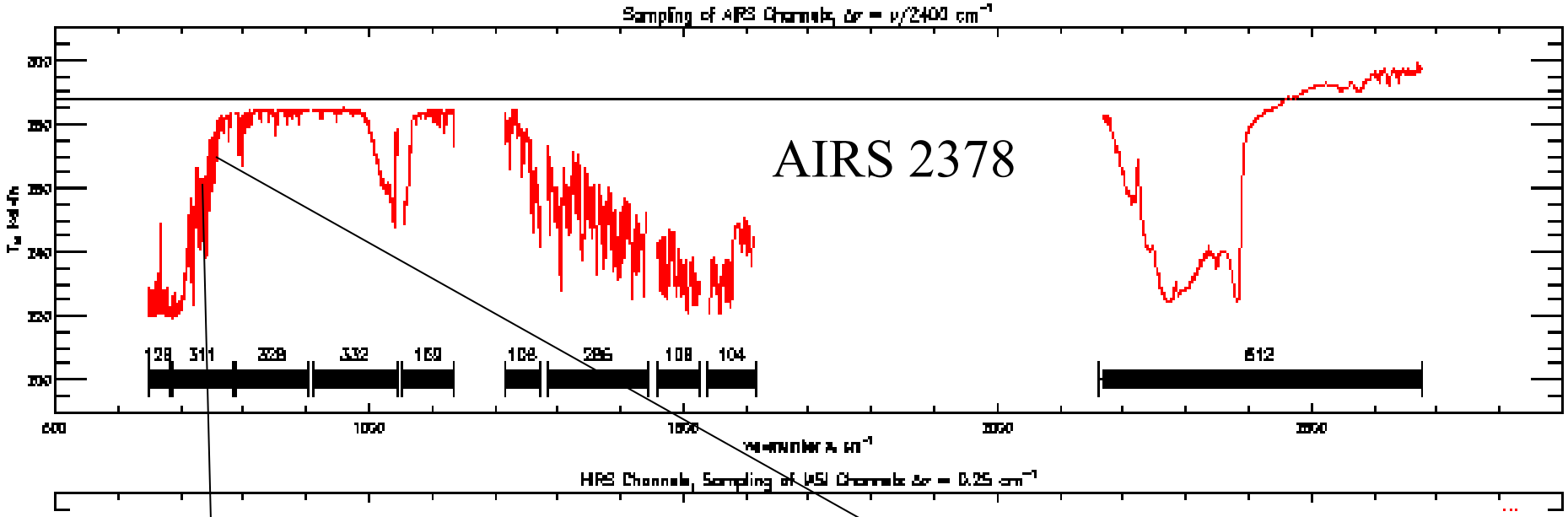

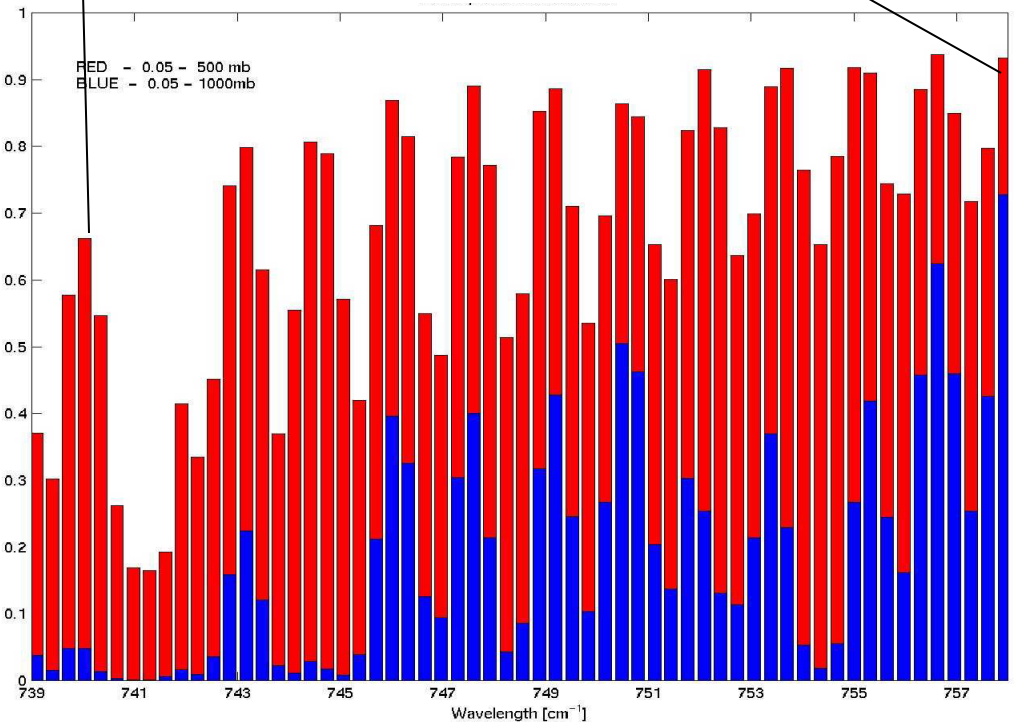

Transmittance within CO2 absorption band

Atmospheric transmittance in CO2 sensitive region of spectrum

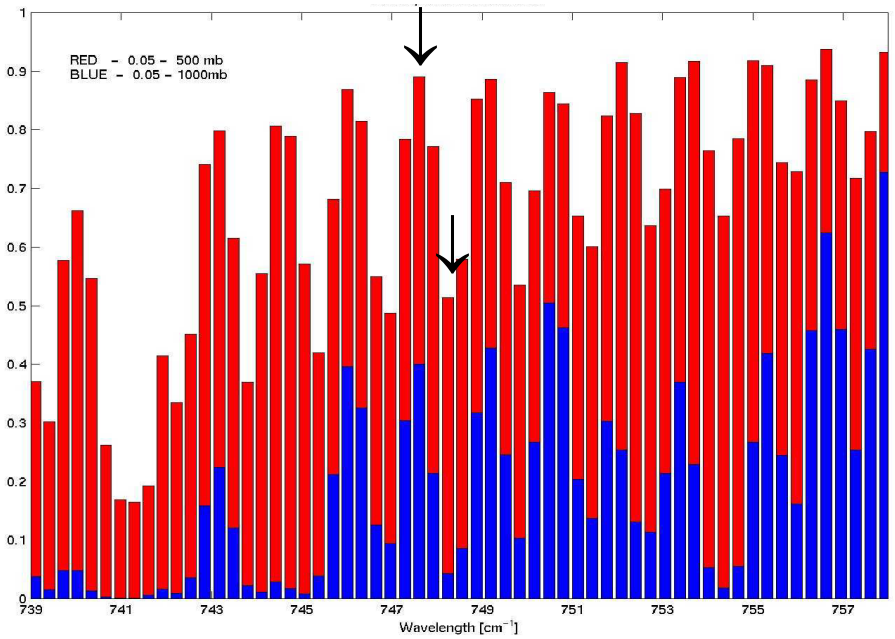

Studying spectral sensitivity with AIRS Data

AIRS BT[747.8] – BT[747.4]

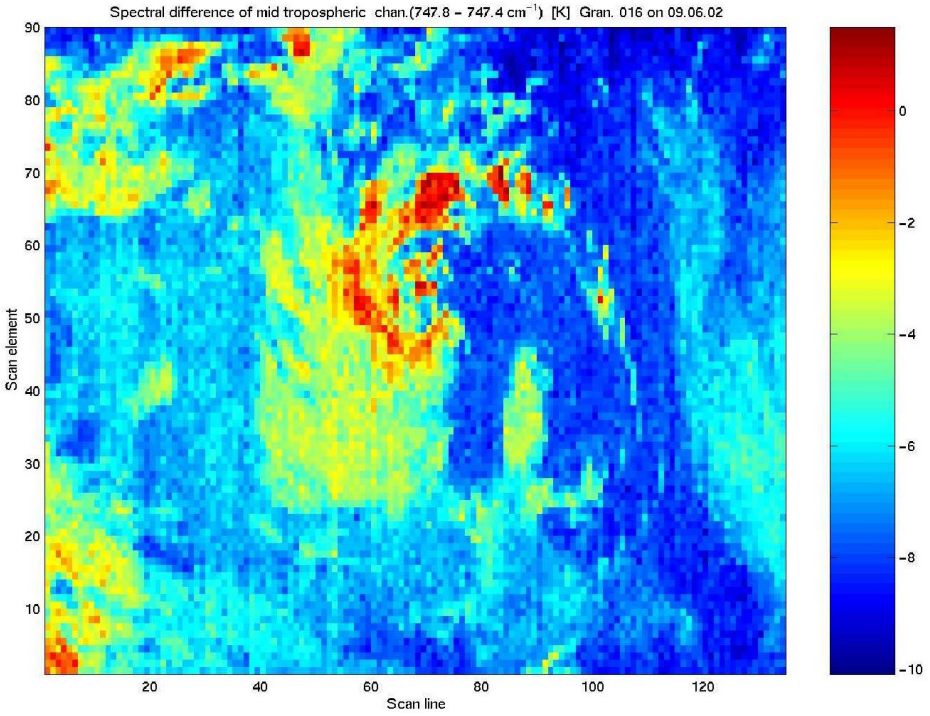

Spectral change of 0.4 cm-1 causes BT changes > 8 C

Radiosonde Validation

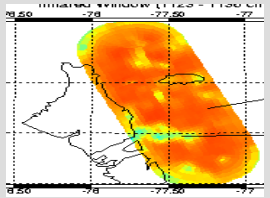

Andros Is. Bahamas, Sept 12, 1998

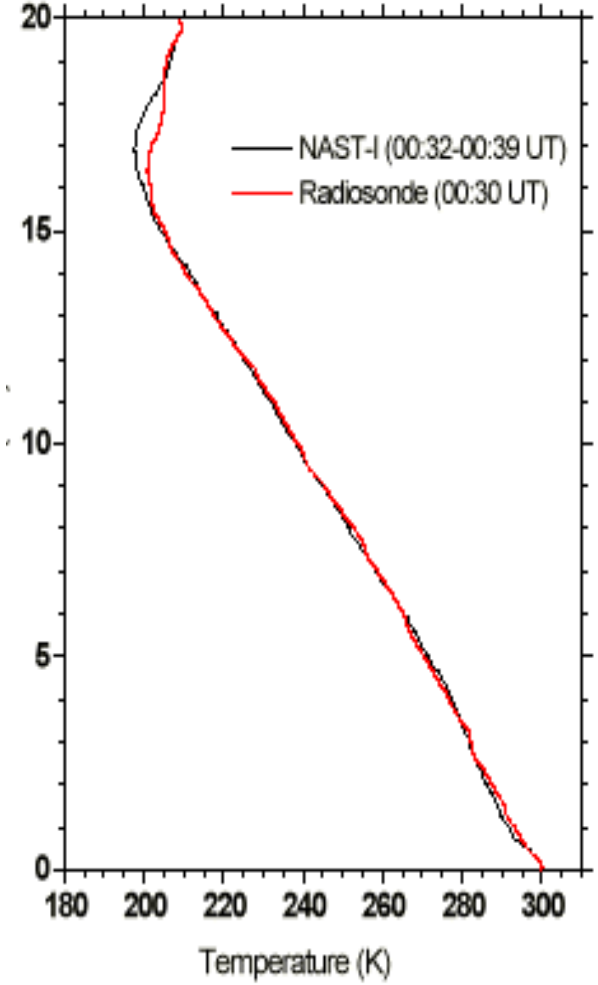

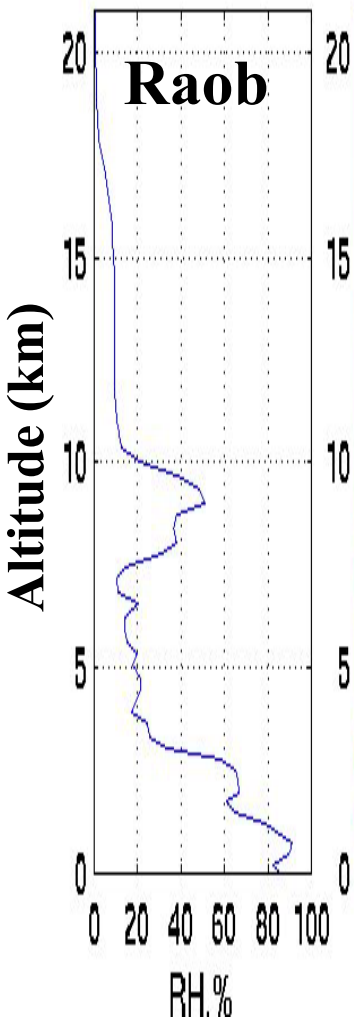

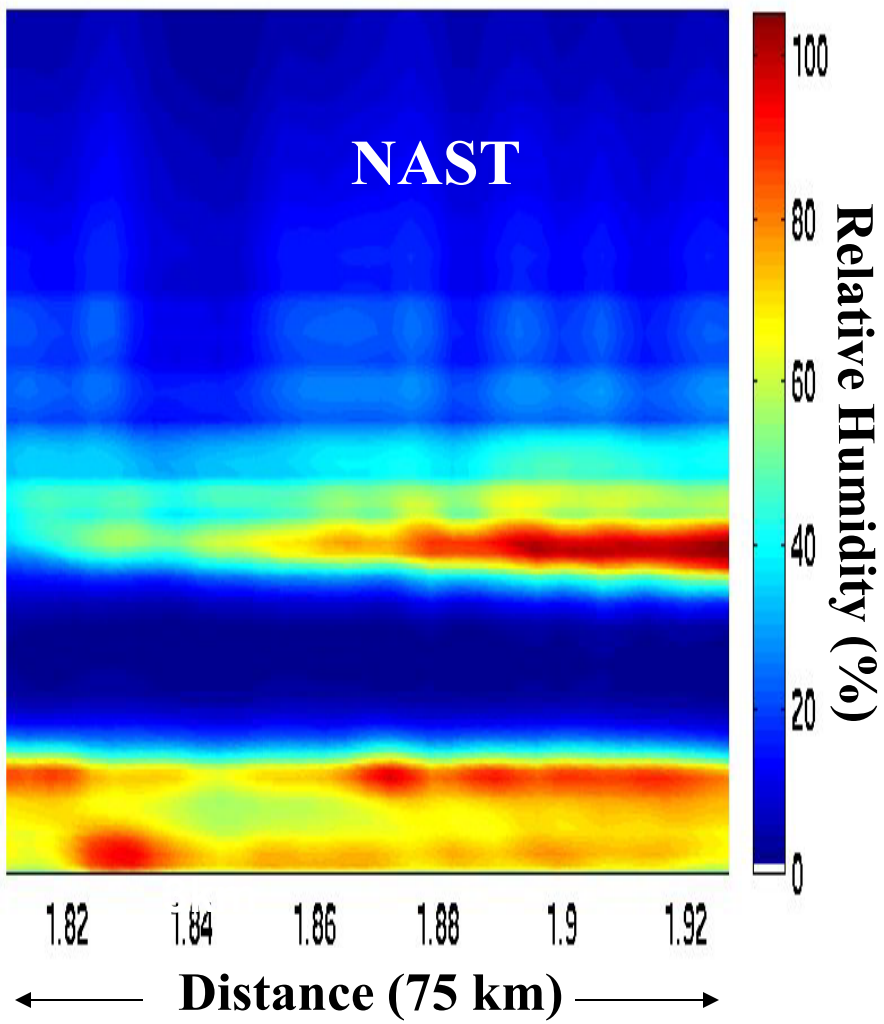

Spectral Signatures seen with AIRS

Lectures in Krakow
May 2006

Paul Menzel
NOAA/NESDIS/ORA

AIRS data from 28 Aug 2005

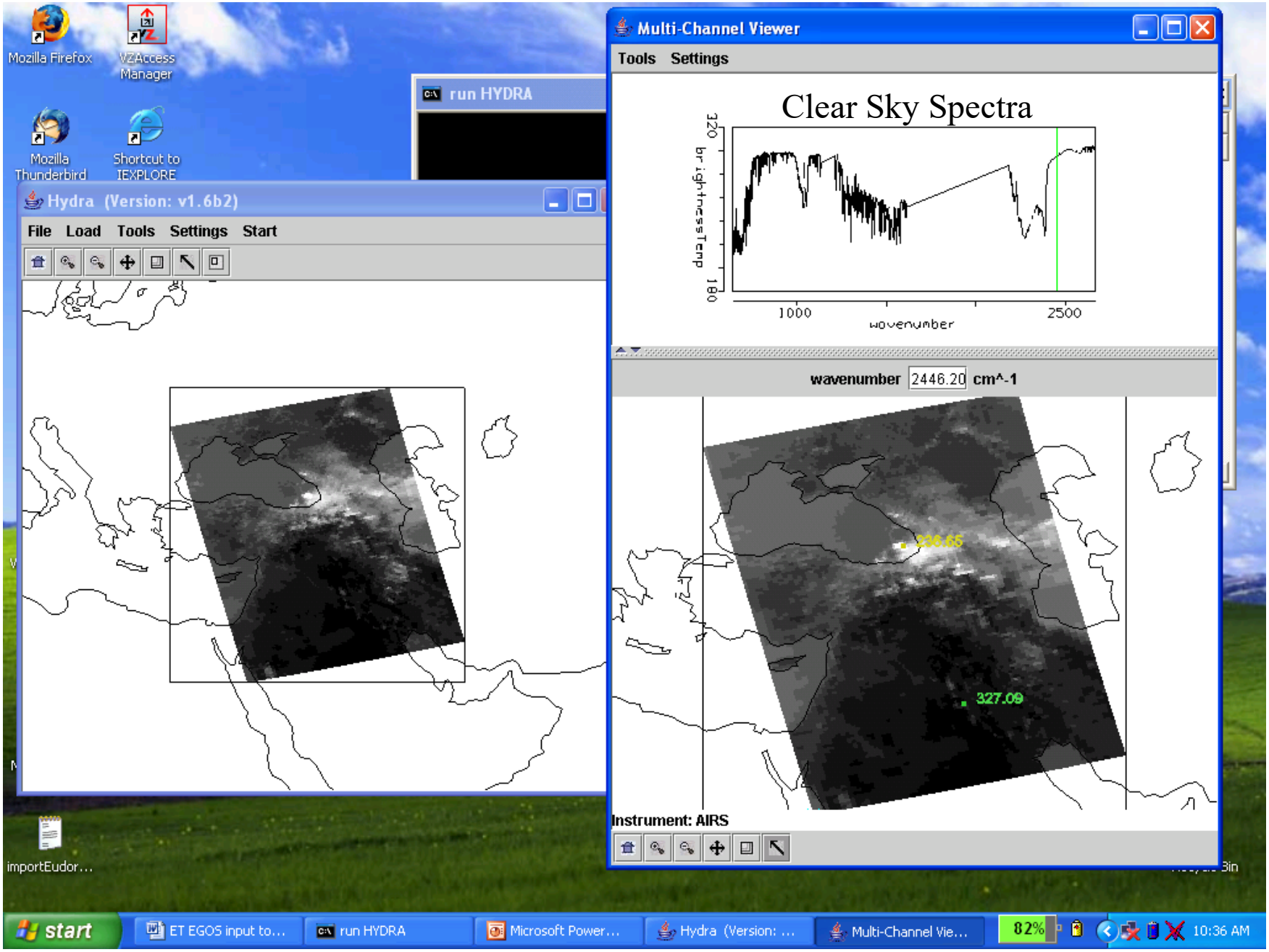

AIRS data from 28 Aug 2005

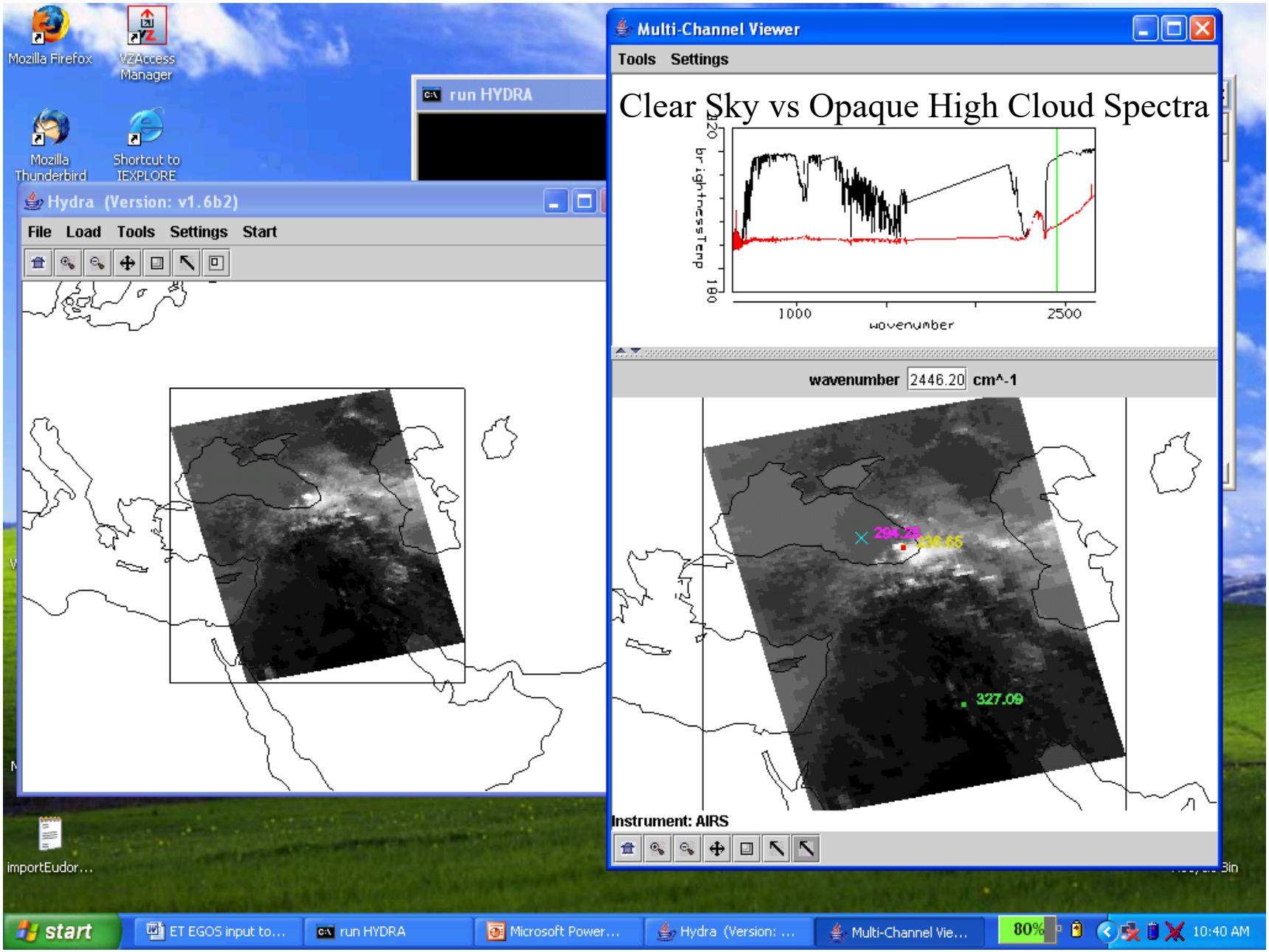

Zoom in
on spectra from cloudy fov
to see warming with height
above tropopause
in O3 absorption band

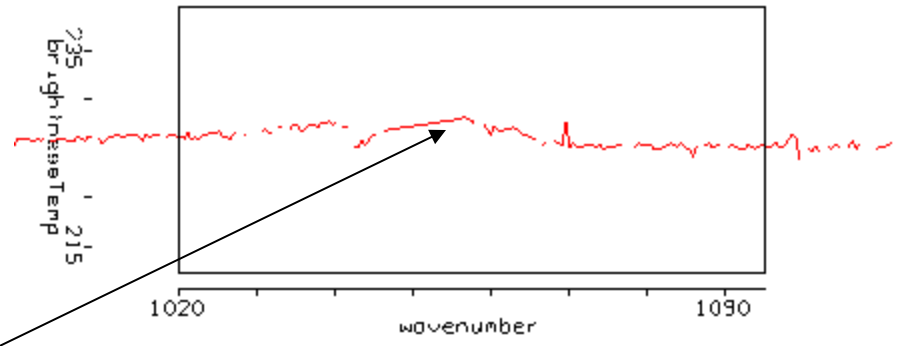

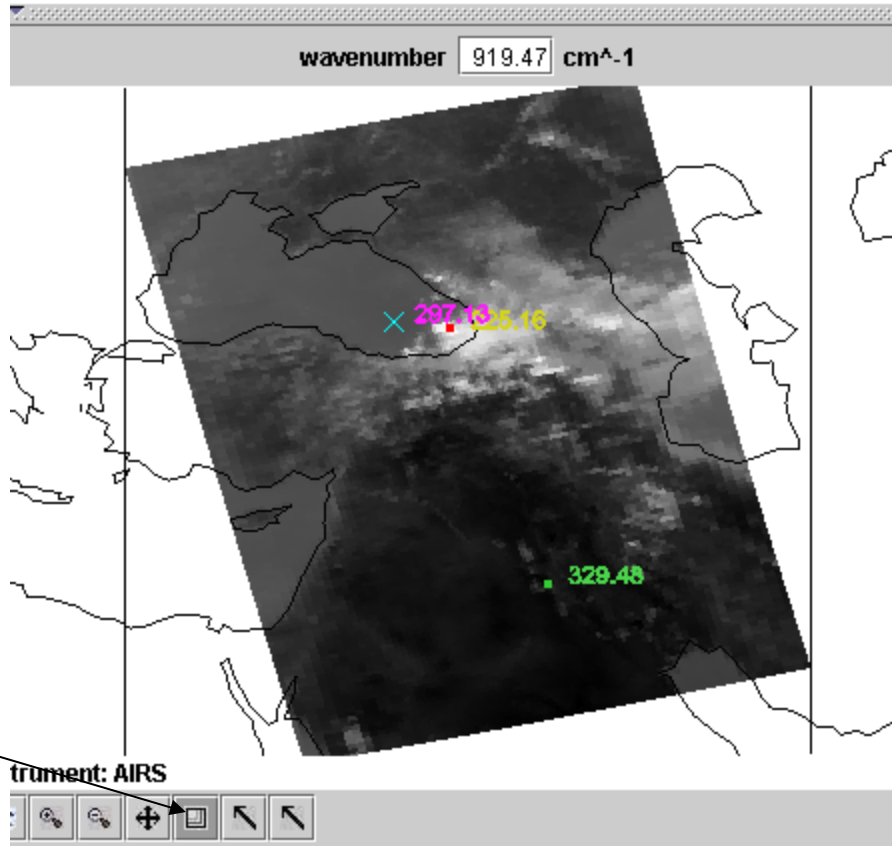

Zoom toolbar

High cloud at 250 hPa

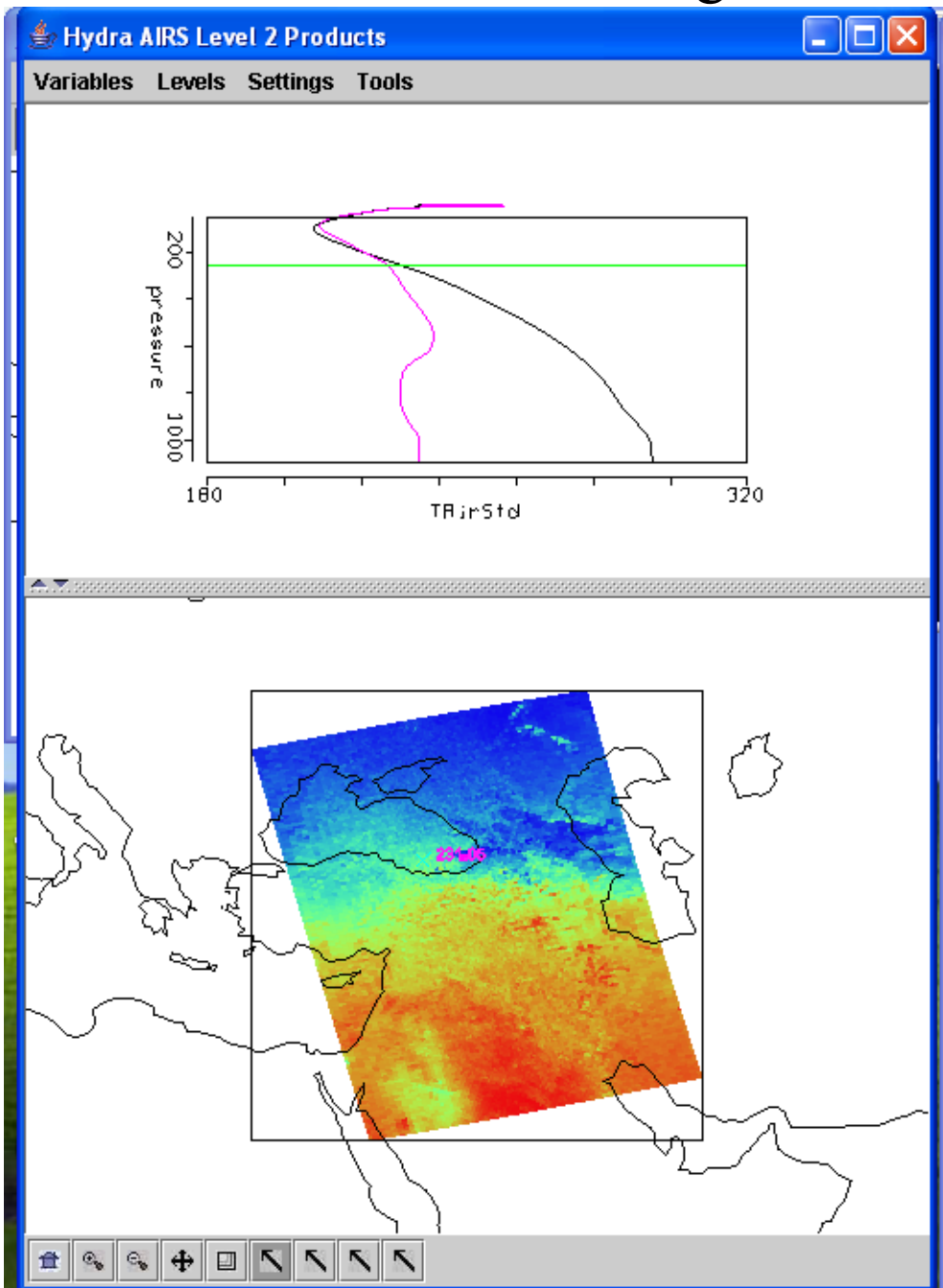

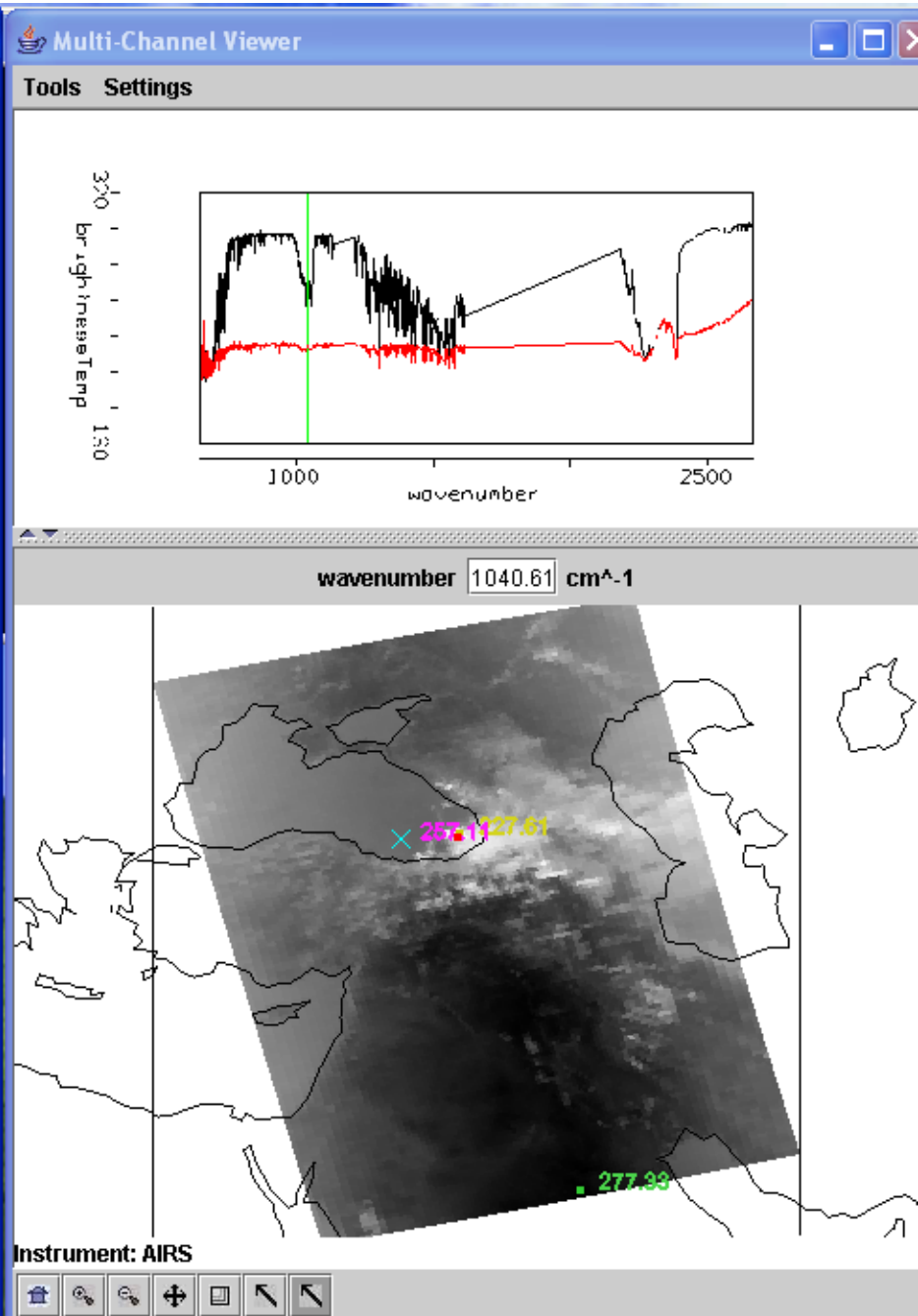

Offline-Online in LW CO2

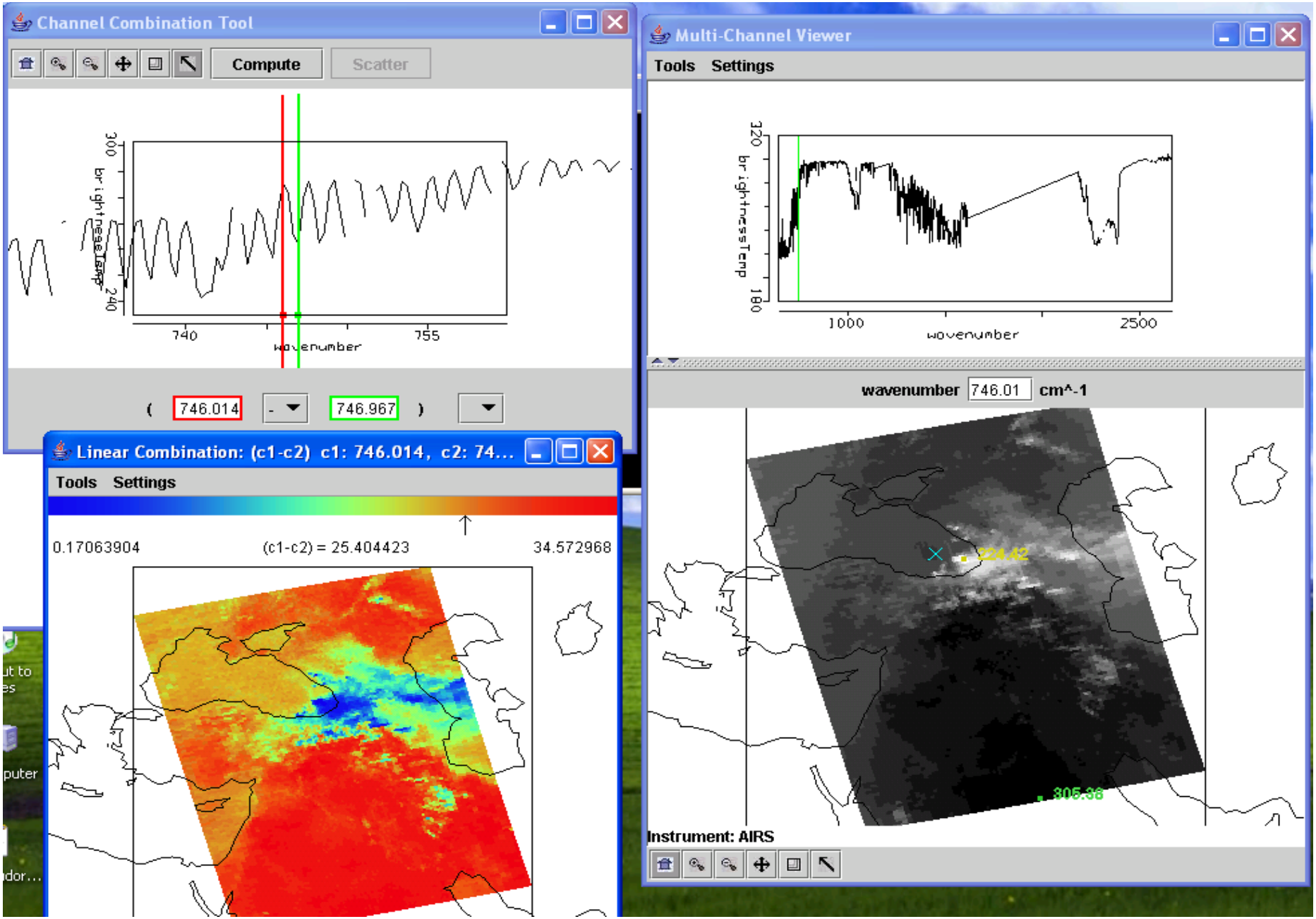

Offline-Online in H2O

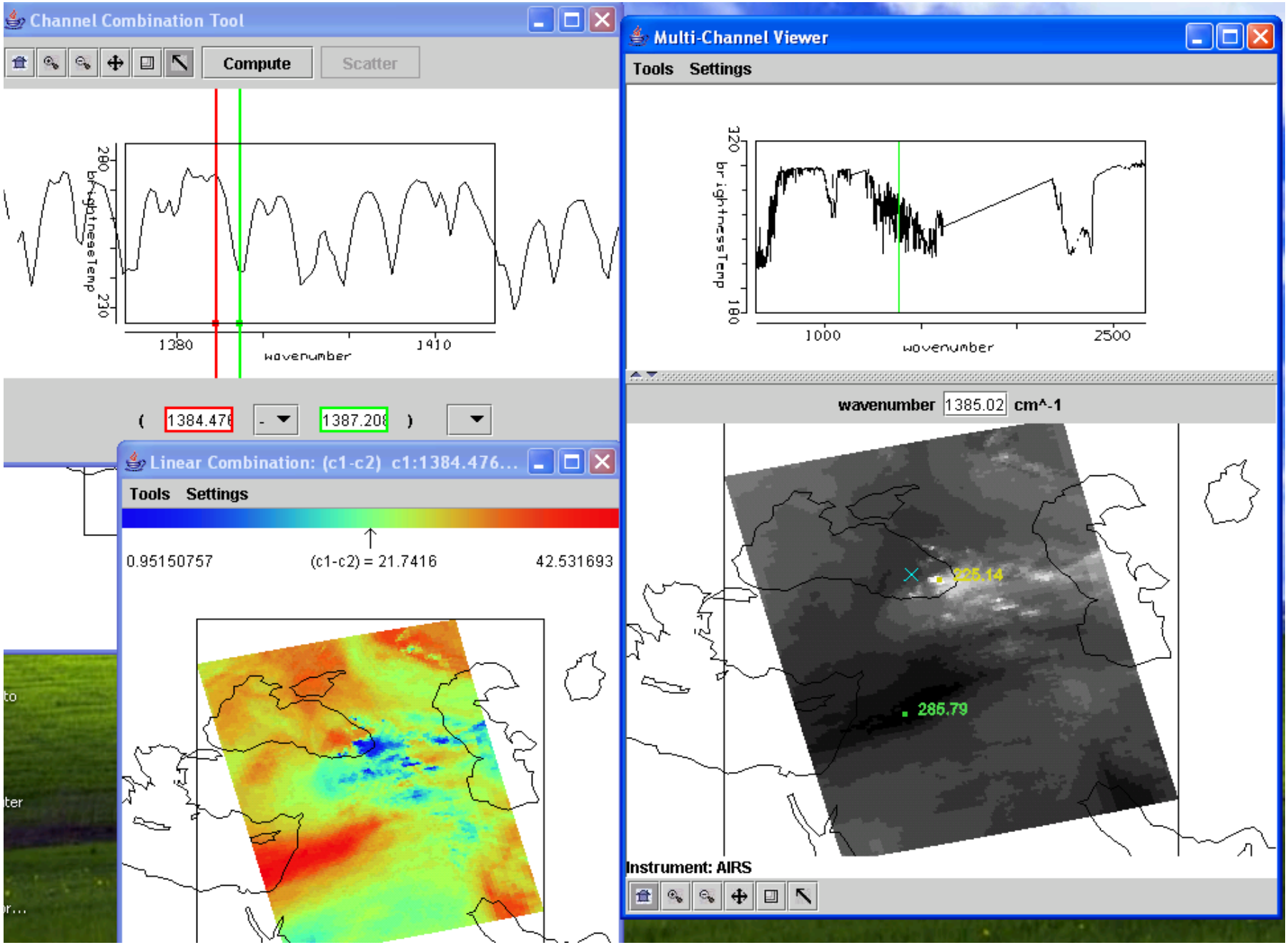

Offline-Online in LW IRW showing low level moisture

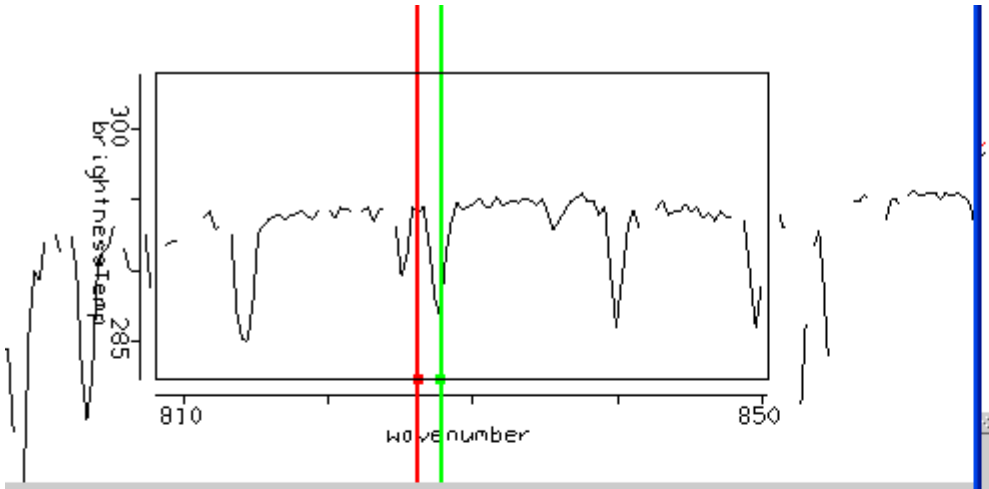

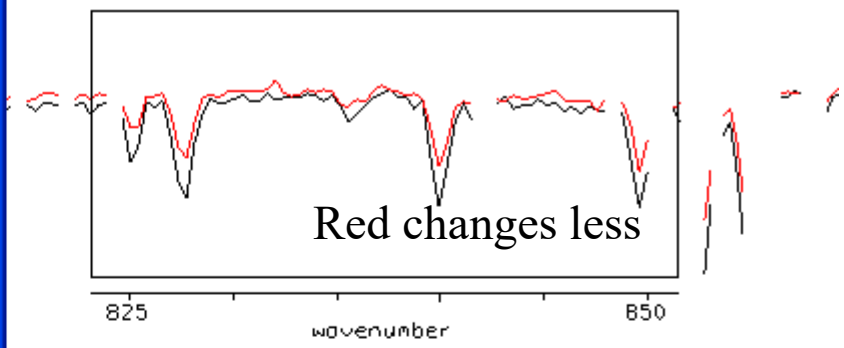

826.202 - 827.748) (------- -------)

wavenumber 919.47 cm^-1

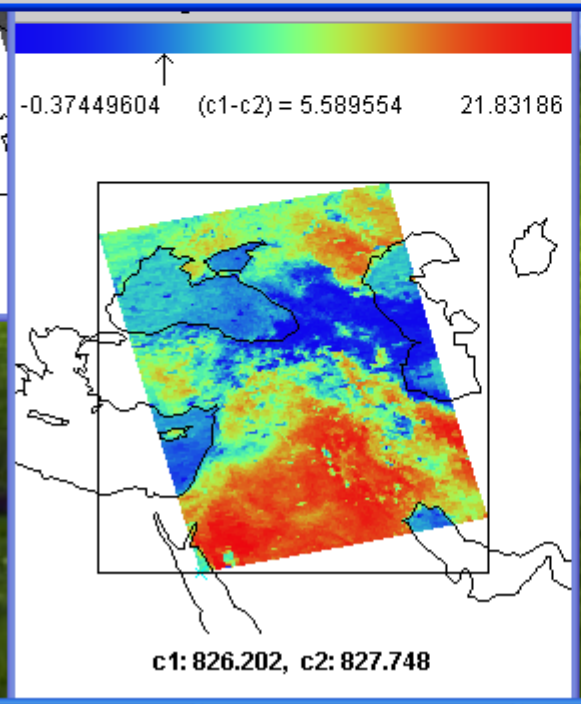

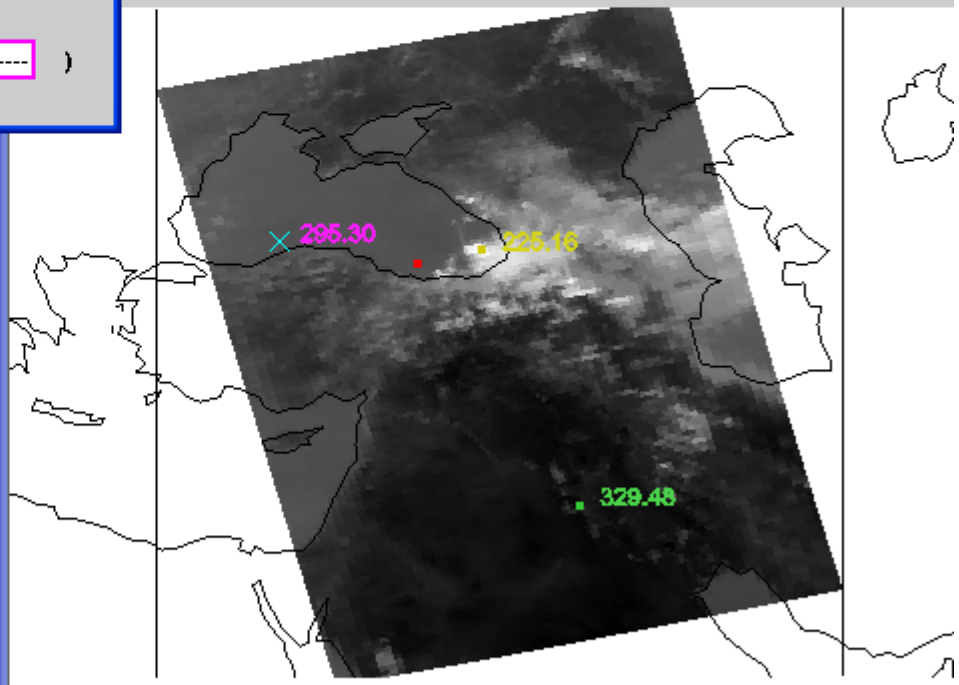

Moisture Profiles (left) confirm west Black Sea (black) is more moist

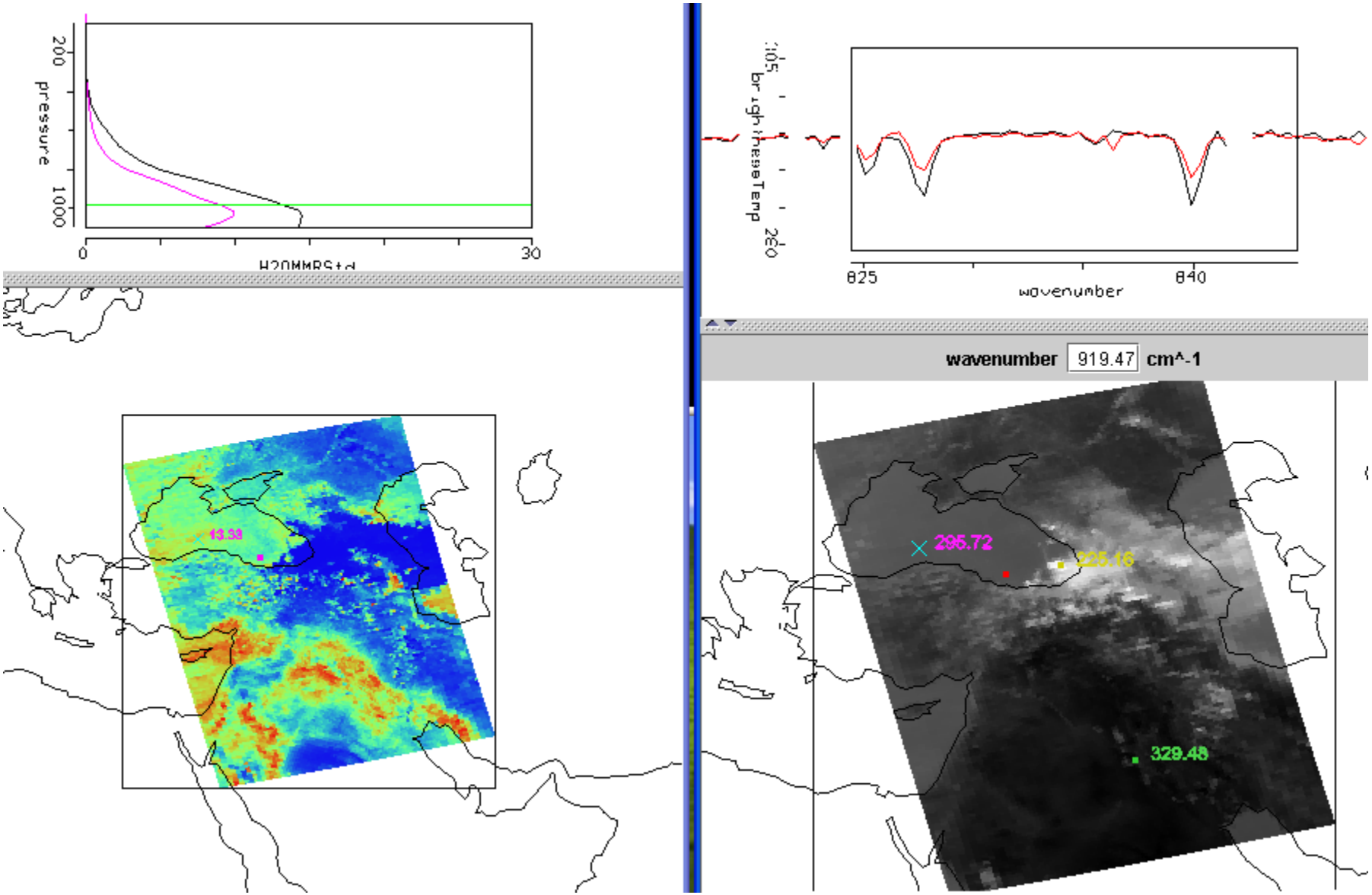

AIRS Spectra from around the Globe

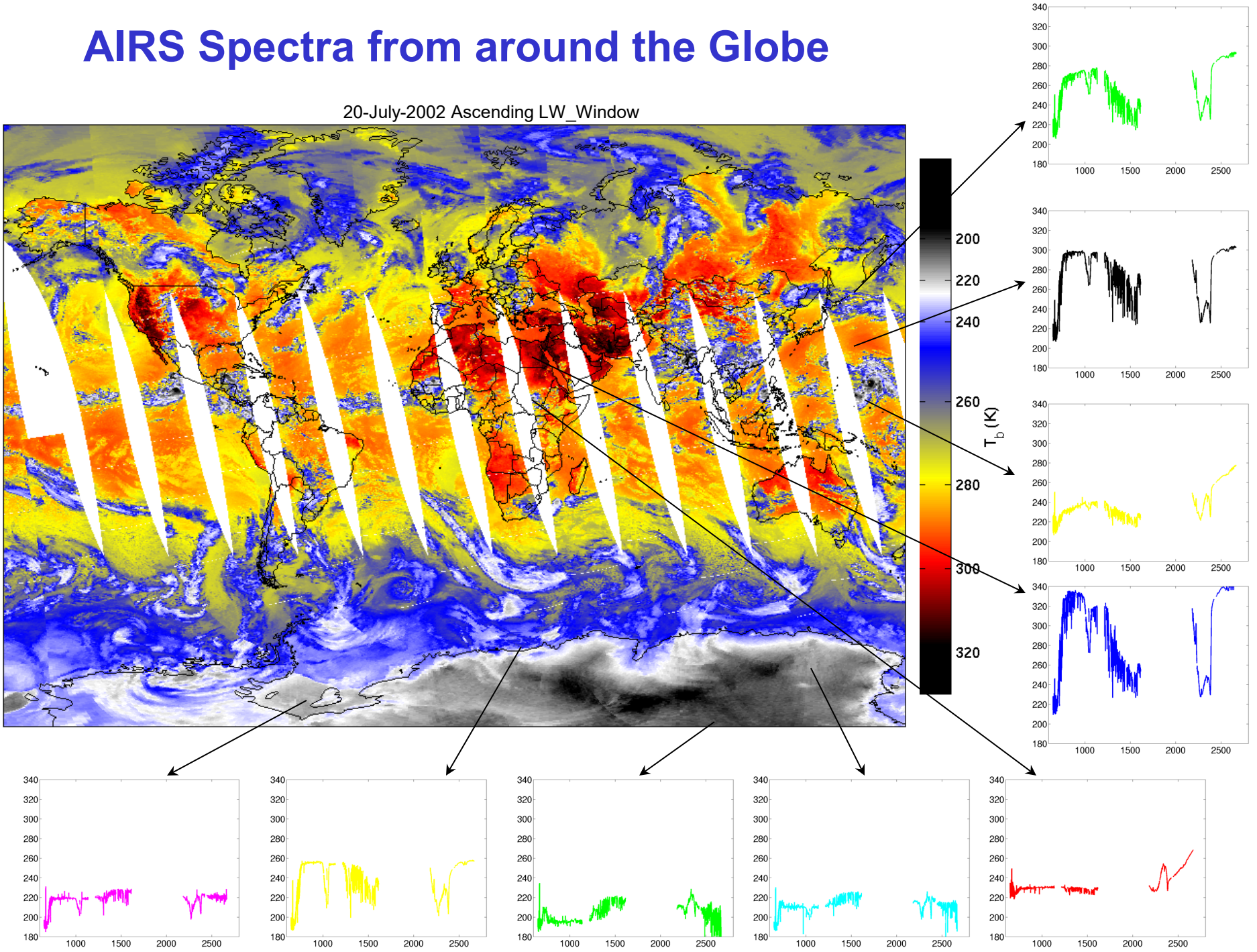

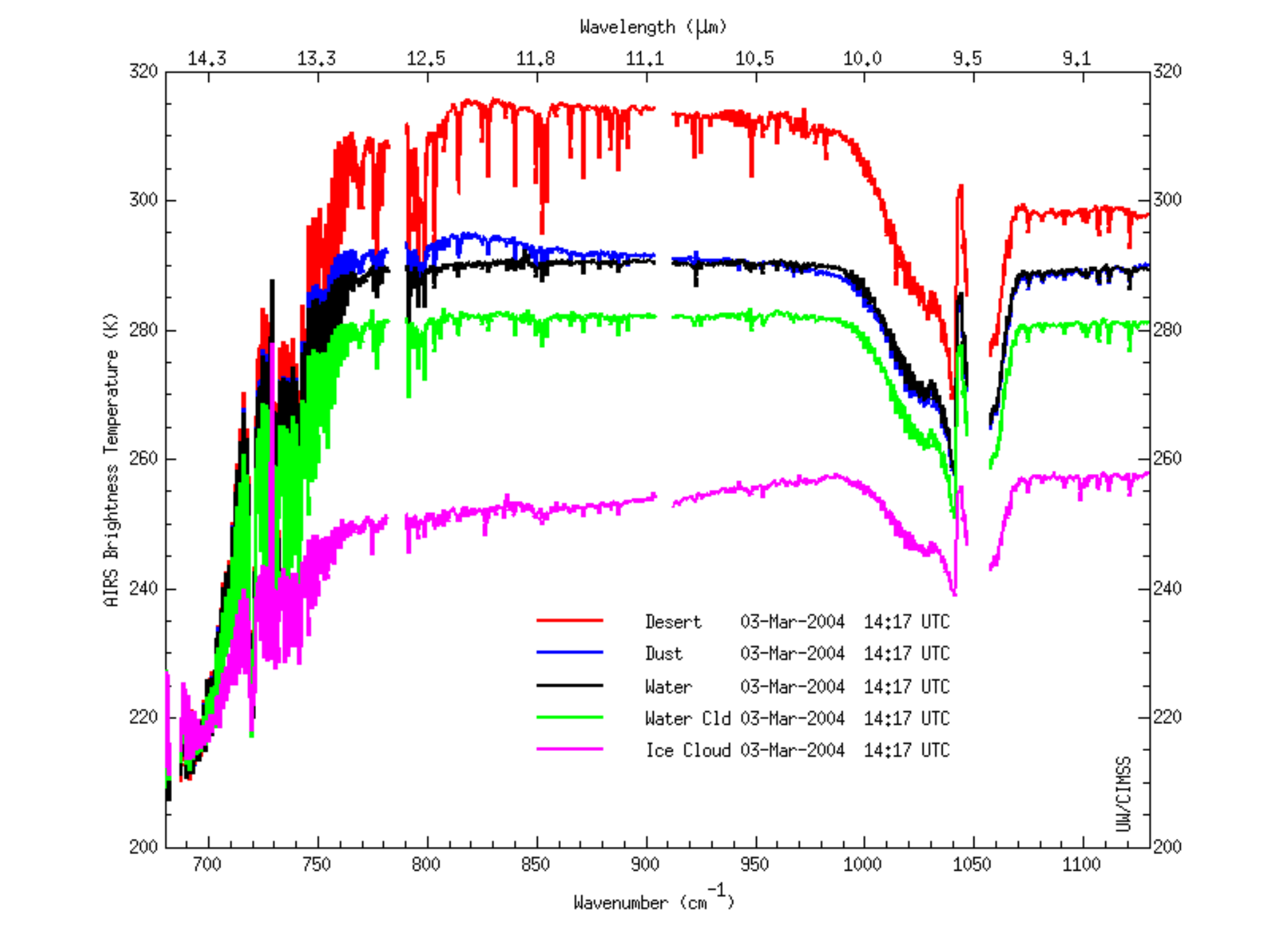
Wavelength (μm)
14.3
13.3
12.5
11.8
11.1
10.5
10.0
9.5
9.1
AIRS Brightness Temperature (K)
320
300
280
260
240
220
200
700
750
800
850
900
950
1000
1050
1100
Wavenumber (cm-1)
Desert 03-Mar-2004 14:17 UTC
Dust 03-Mar-2004 14:17 UTC
Water 03-Mar-2004 14:17 UTC
Water Cld 03-Mar-2004 14:17 UTC
Ice Cloud 03-Mar-2004 14:17 UTC
UW/CIMSS

Brightness Temperature Spectra reveal changes in atmosphere from eye to boundary of Tropical Cyclone

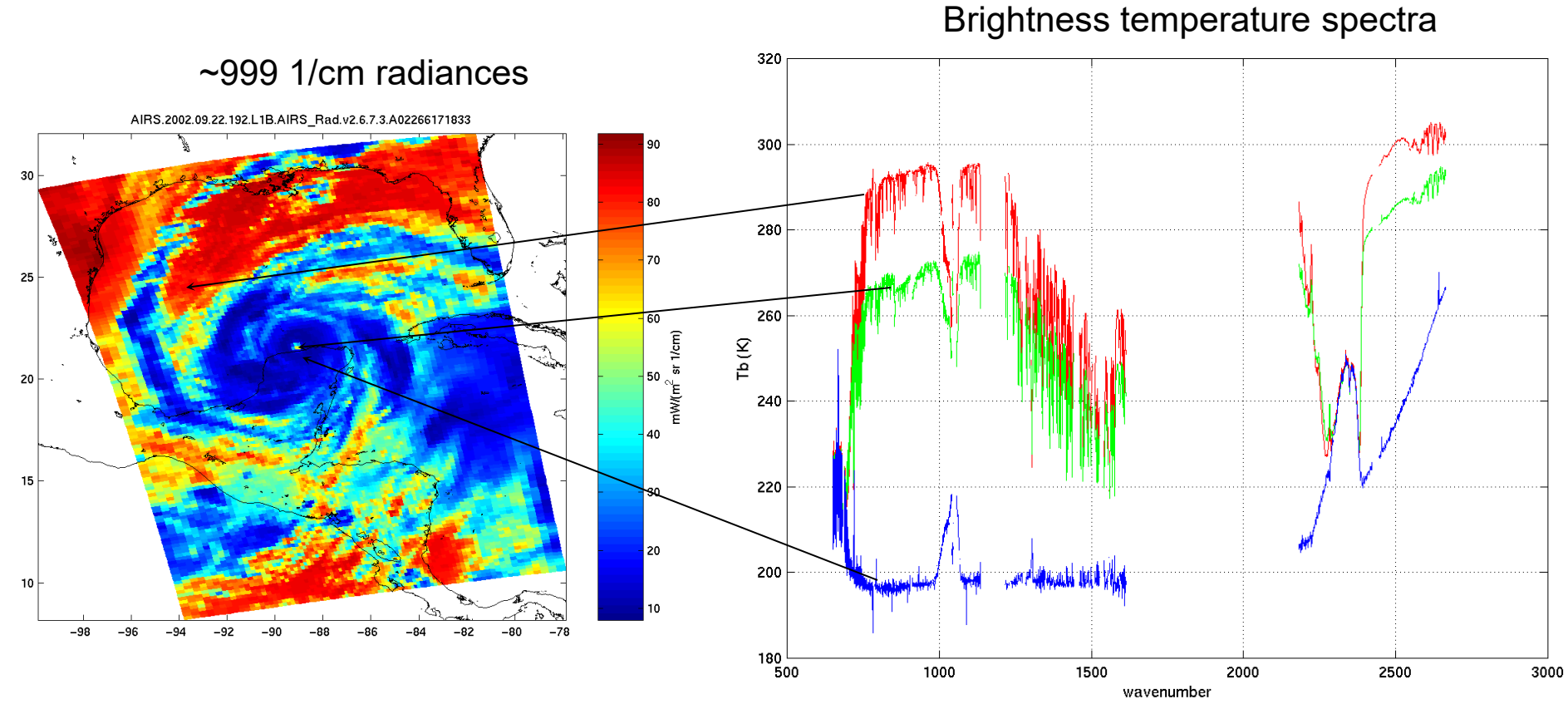

AIRS observations of tropical storm Isadore
on 22 Sept 2002 @ ~19:12-19:18 UTC

Inferring surface properties with AIRS high spectral resolution data

Barren region detection if T1086 < T981

Barren vs Water/Vegetated

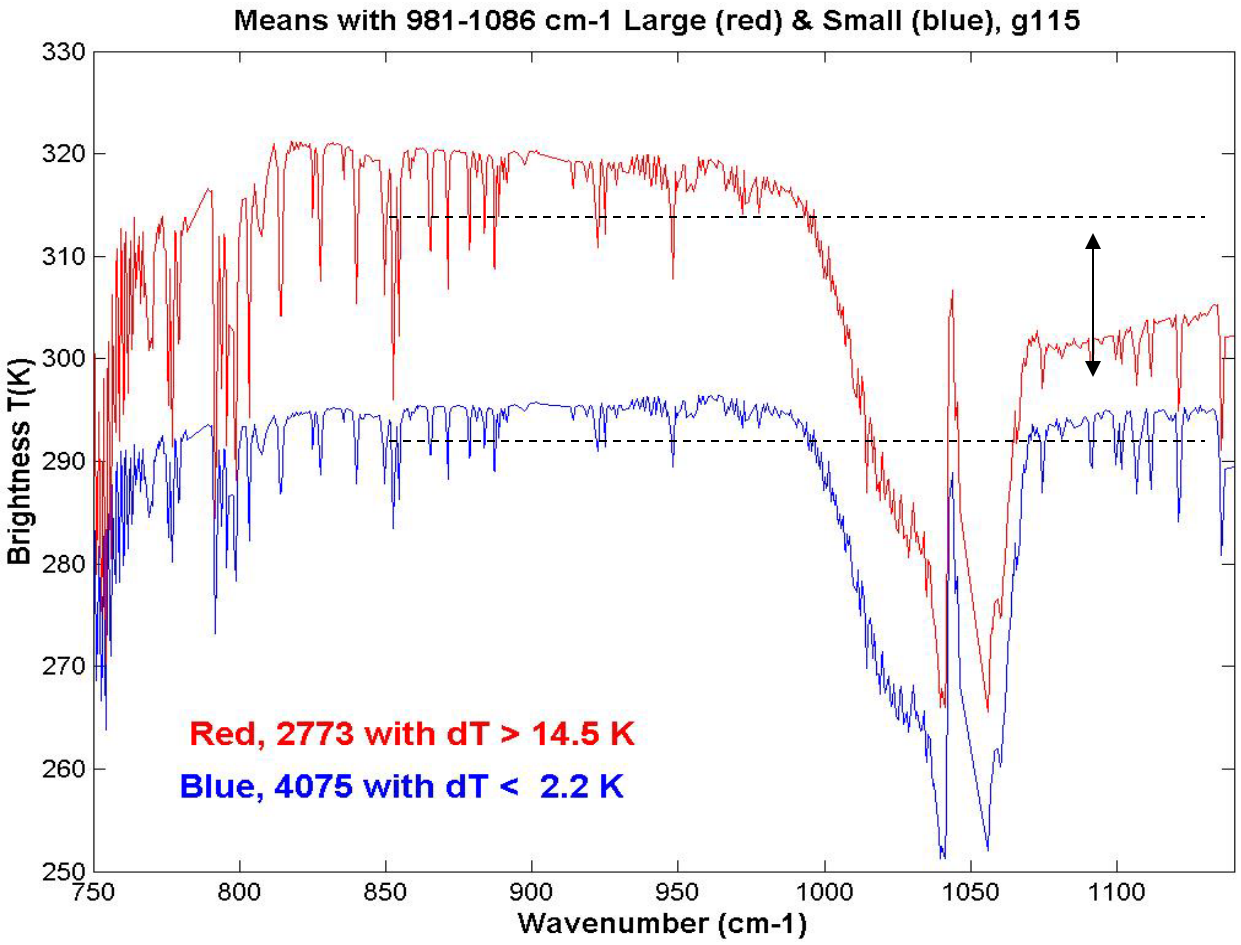

AIRS data from 14 June 2002

T(981 cm^{-1})-T(1086 cm^{-1})

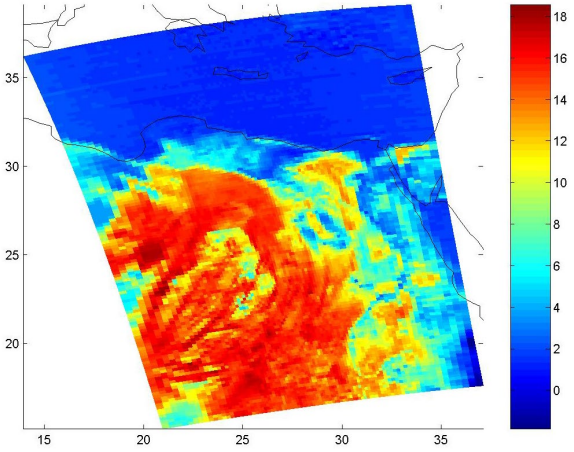

T(1086 cm^{-1})

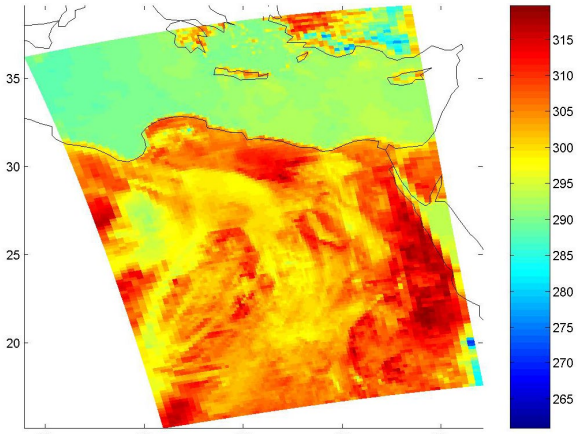

from Tobin et al.

Mt Etna eruption

28 October 2002
ISS photo

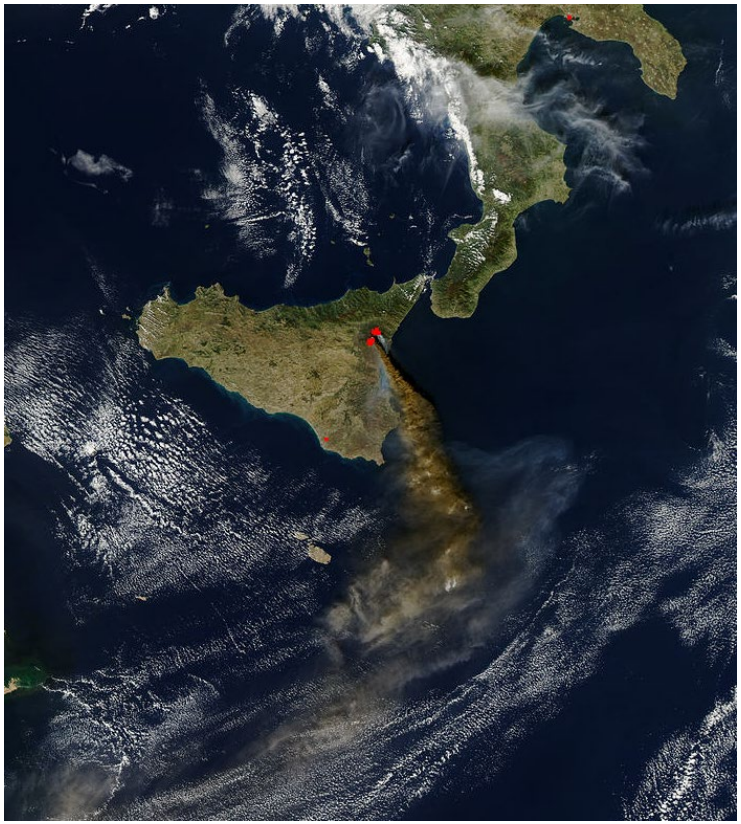

28 October 2002
MODIS Aqua

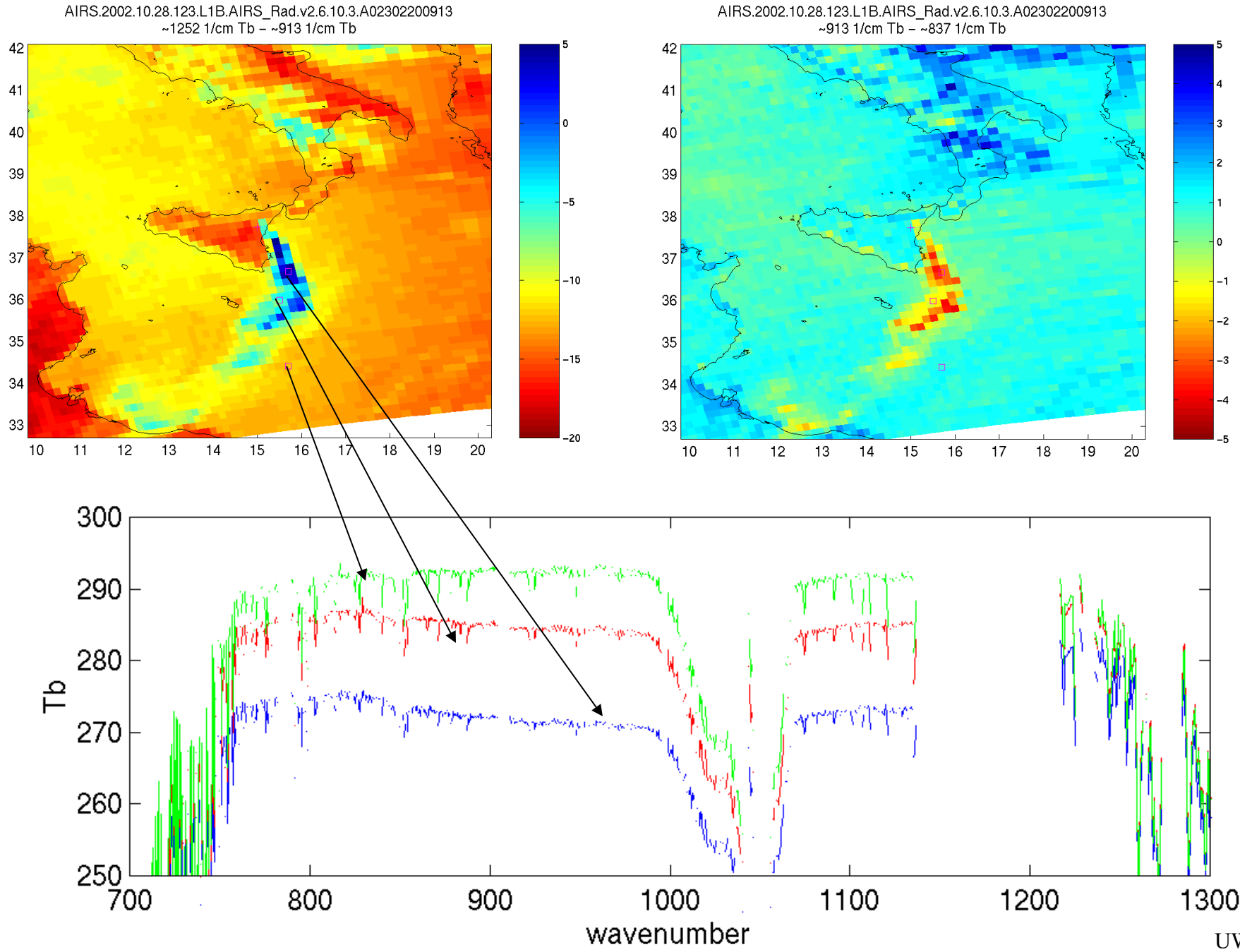
AIRS.2002.10.28.123.L1B.AIRS_Rad.v2.6.10.3.A02302200913
~1252 1/cm Tb – ~913 1/cm Tb
AIRS.2002.10.28.123.L1B.AIRS_Rad.v2.6.10.3.A02302200913
~913 1/cm Tb – ~837 1/cm Tb
Tb
wavenumber

UW
CIMSS

Mt Etna Ash cloud at 500 hPa

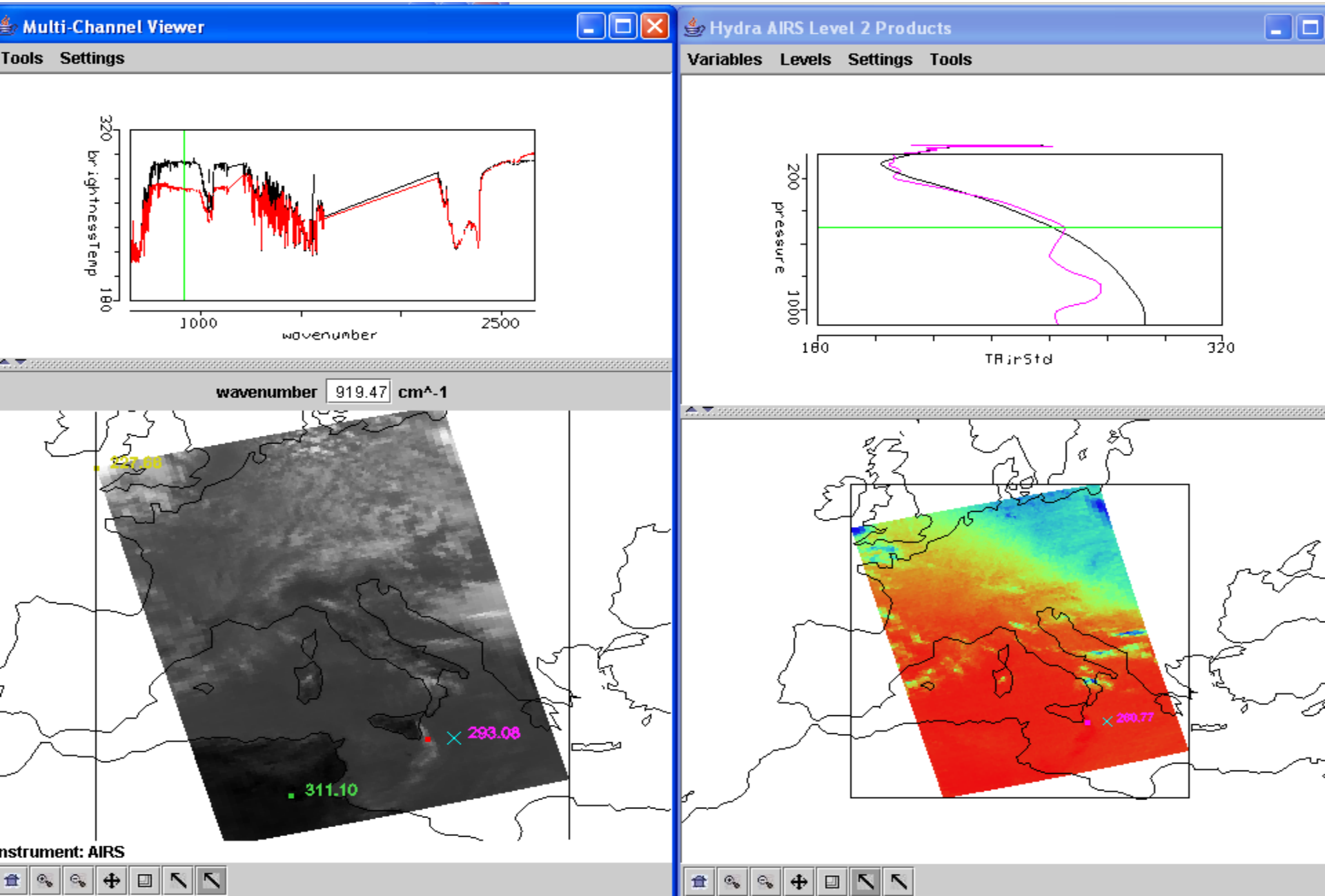

Ash cloud and clear sky spectra

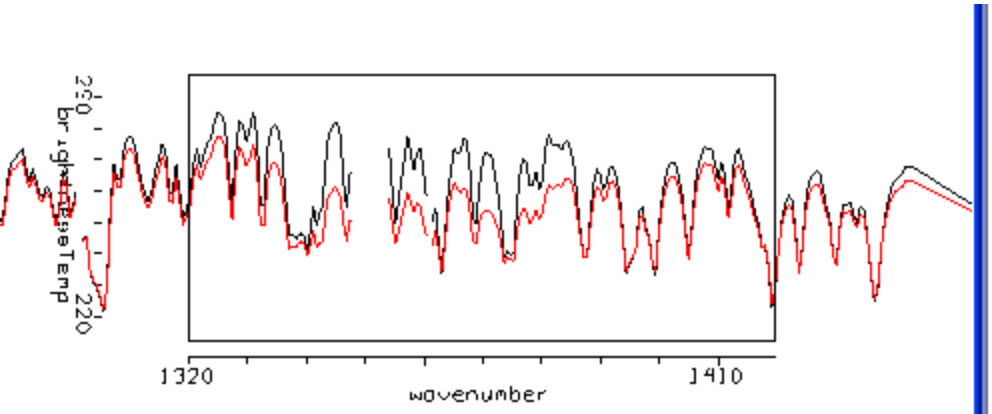

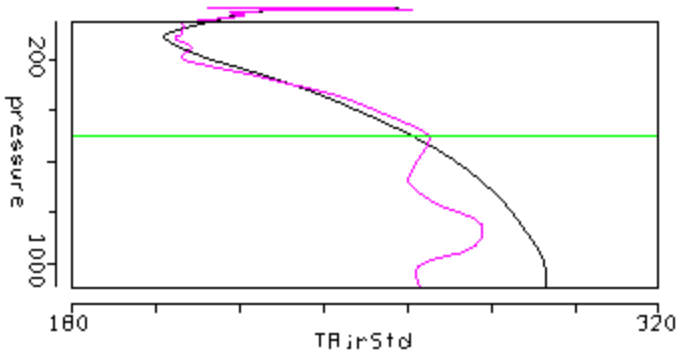

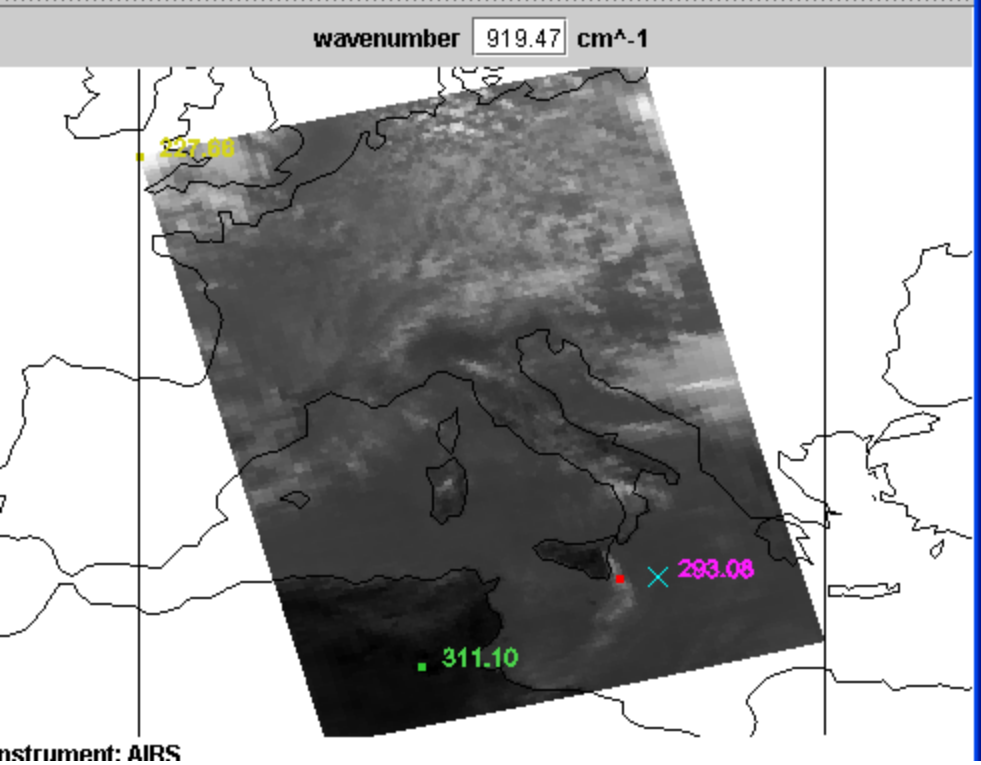

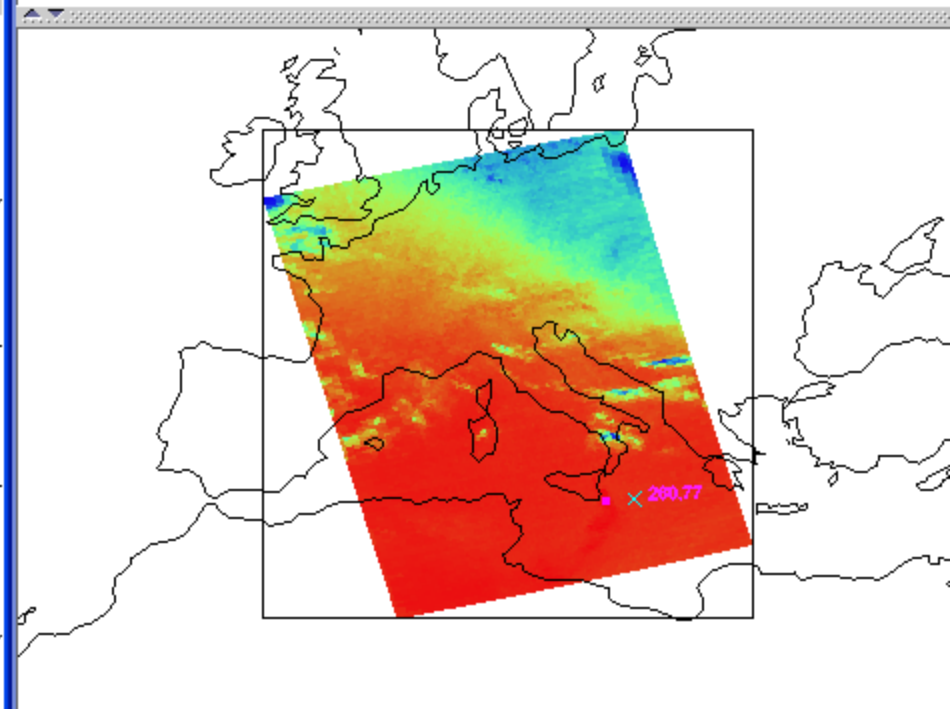

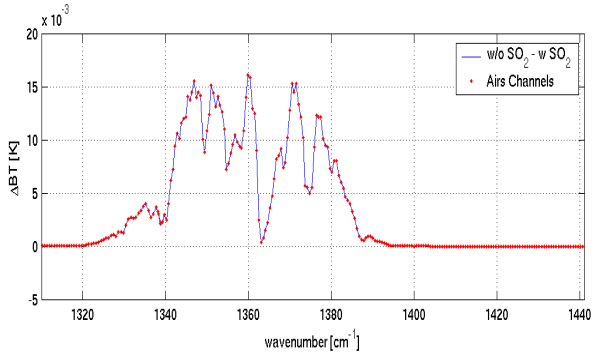

Mt Etna volcanic plume
SO2 (left) from 1284-1345
Ash (right) from 832-900

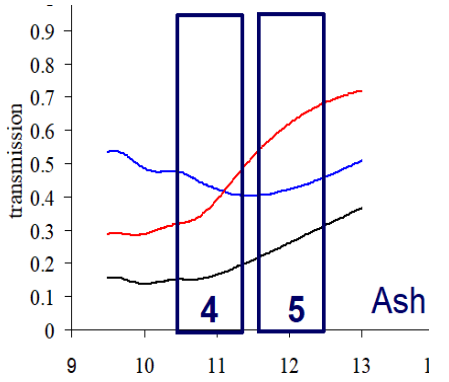

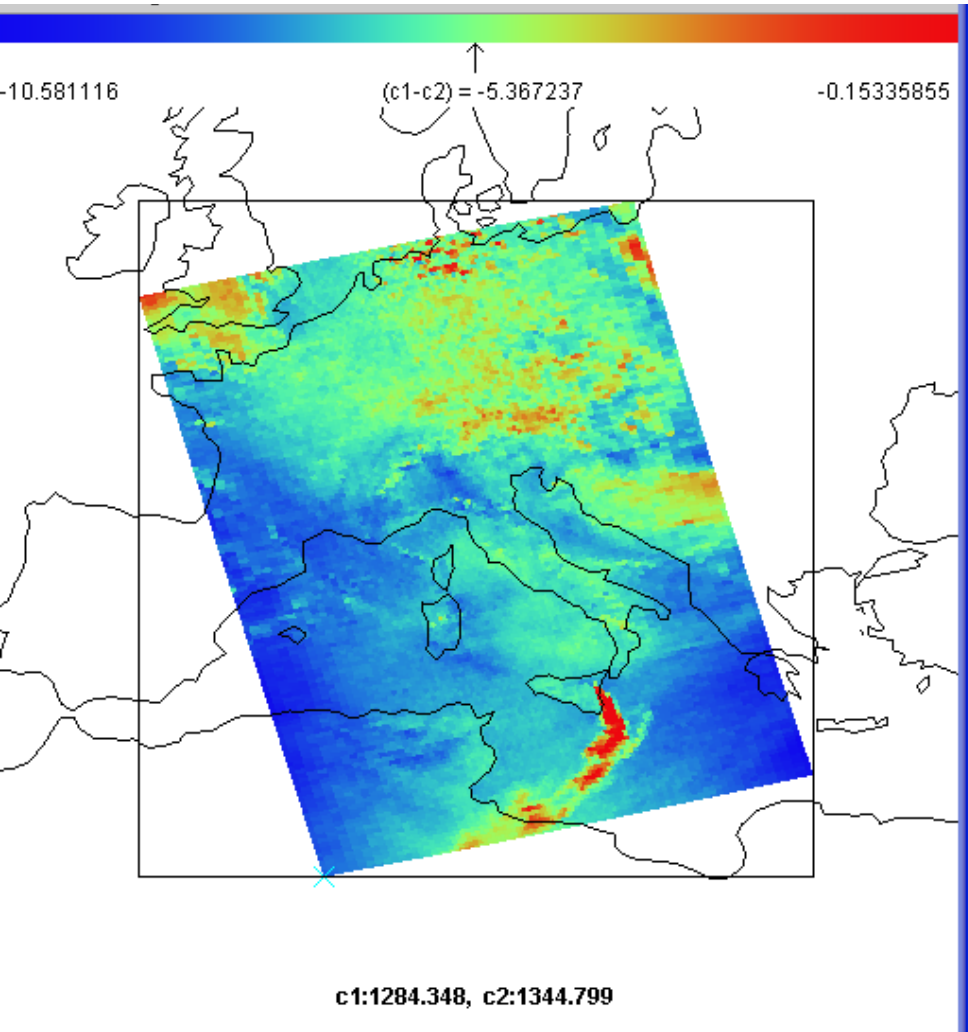

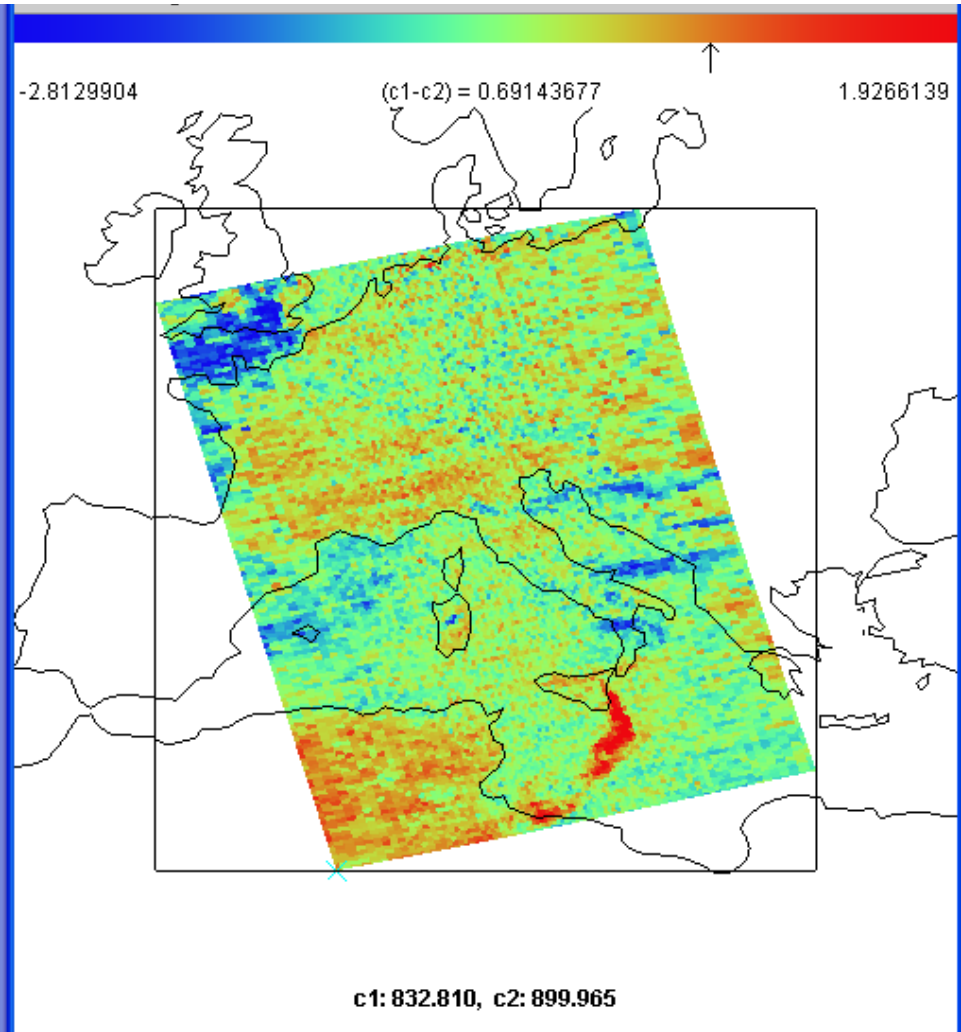

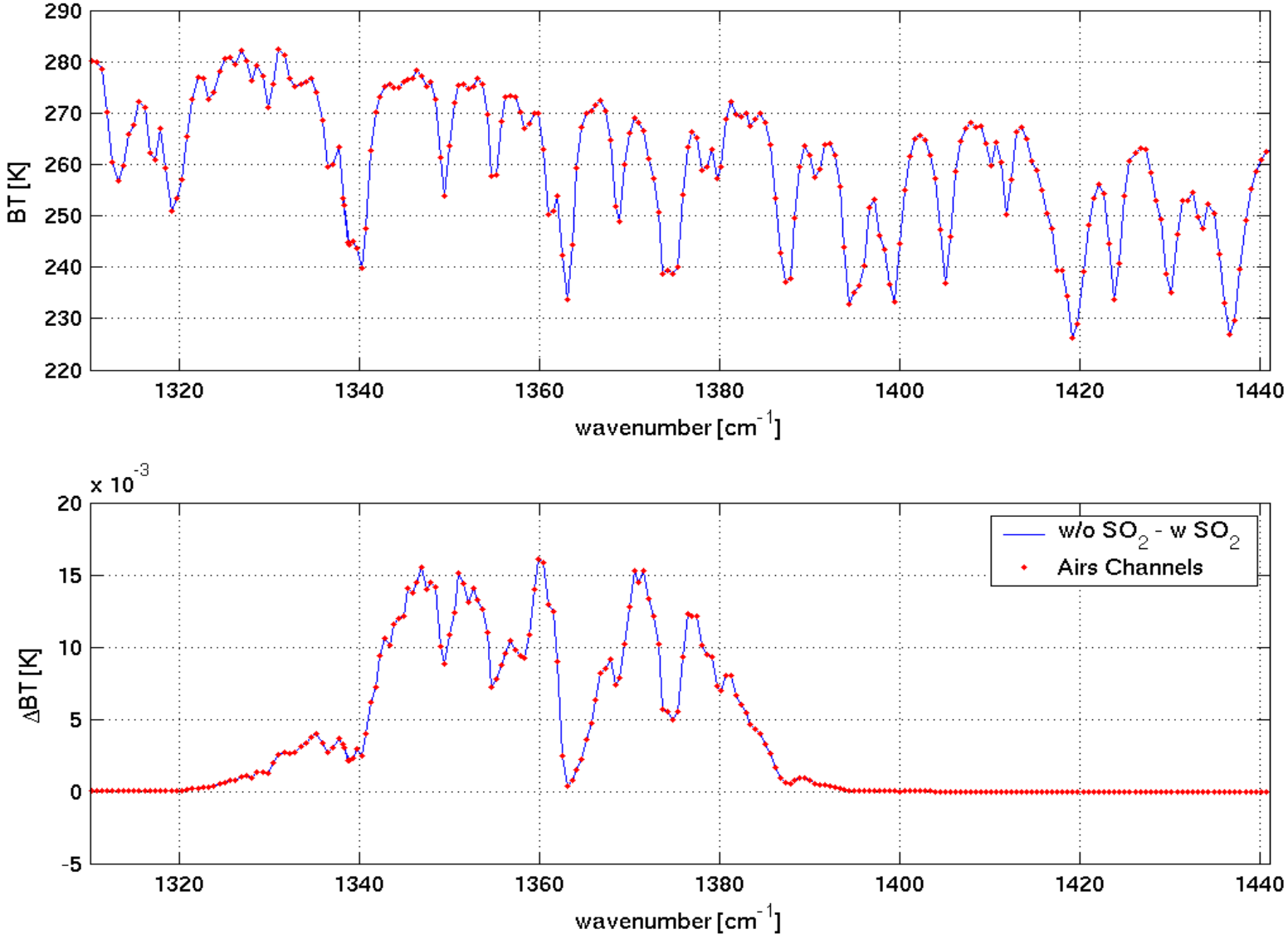
290
280
270
260
250
240
230
220
BT [K]
1320
1340
1360
1380
1400
1420
1440
wavenumber [cm-1]
x 10-3
20
15
10
5
0
-5
ΔBT [K]
w/o SO2 - w SO2
Airs Channels
1320
1340
1360
1380
1400
1420
1440
wavenumber [cm-1]

Anatahan Volcano viewed with AIRS

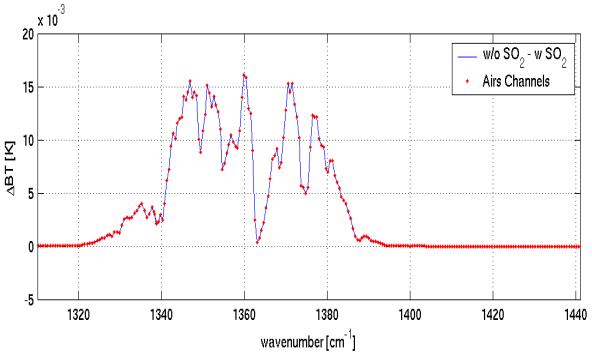

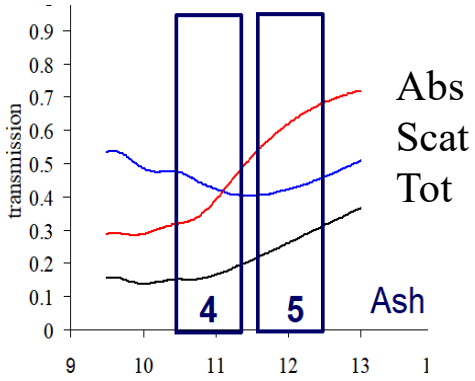

SO_2 signal

1284-1345 cm^{-1}

Ash signal

1228-995 cm^{-1}

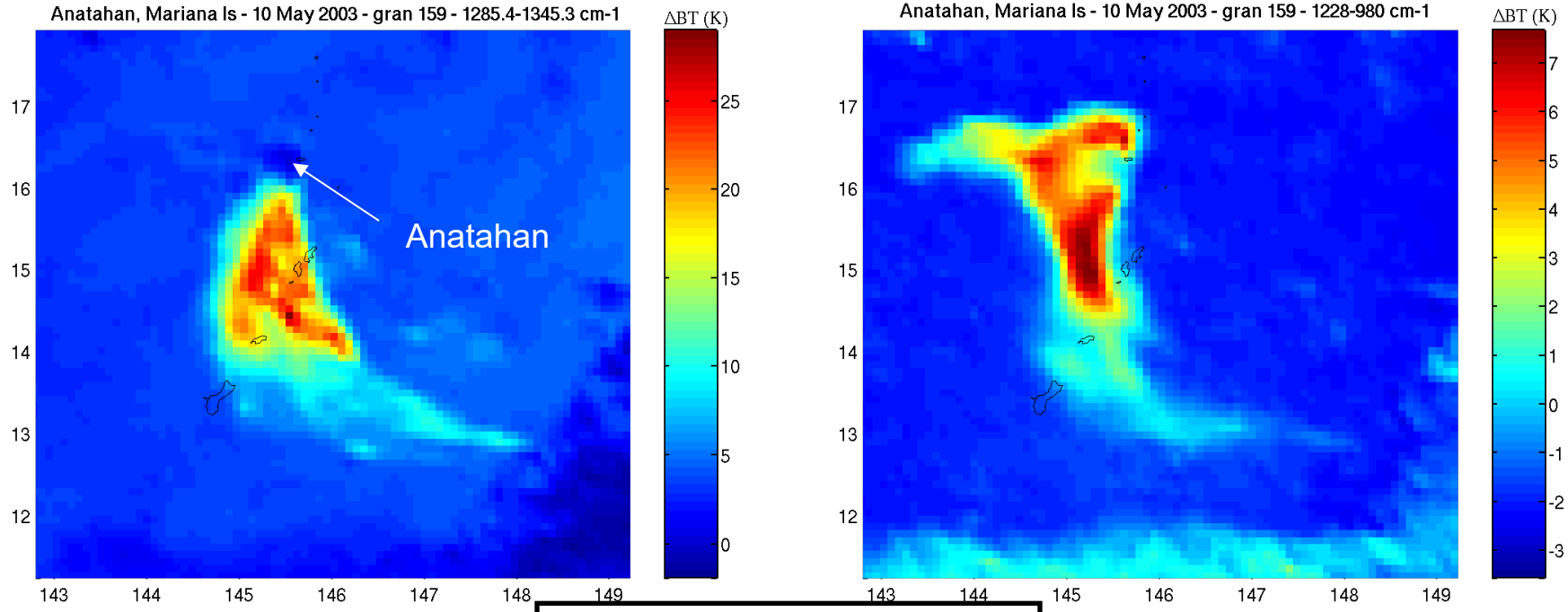

10 May 2003 (1554 UT)

Dust and Cirrus Signals

Imaginary Index of Refraction of Ice and Dust

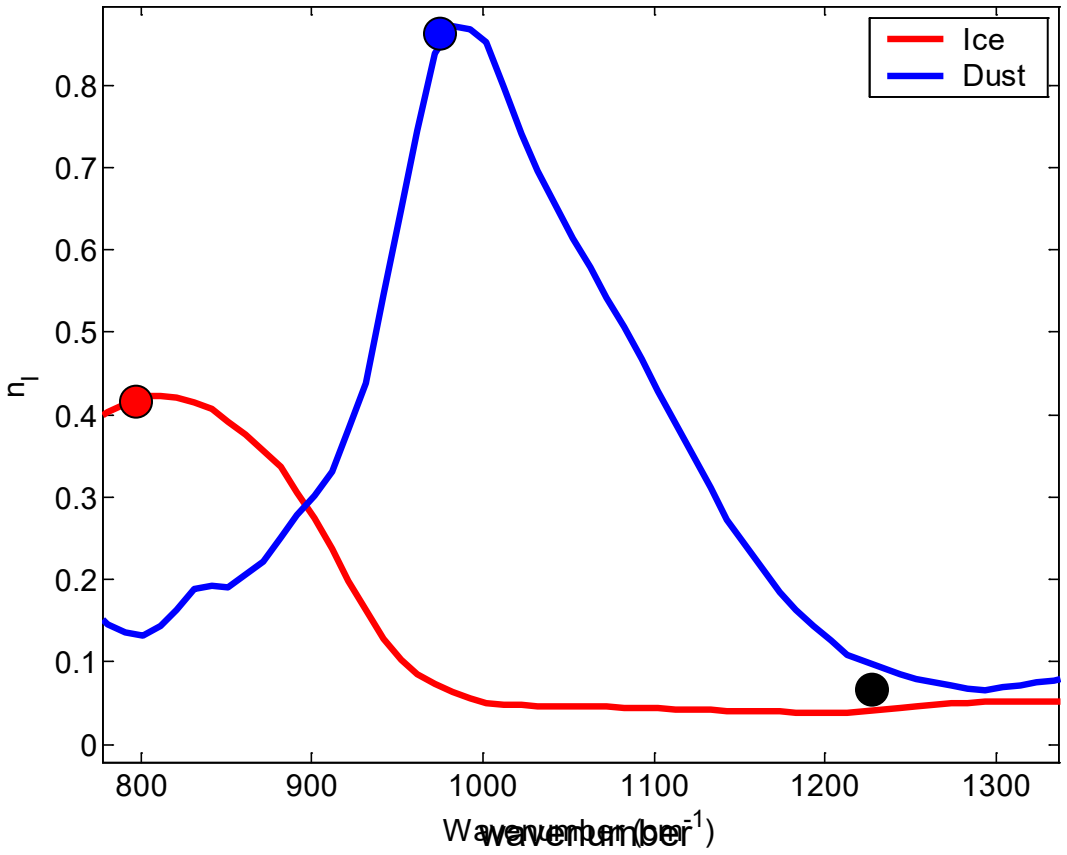

- Both ice and silicate absorption small in 1200 cm^{-1} window
- In the 800-1000 cm^{-1} atmospheric window:

  Silicate index *increases*

  Ice index *decreases*

  with wavenumber

Volz, F.E. : Infrared optical constant of ammonium sulphate, Sahara Dust, volcanic pumice and flash, Appl Opt 12 564-658 (1973)

Hyperspectral Dust Observations

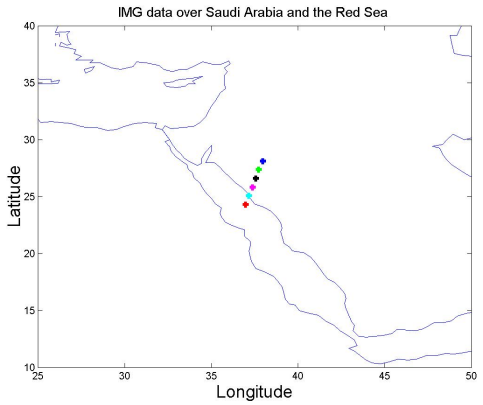

Desert

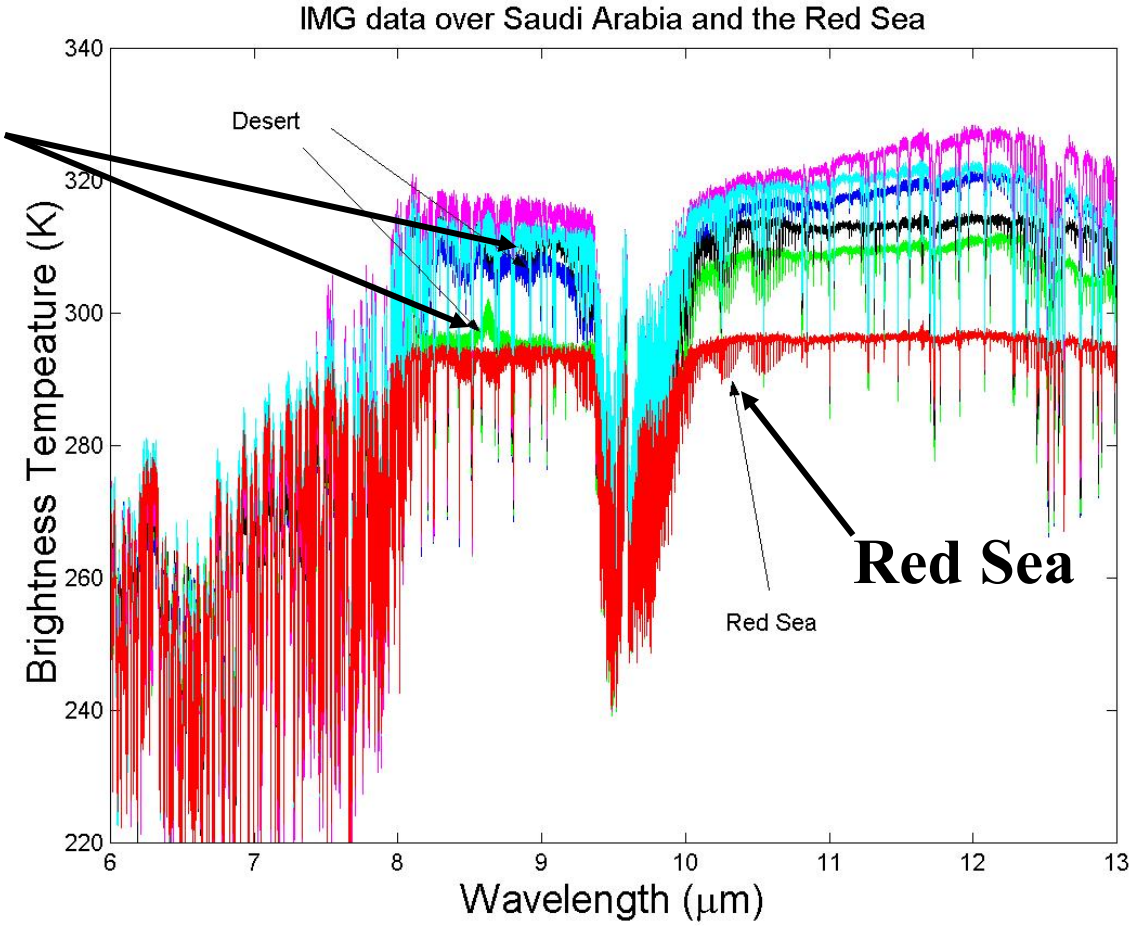

Hyperspectral Dust/Aerosol Modeling

Negative Slope 880 to 920 cm-1– The Dust Signature

Green – Clear Spectrum

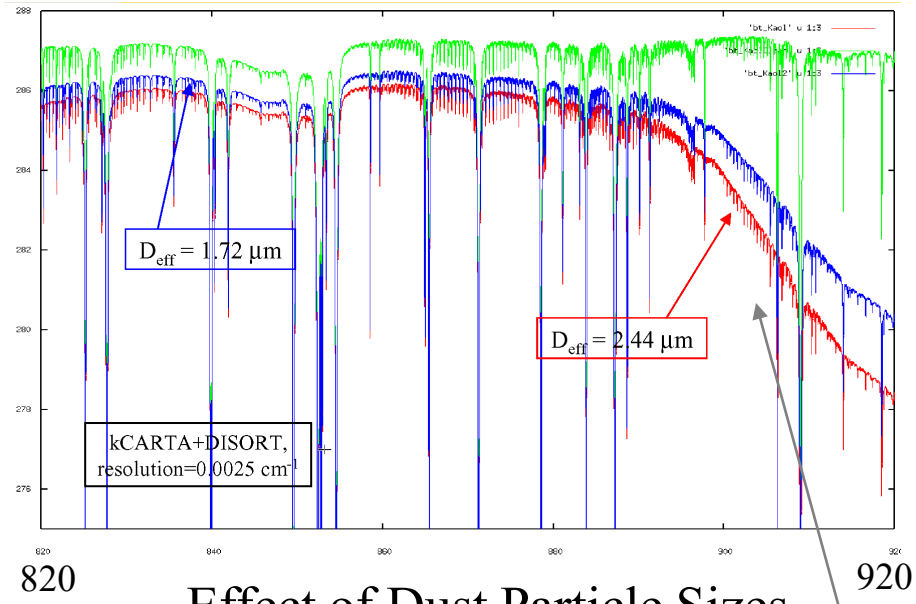

Effect of Dust Particle Sizes

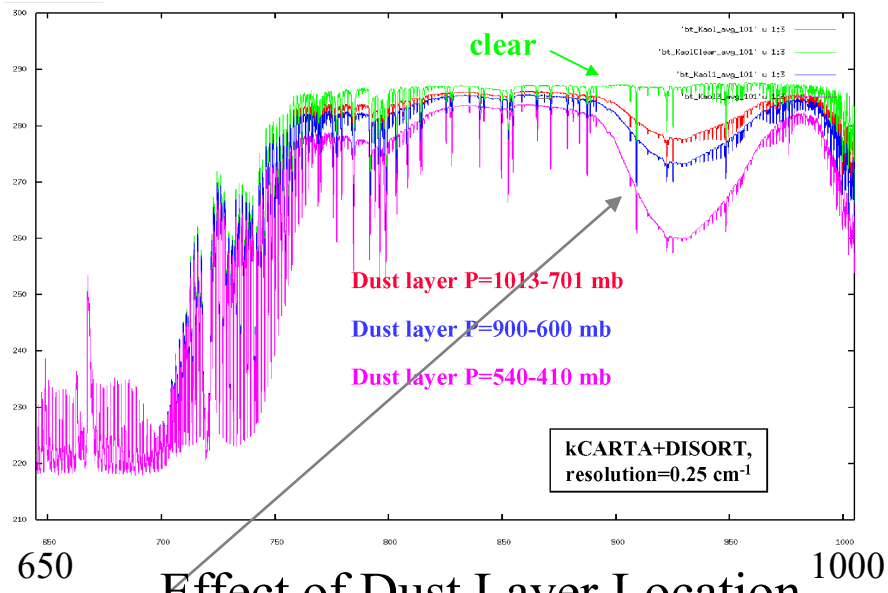

Effect of Dust Layer Location

Negative slope

kCARTA+DISORT, spectral resolution = 0.0025 cm^{-1}

Sokolik, Univ Colo, 2002

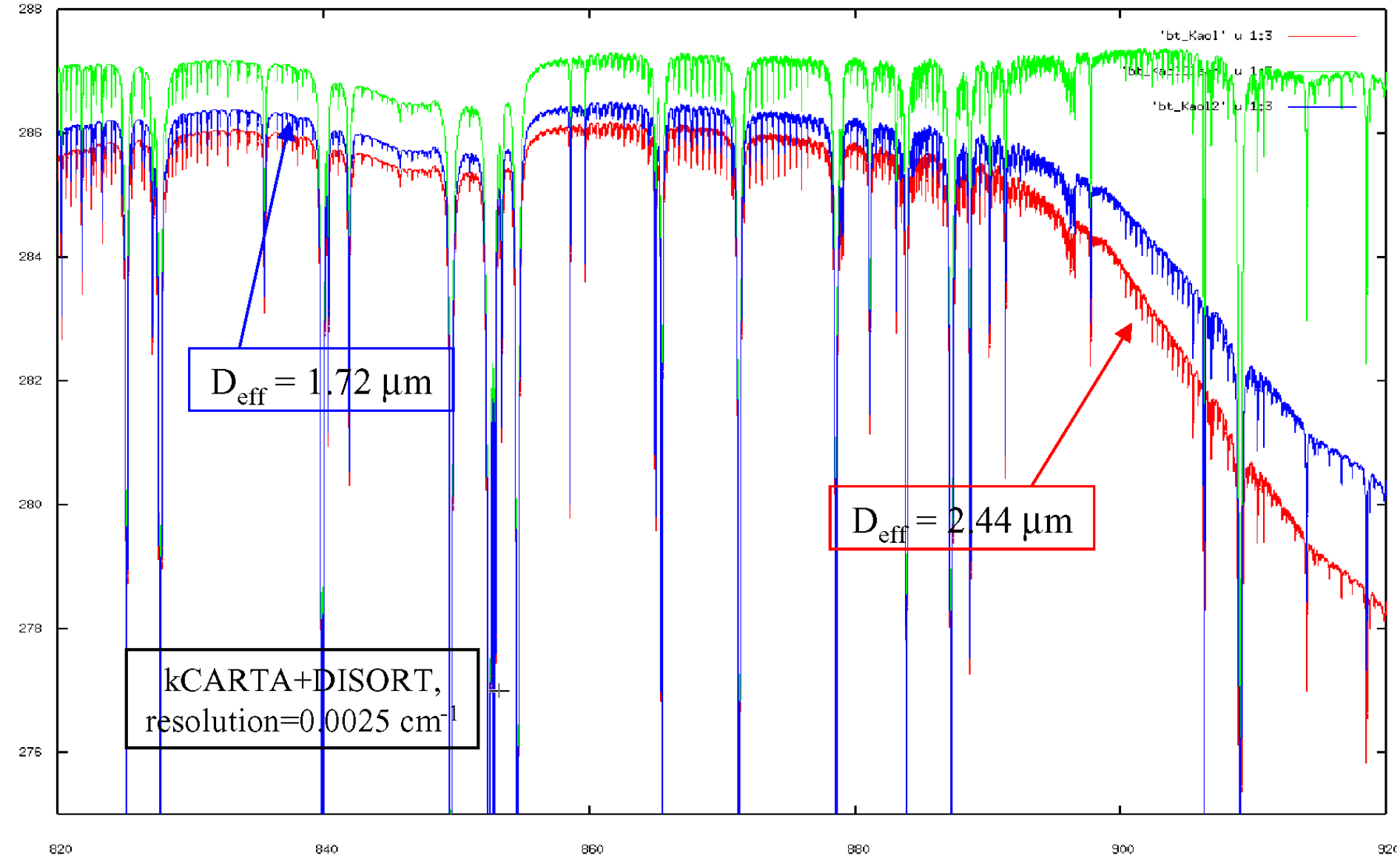
'bt_Kao1' u 1:3
'bt_Kao12' u 1:3
288
286
284
282
280
278
276
820
840
860
880
900
920
D_{eff} = 1.72 µm
D_{eff} = 2.44 µm
kCARTA+DISORT,
resolution=0.0025 cm^{-1}

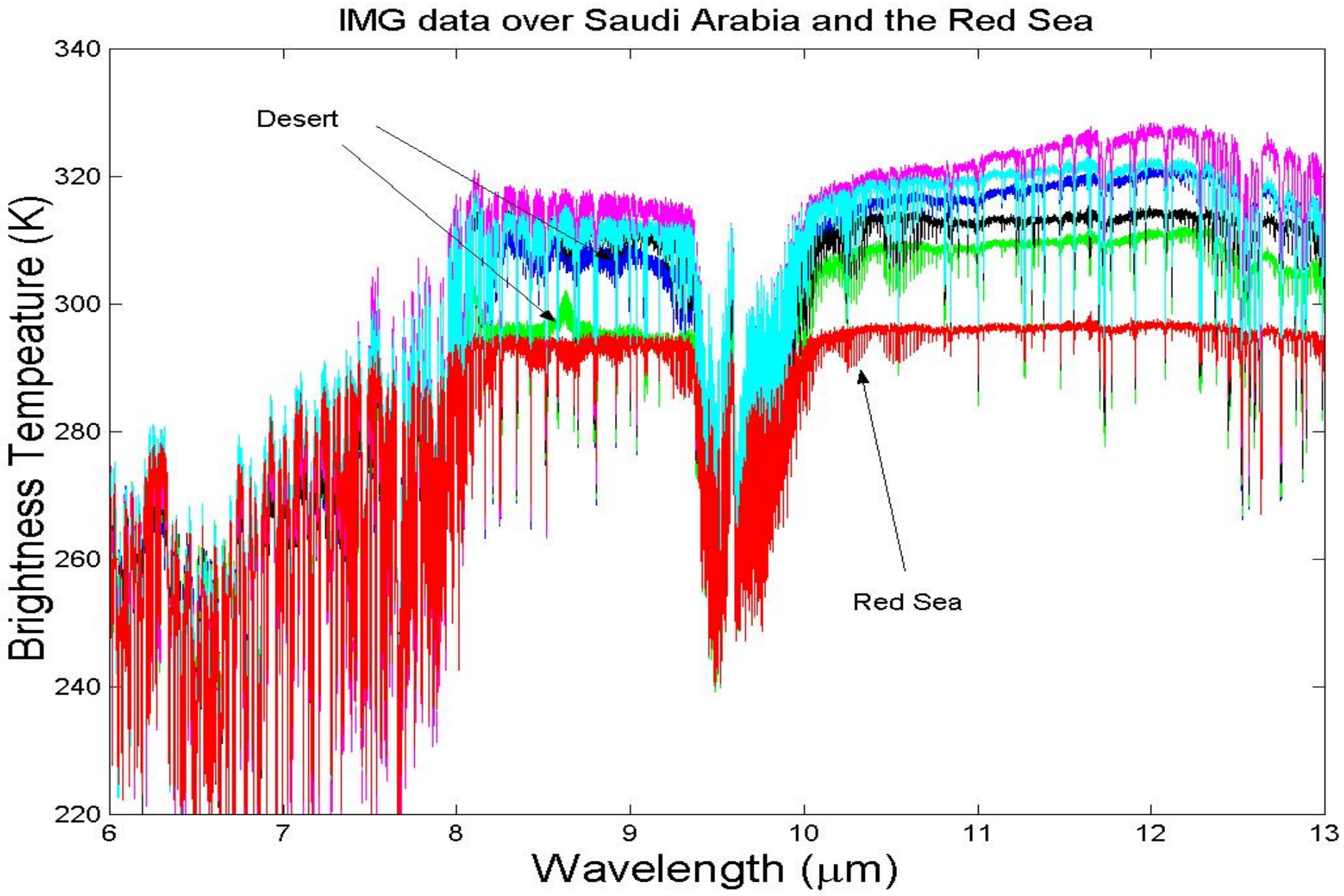
IMG data over Saudi Arabia and the Red Sea
Desert
Red Sea
Brightness Tempeature (K)
Wavelength (μm)
340
320
300
280
260
240
220
6
7
8
9
10
11
12
13

Silicate (ash cloud) signal at Anatahan, Mariana Is

Image is ECMWF bias difference of 1227 cm^{-1} – 984 cm^{-1} (double difference)

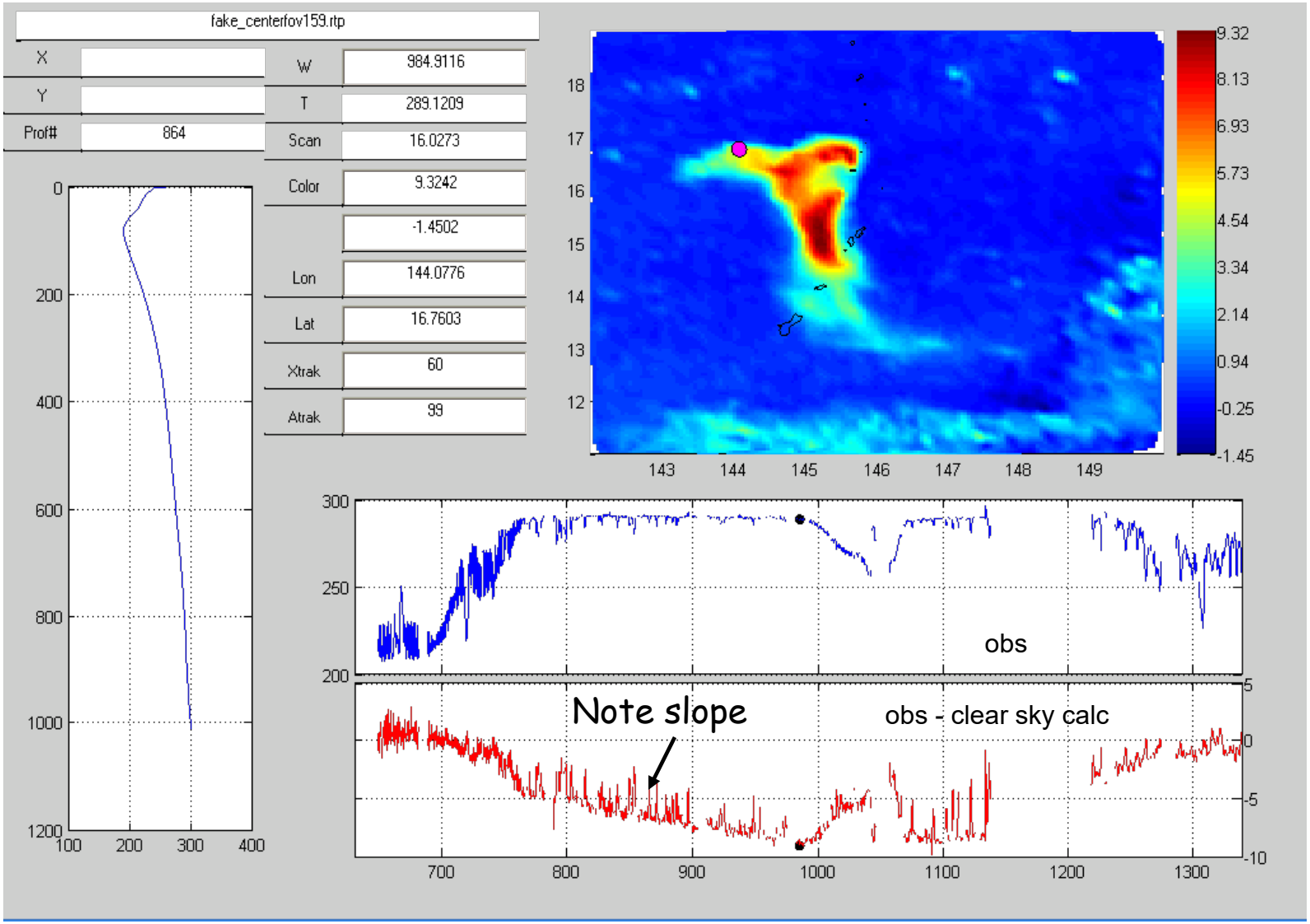

Cirrus signal at Anatahan

Image is ECMWF T_b bias difference of 1227 cm^{-1} – 781 cm^{-1} (double difference)

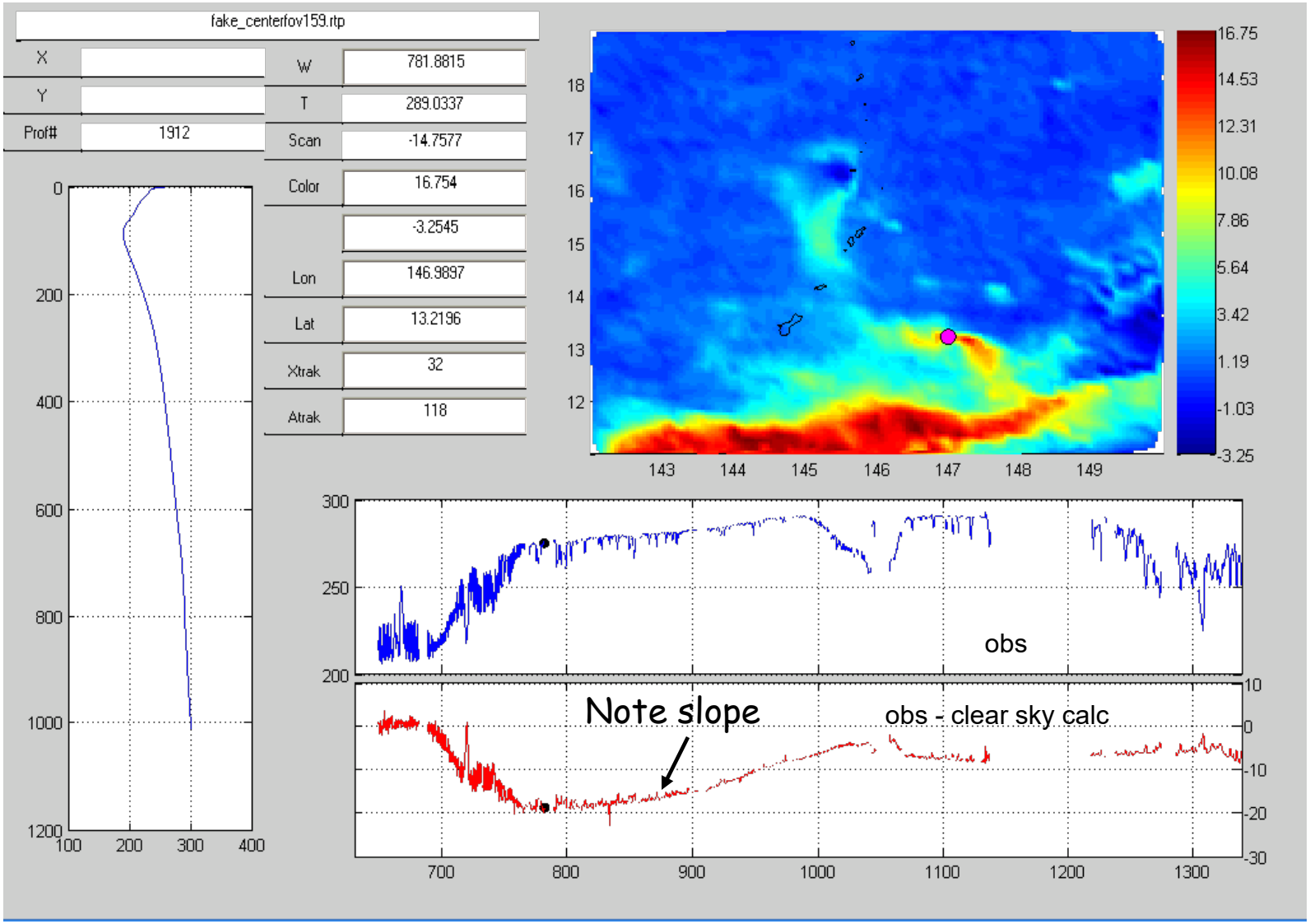

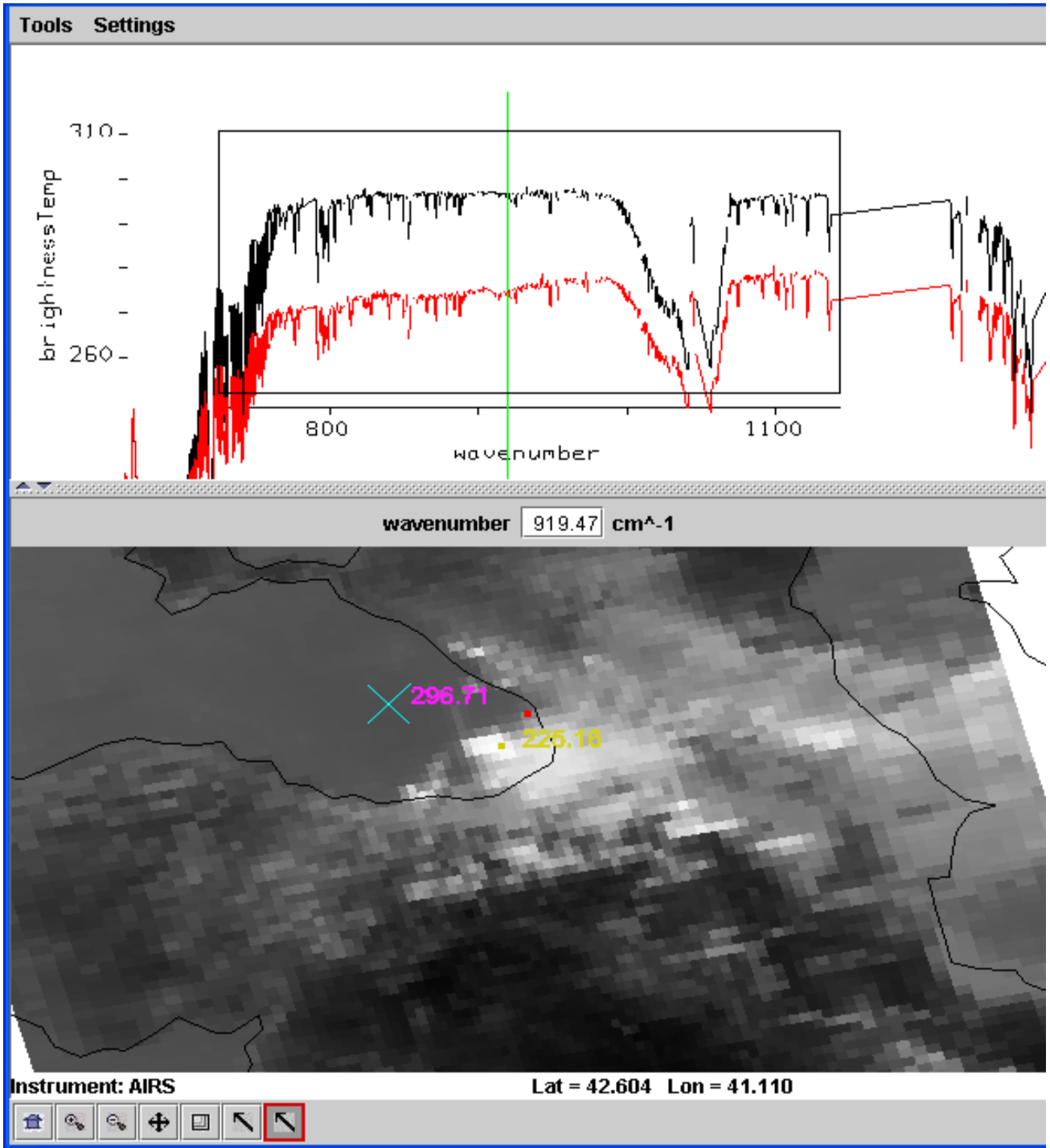

Cirrus
vs
Clear Sky
Spectra

Investigating the Eye of a Tropical Cyclone with AIRS

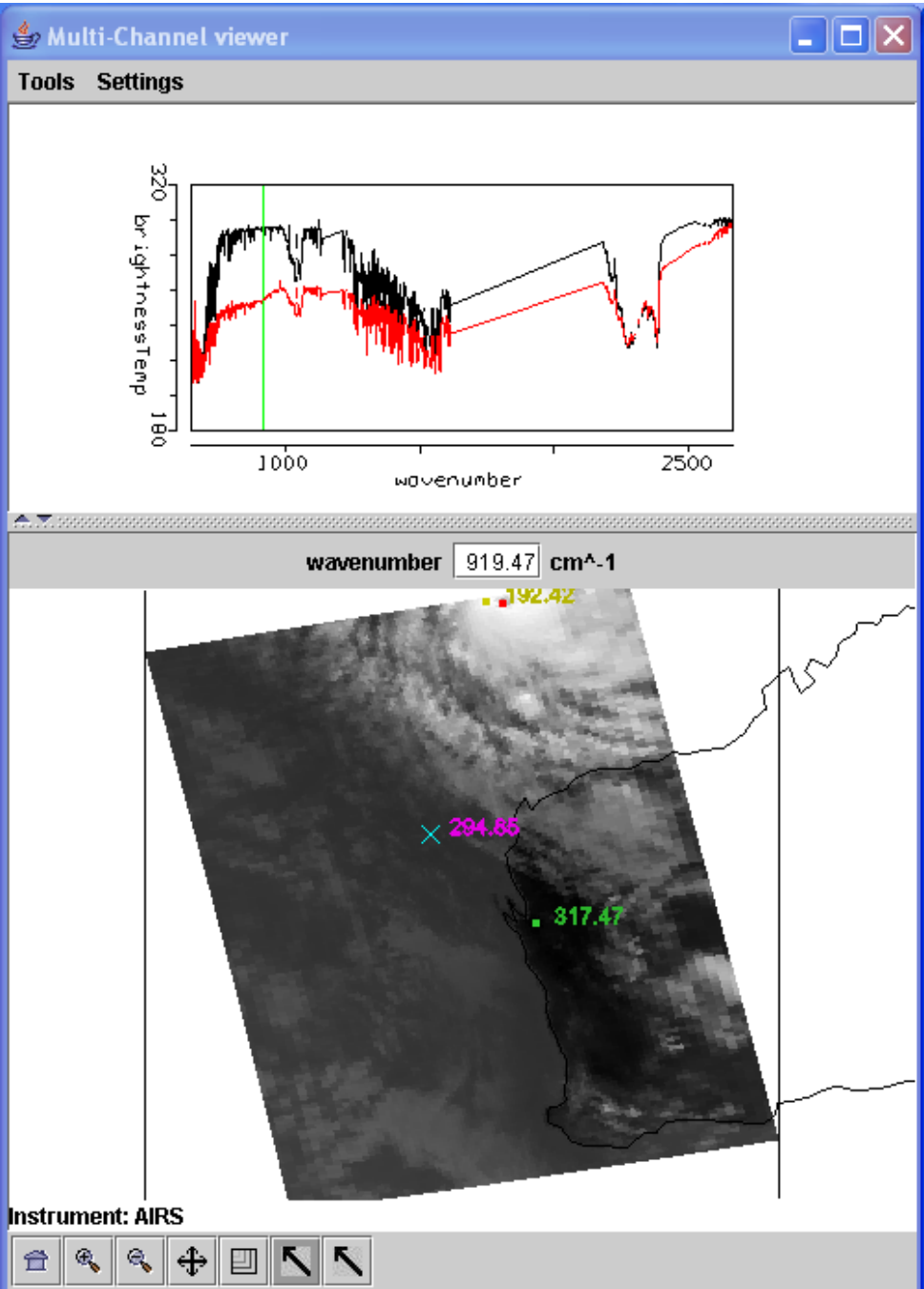

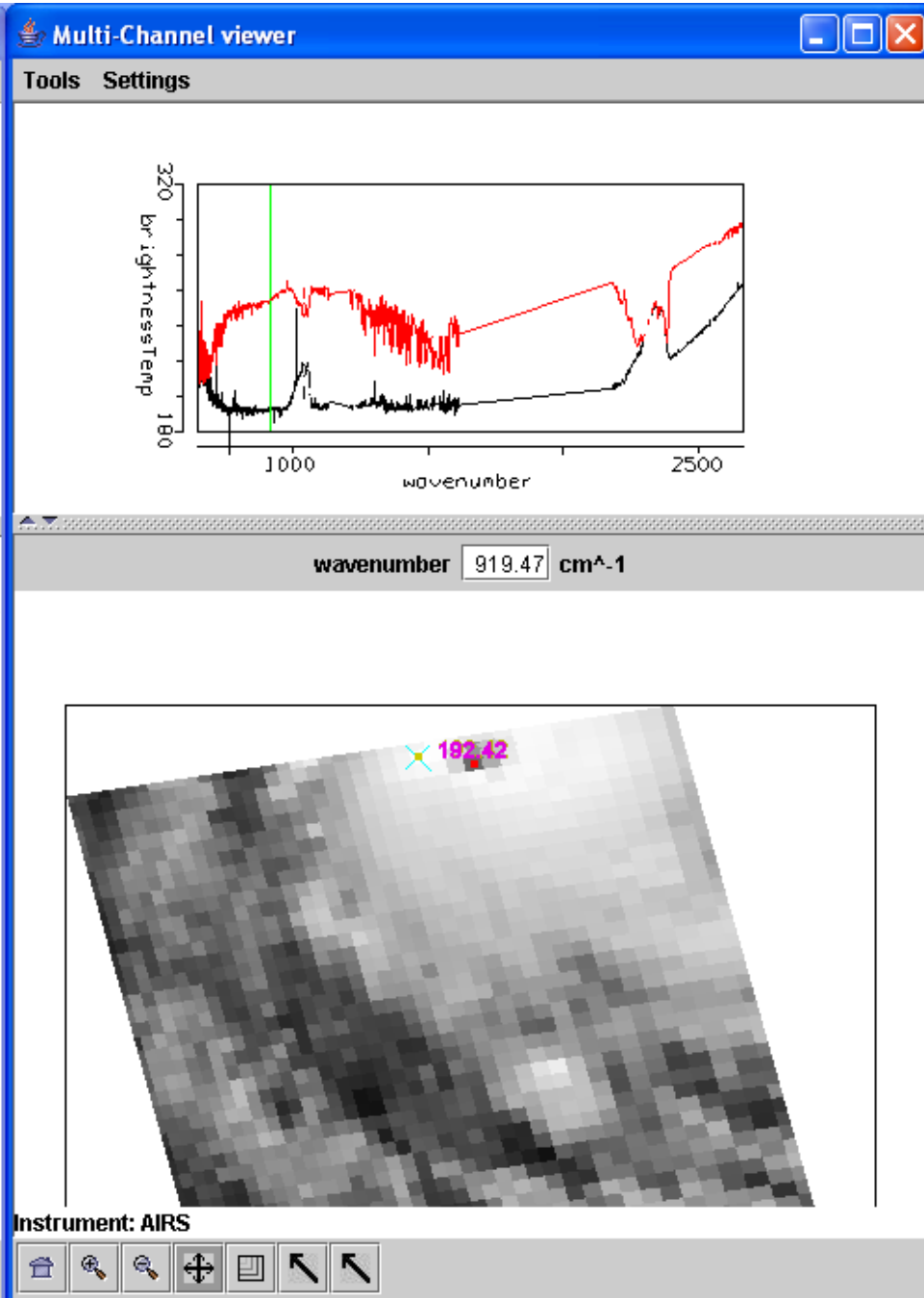

Isabel Eye Sounding from AIRS

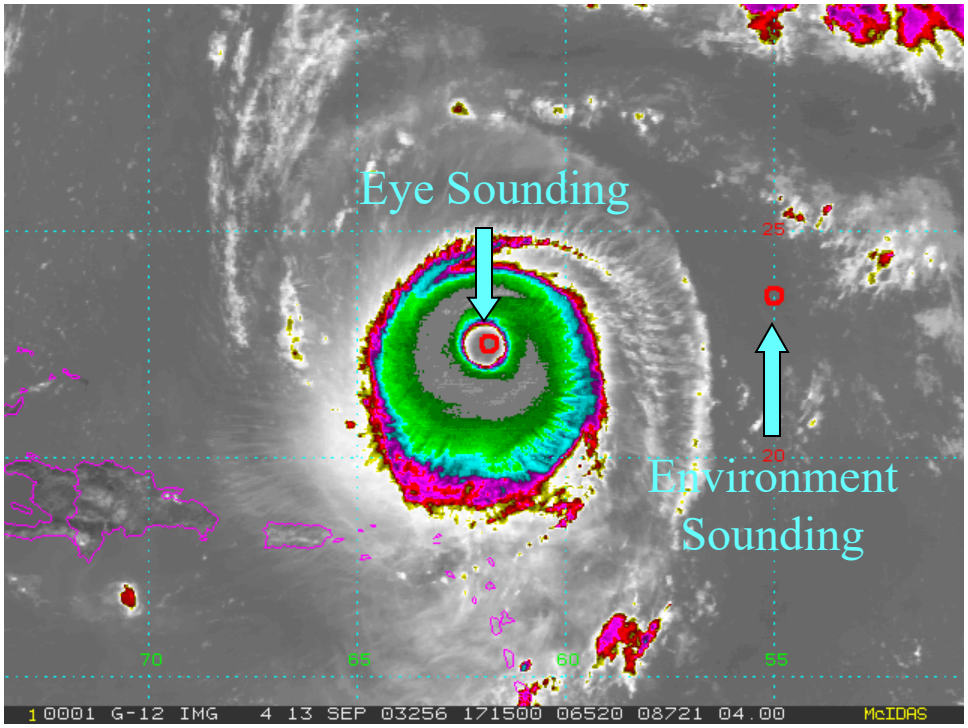

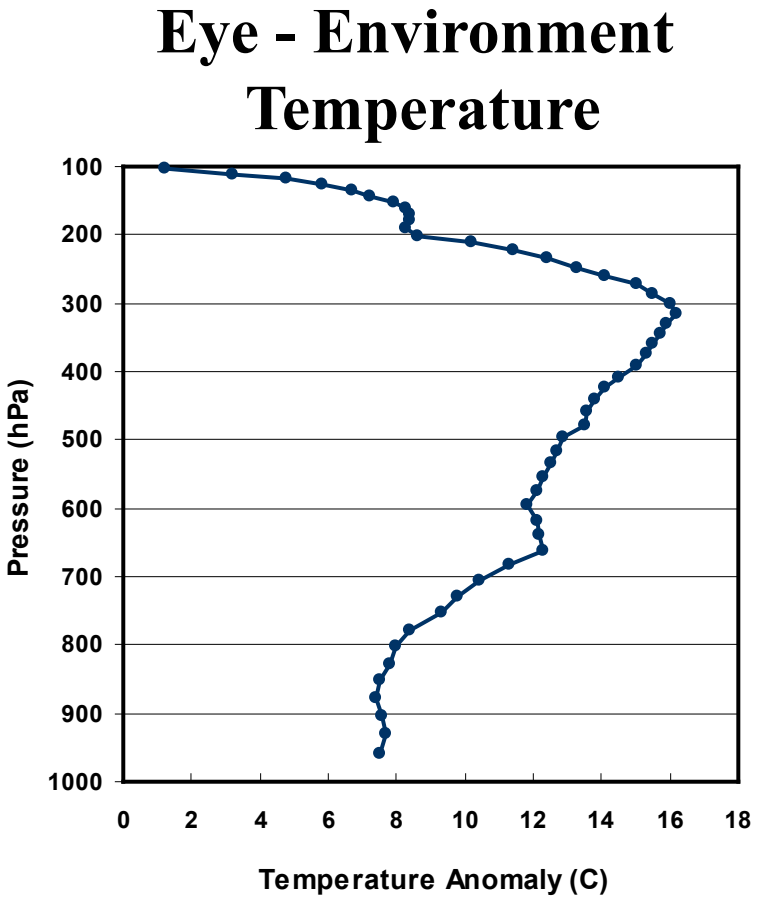

Integrate Hydrostatic Equation Downward from 100 hPa to Surface

Environment Sounding: P_s = 1012 hPa

Eye Sounding: P_s = 936 hPa

Aircraft Recon: P_s = 933 hPa

DeMaria, CIRA, 2004

Example Spectra

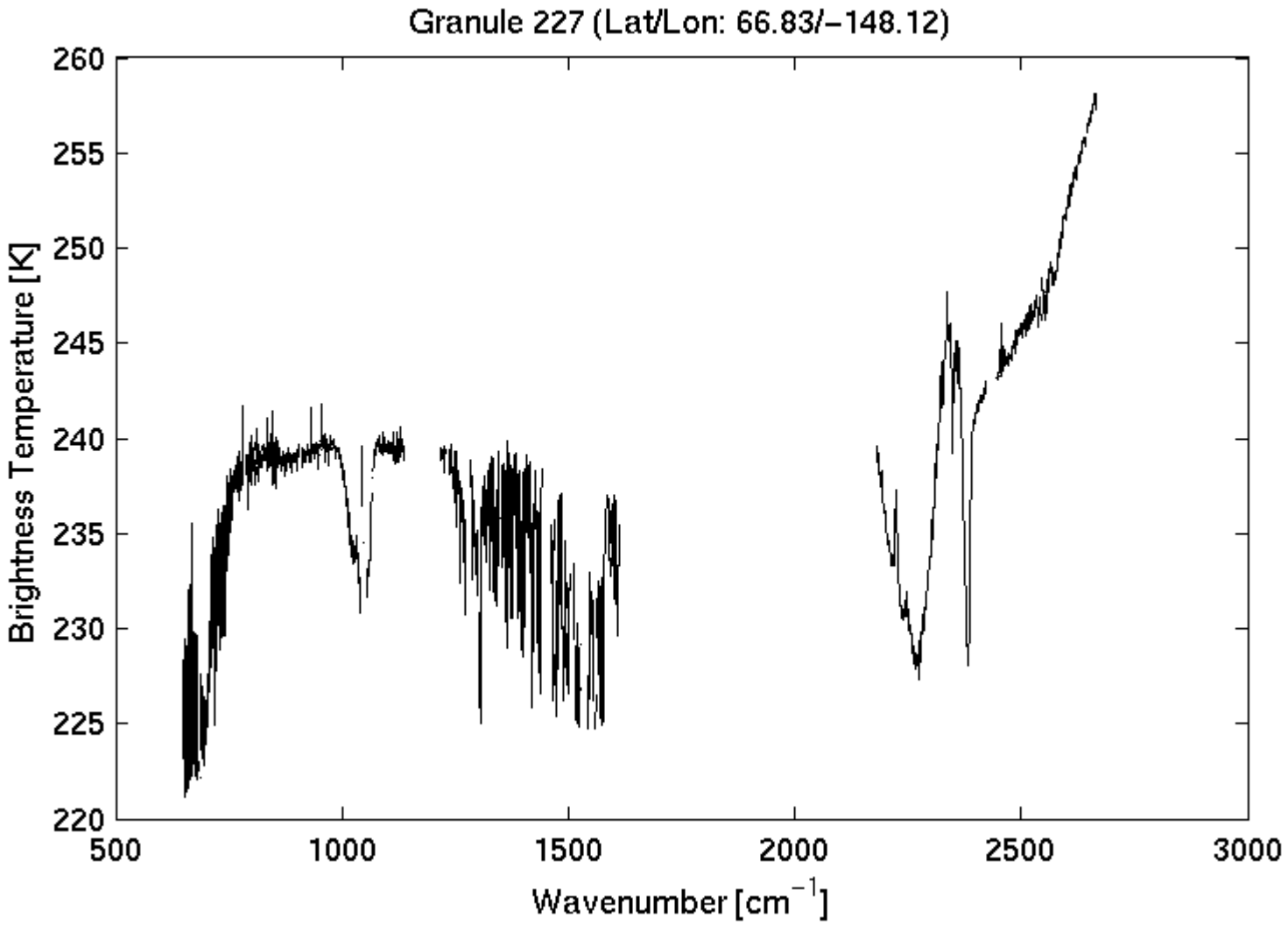
Granule 227 (Lat/Lon: 66.83/−148.12)
Brightness Temperature [K]
260
255
250
245
240
235
230
225
220
500
1000
1500
2000
2500
3000
Wavenumber [cm^{-1}]

Day or night?

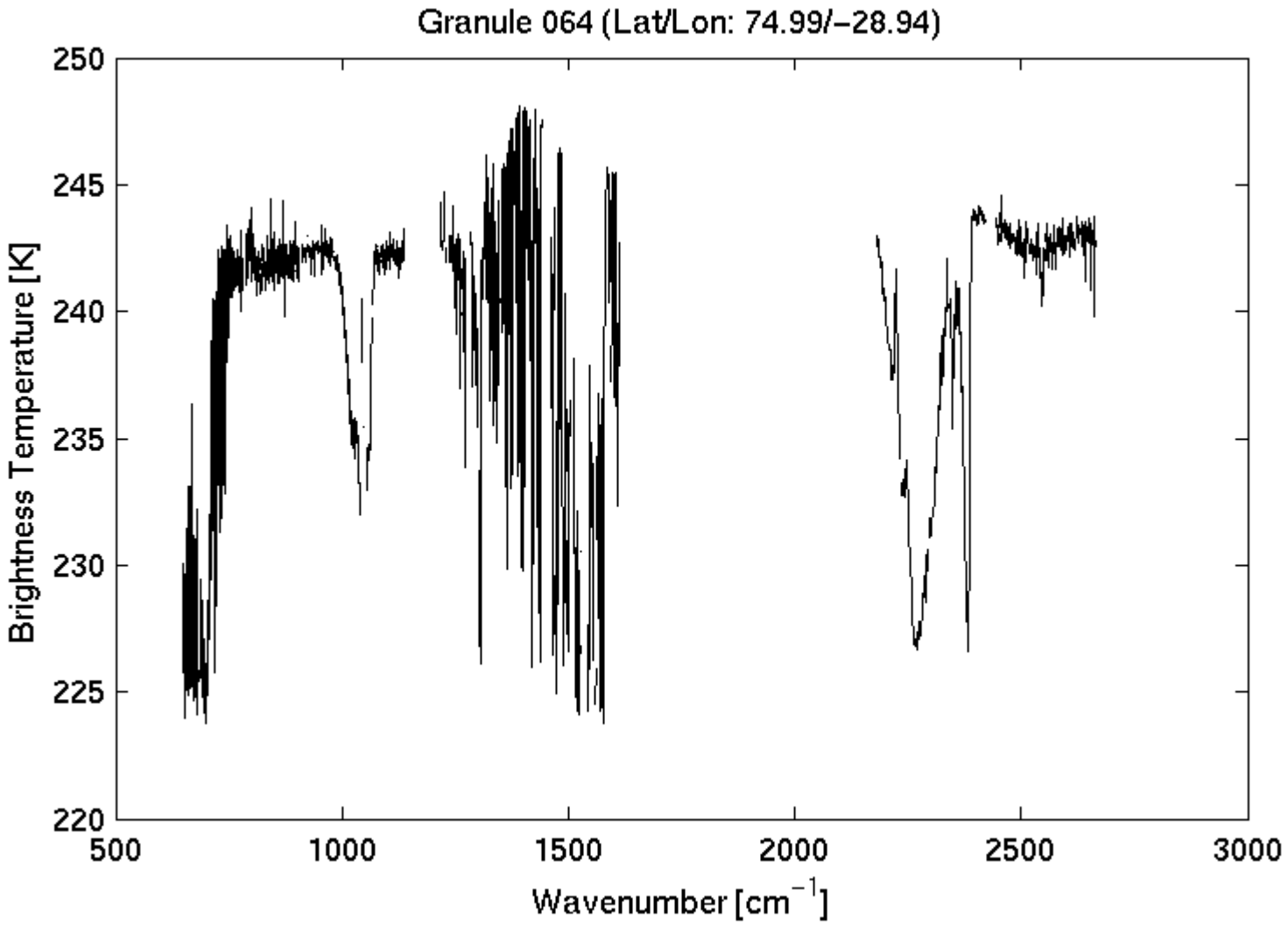

Day, night, desert, or ice/snow?

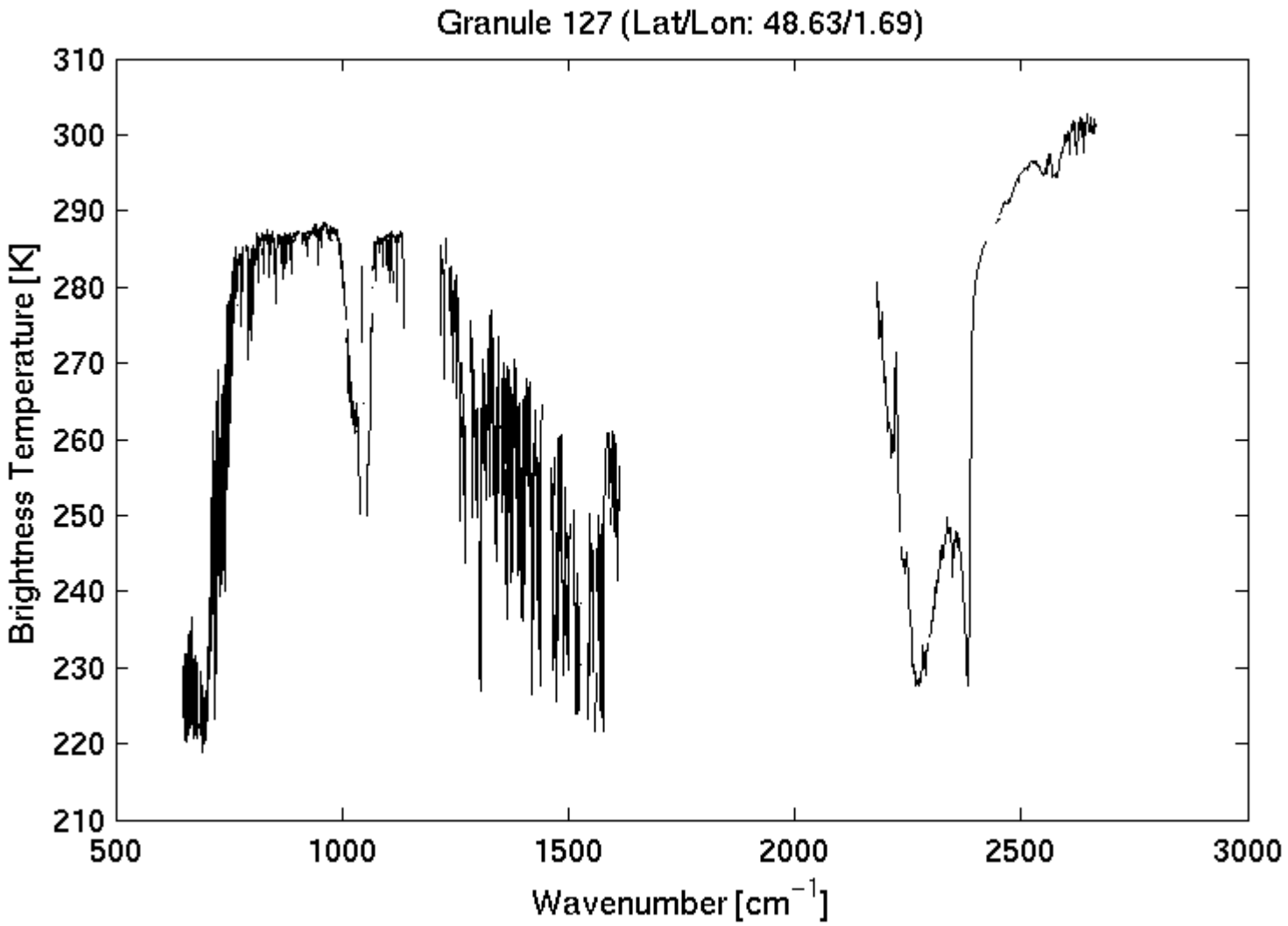
Granule 127 (Lat/Lon: 48.63/1.69)
Brightness Temperature [K]
310
300
290
280
270
260
250
240
230
220
210
500
1000
1500
2000
2500
3000
Wavenumber [cm^{-1}]

Day or night?

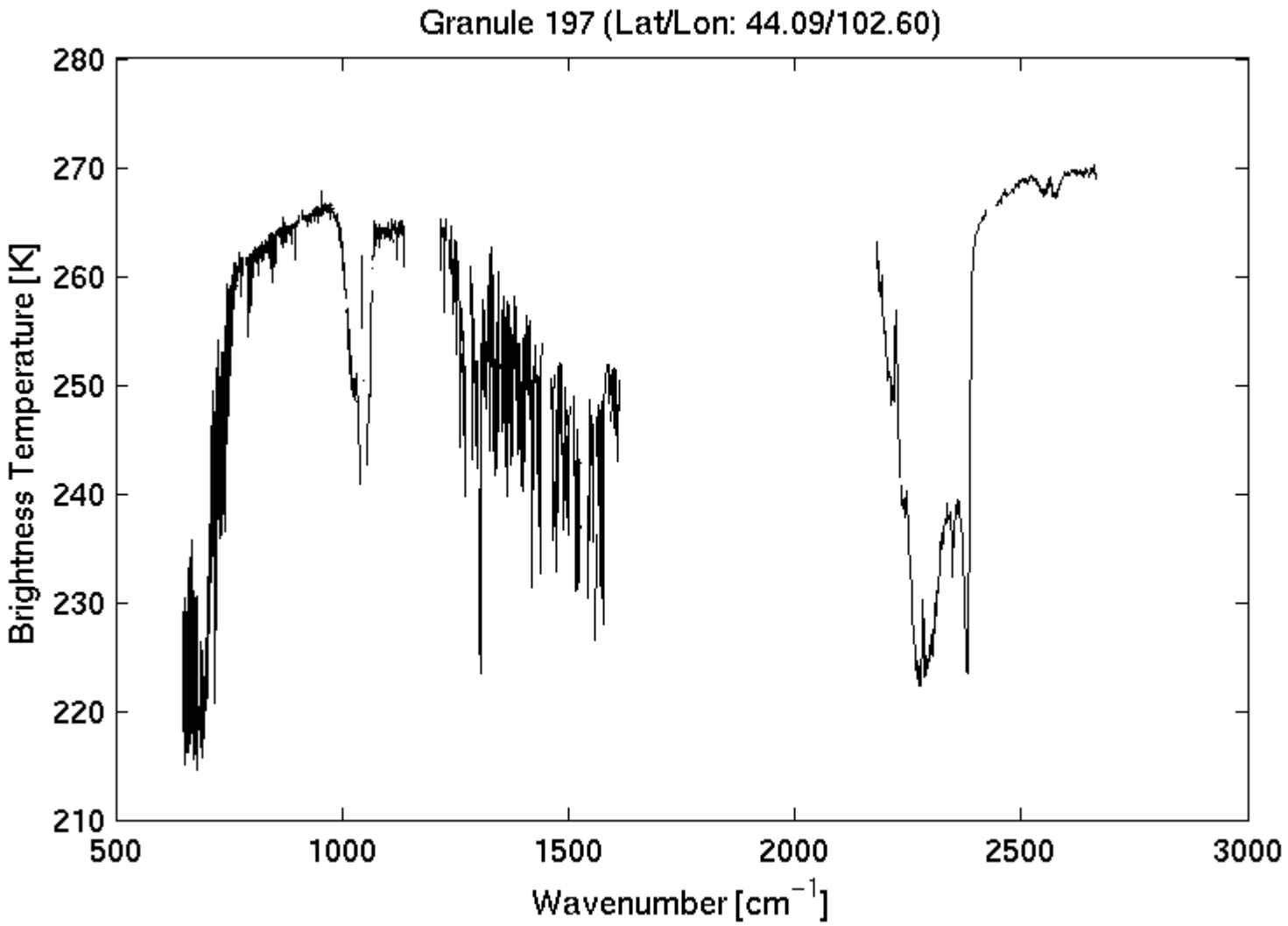

Land or ocean?

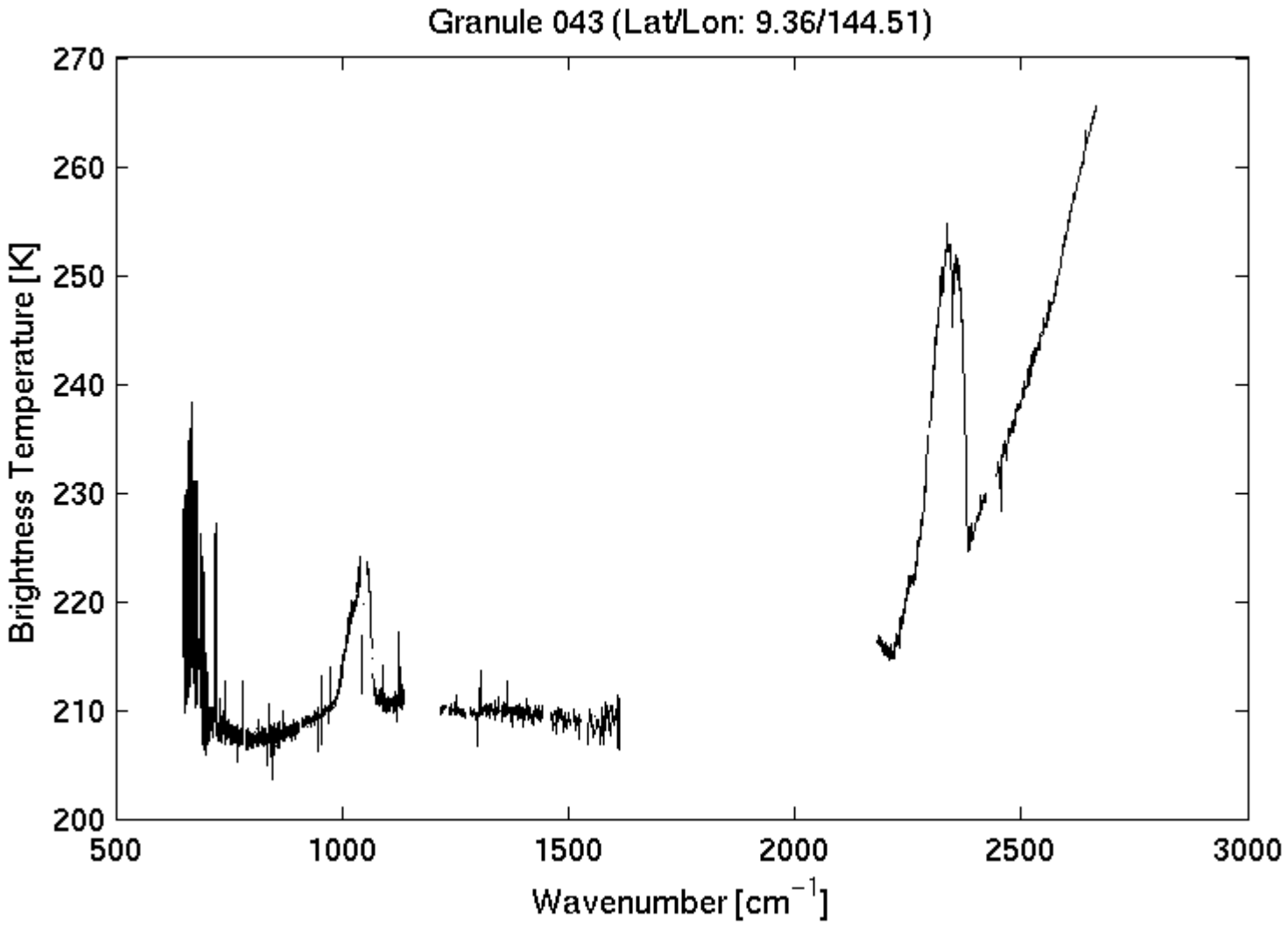

Desert, ocean, or cloudy?

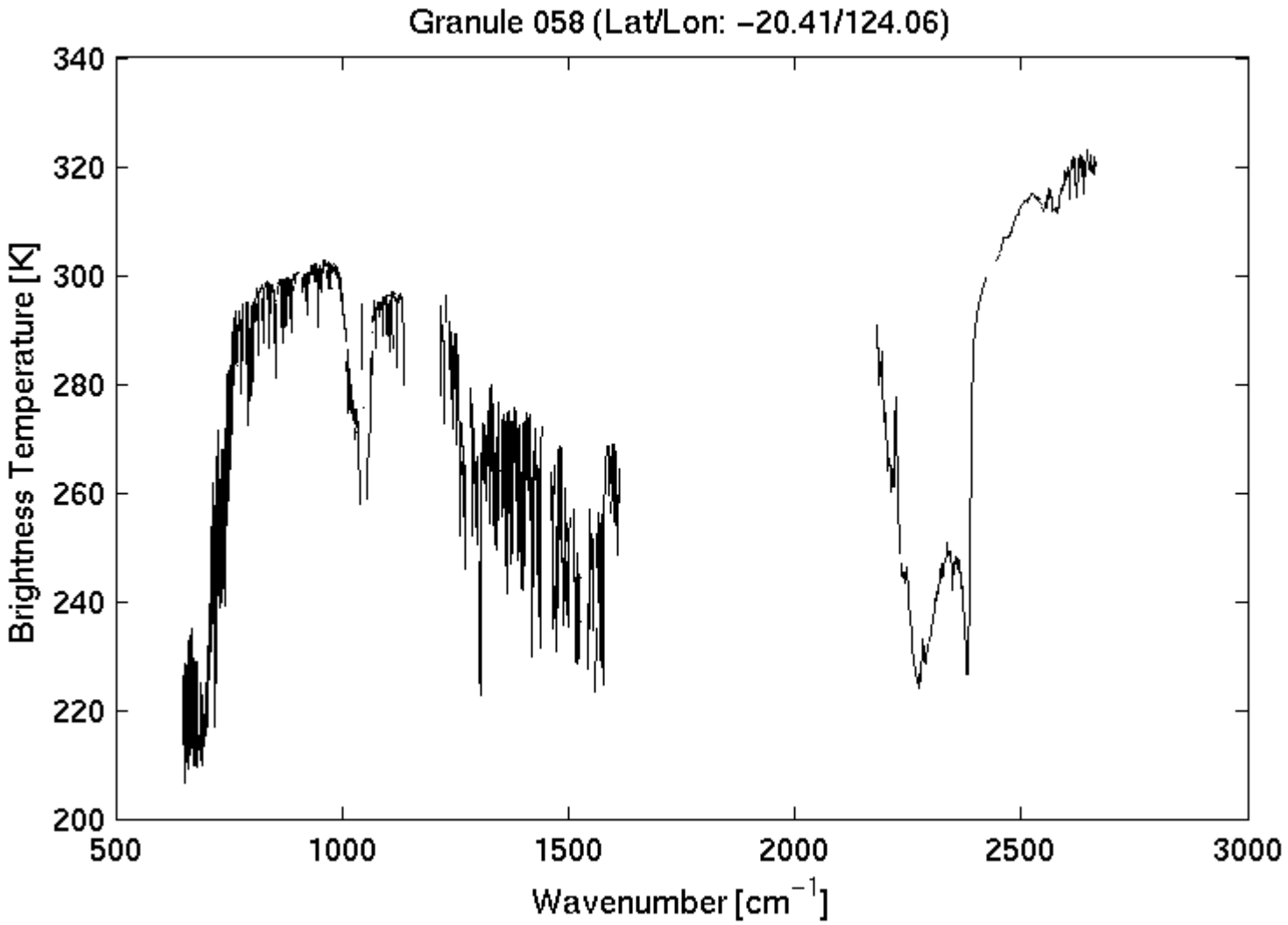

Day, night, desert, or ocean?

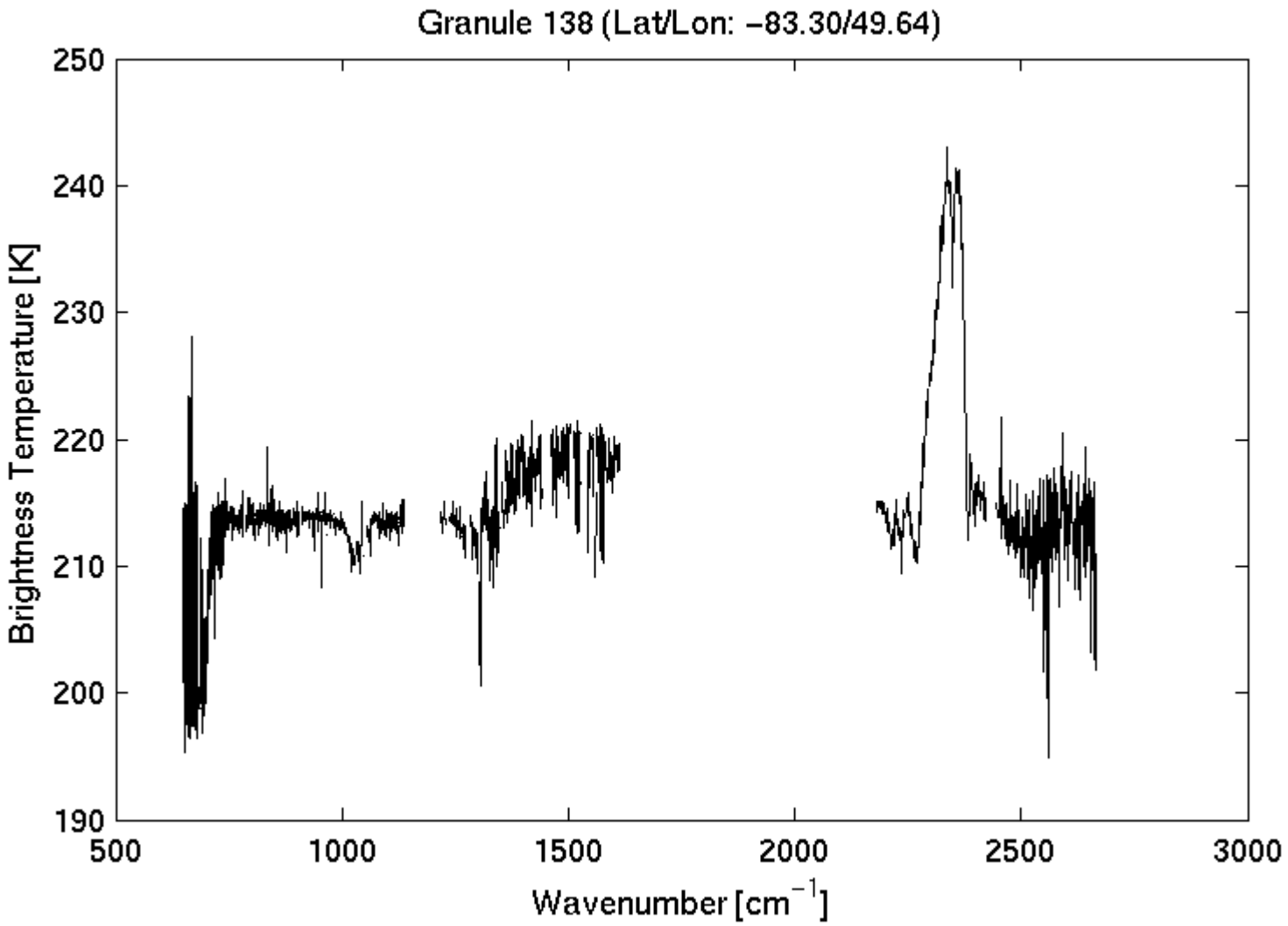

Ocean, cloudy, snow/ice, or desert?

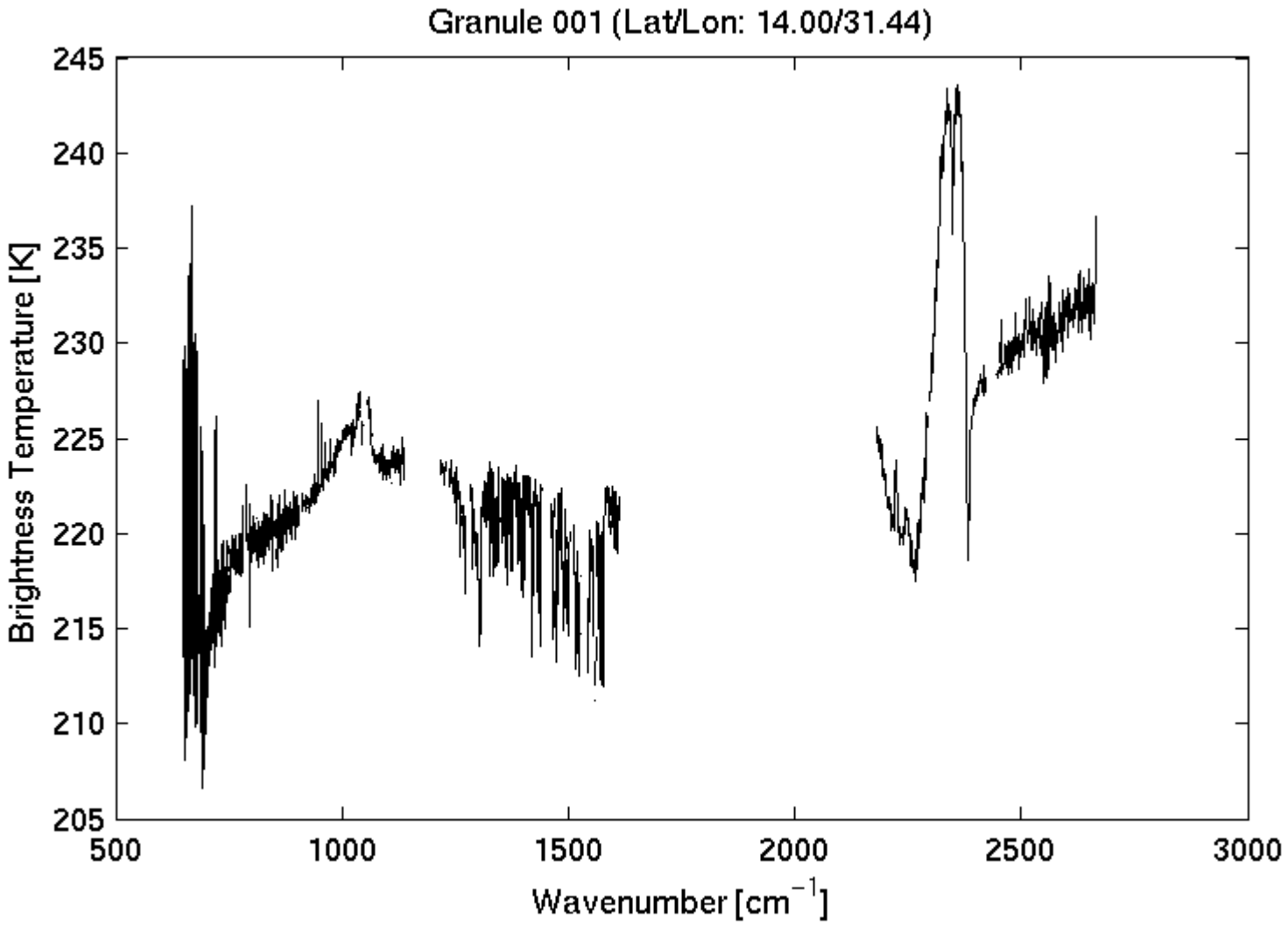

Day, night, desert, or cloudy?

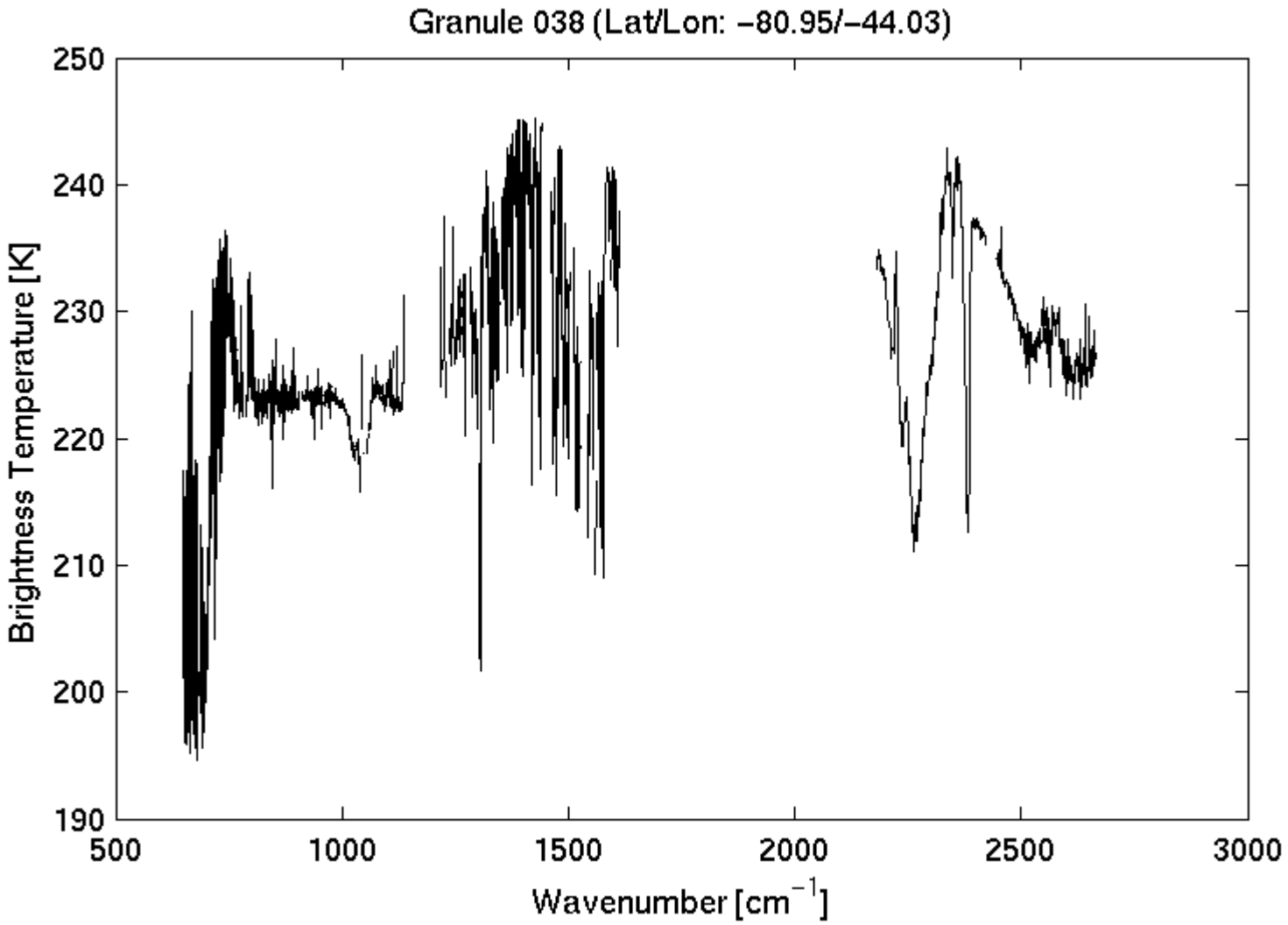

Cloudy, desert, or ocean?

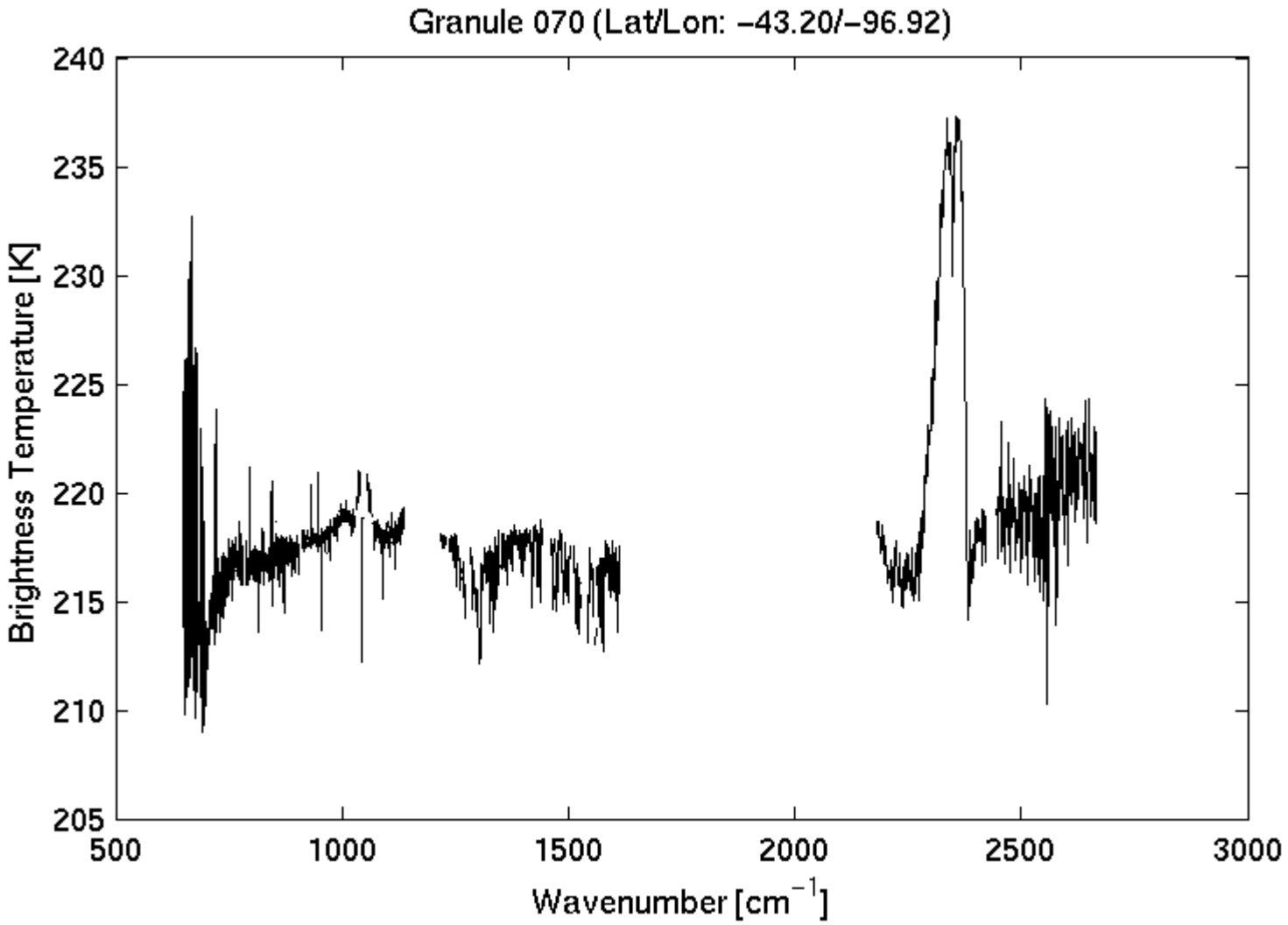

Land, desert, ice/snow, or ocean?

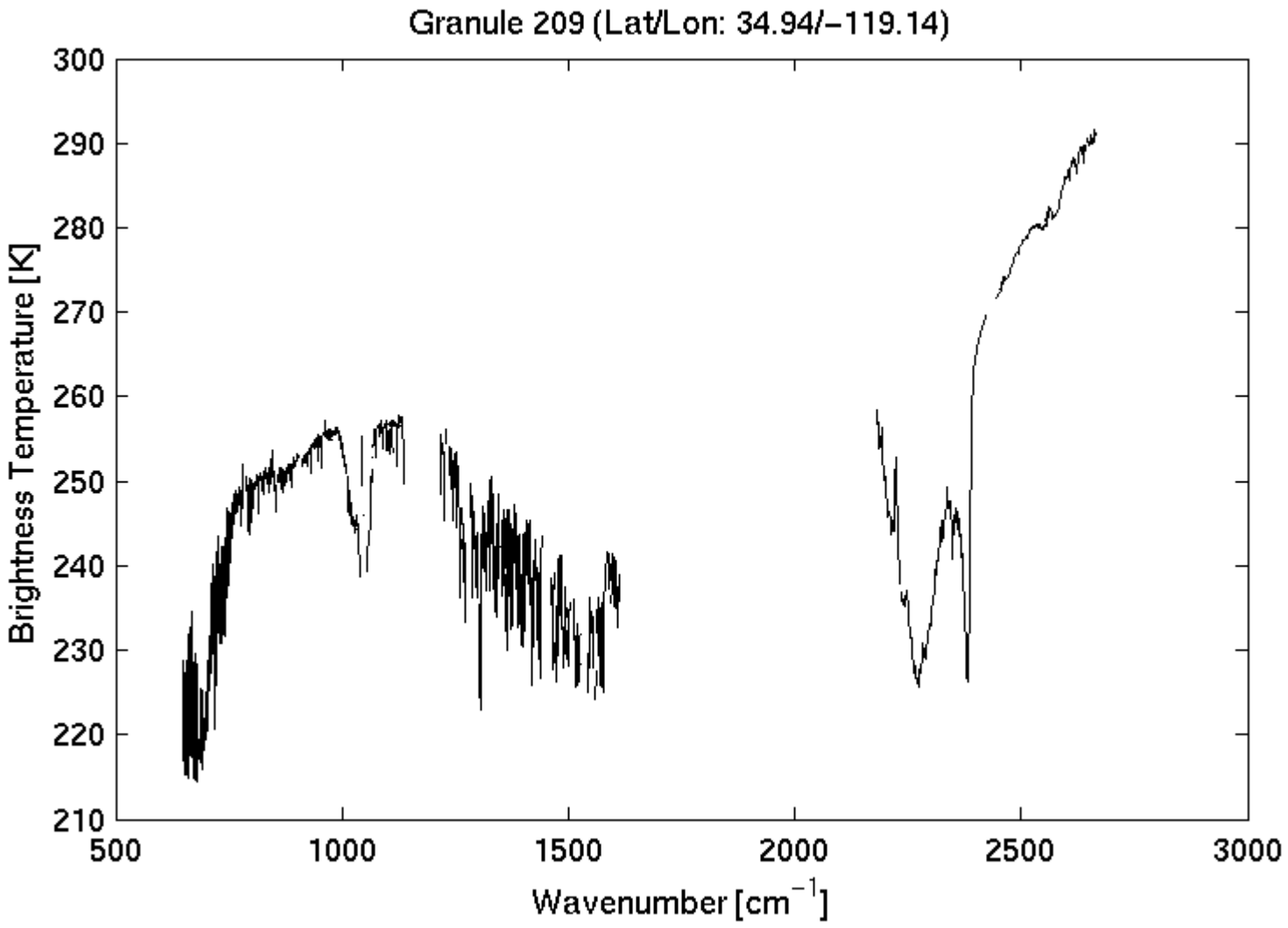

Day, night, desert, or cloudy?

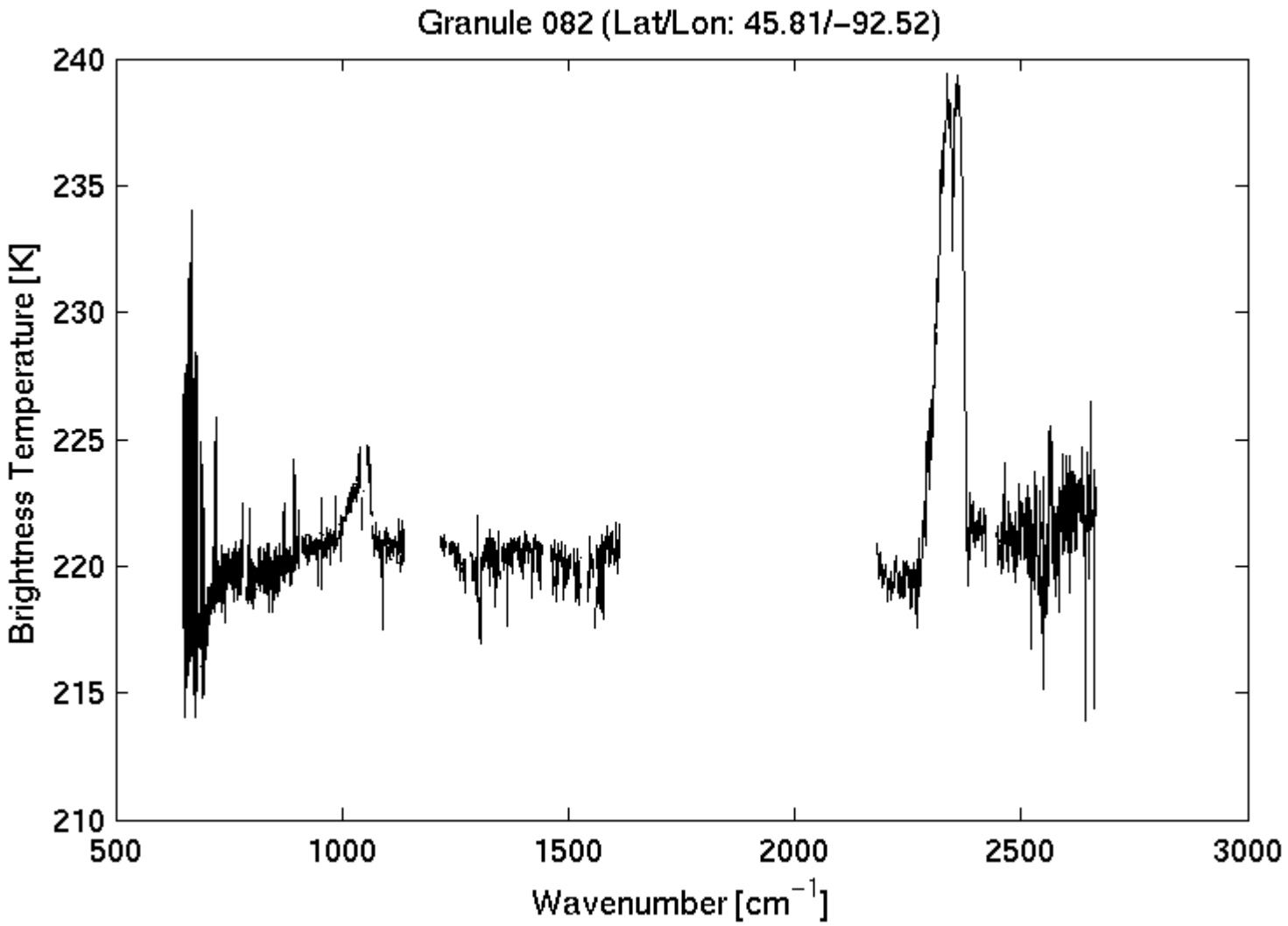

Day, night, ocean, or cloudy?